Interactive comment on "Space Weather Forecasting: What We Know Now and What Are the Current and Future Challenges?" by Bruce T. Tsurutani et al.

Anonymous Referee #1 Received and published: 21 August 2019

The manuscript "Space Weather Forecasting: What we know now and what are the current and future challenges" submitted to NPG, 2019, by Tsurutani et al., represents overall an excellent summary of the physics background of geomagnetic storms and substorms, solar energetic particle fluxes, enhanced energetic magnetospheric electron fluxes and radiation belt formation, as well as ionospheric TEC changes. The focus is placed on the physics of the different space processes and the interplanetary causes and solar origins.

It is very understandable that a summary on space weather cannot easily cover all aspects (incl. the glossary), ranging from new solar observations from SDO, 3D CME modelling results based on STEREO observations, new heliospheric imaging results for ICMEs also from STEREO, CME/ICME kinematics and new projects (e.g., FLARECAST, HESPERIA, AFFECTS, HELCATS, etc. and also other US and int. projects). However, before publication I suggest to state this in the paper and to add ref. about ongoing projects and literature covering those issues. I am not pointing out special references because they are easy to find through the internet or by browsing the Space Weather Journals of AGU and Int. Journal on Space Weather and Climate. I suggest adding clarifications of the focus and limitations of the paper at the beginning and end of the manuscript, see also the specific comments below. I also suggest to name some books on space weather (e.g., Hanslmeier: The Sun and space weather; Koskinen: The physics of space storms, etc.). Eventually even the title maybe modified to these suggestions to be more specific.

I further suggest adding more specific details on how new missions (PSP, SO) will help answer the addressed questions, or if it is not possible, to leave it out.

With these modifications the paper will certainly be a very good overview on space weather processes, written in a clear way.

We thank the referee for his/her helpful comments. Based on your comments and that of the other referee, we now reduce the usage of the word "forecasting" and speak mainly of the physics of space weather, a point that you have emphasized. This is now in the title of the paper. This was our original intent. We thank you for the references to the Hanslmeier and Koskinen books. We have mentioned those, some earlier ones and one more very recent publication (Buzulukova, 2018) in the Introduction section and state that Space Weather is an extremely broad field and that even those many books have not covered all areas of importance. Our present effort is not only to fill in the cracks but to give a different slant to the topic of Space Weather and what fruitful research can be done today and in the next 10 to 25 years. This is now explicitly stated in the paper.

We now give more specific ideas on how current and future missions could help solve outstanding questions.

Minor comments:

1) p.1, l.11: Since also the solar wind speed plays a role because of E=-v x Bz, I suggest to add the word "major" at the beginning, i.e., "Major geomagnetic storms are caused by ...". Or some similar clarification.

Yes, Corrected.

2) Same p., l.17: I suggest adding a sentence on SEPs because the topic start a little abrupt.

Done. A phrase was added.

3) p.2, l.35: I suggest removing the word "old" by a more elegant sentence stating an evolution of space weather from solar terrestrial research over the years, or something similar. Several space missions over the last decades have made significant progress in terms of interdisciplinary research (SOHO, Cluster, ACE, STEREO, etc.) between the solar, magnetospheric, ionospheric disciplines and space physics in general. And the new data have led to fundamental new insights into solar storms (e.g., CME 3D structure and propagation to Earth).

Okay. Done. The main point that we wanted to make to the reader is that many of the physical phenomena have already been discovered and much of the future work is fine tuning, and understanding of the detailed physics.

4) p. 3, l. 70: I suggest adding "that occur more frequent during ...".

Corrected. Thank you.

5) Same p., next lines: I suggest to rephrase " We will explain to solar scientists ...". There are also solar scientists knowledgeable of space physics.

Yes, corrected. We now address this "to the reader". Sorry. This phrase came when one of us gave a talk on space weather at a meeting and afterwards he was collared by a very prominent solar physicist who thanked the speaker for defining why space weather people talk about ICMEs. This person in the audience did not know.

6) p.6, 1st par.: I suggest to not completely neglect the role of v solar wind here. I see it is addressed later on.

Yes, okay. Done. It should be mentioned to the referee that the variation in V typically ranges from ~400 km/s to 1,000 km/s, a factor of about 2. However the Bsouth component varies from

about 0 nT to say -60 nT for a major magnetic storm. The variation in Bsouth is the greater of the two.

7) P.7, l.180: lASCO has observed by now far more then 10.000 CMEs, but only about 5% are faster than 700 km/s in the plane of sky. Only a very few have speeds of >2.000 km/s and these are coming preferentially from coronal regions above enhanced photospheric fields, so that higher field strengths and compression effects are pronounced. That means only a subset of CMEs produces strong fields in ip space. Please add some clarifications.

Thank you very much for the information. We have paraphrased your comments in quotation marks and have added it to the paper. We did not know this. Very important.

8) p.8, 2nd par.: Results from STEREO observations are missing here. It is also pointed out that new missions will provide new insights, but do they really do for these research topics? And if so, how?

Corrected. Thank you. It is obvious that STEREO should have addressed this issue already (but haven't). In our initial writeup we were only focusing on future missions. A reference to STEREO has been added.

9) p.11, l. 268-272: There are results that relate MC magnetic field structures back to their solar source regions. I suggest including a few sentences.

Corrected.

10) Same p., next par.: Again, how do PSP and SO help specifically?

Corrected. We now mention that they would have to study the same ICME at different distances from the Sun.

11) p.17, l.414: Only "intensities that some MC fields do". Many MCs have weaker fields.

Corrected.

12) Same p., l.422: "having said"?

Corrected.

13) p.18, caption Fig.7: I suggest to write: "A large coronal hole at the ..."

Thank you. Corrected.

14) p.19, l.442-444: LASCO C2 is also included.

Now corrected.

15) p.21, l.480: How will these missions be useful? Be specific.

Amplified and corrected.

16) p.23, l.533: same as 15).

Corrected.

17) p.32, l.724: “stronger”

Corrected.

18) same p., l.727: wording of sentence

Corrected.

19) p.35, l.805-812: I missed some results from STEREO in this context.

Corrected.

20) Same p., 816-824: I suggest including here some sentences on the established drag modelling for CME propagation I the heliosphere.

Corrected.

21) p.37, l.865: “have shown”

Corrected.

22) p.38, l. 887: wording of sentence

Corrected.

23) p.39, caption Fig.18: I suggest adding clarifying text about the shock creation.

Corrected. We have added more explanation of the figure in both the figure caption and within the text.

24) p.42, l.962: I suggest removing the word “poor”. Either there is connection or not.

Corrected.

25) p.50, l.1100: Why is the magnetic profile unlike those of other ICMEs? Please explain.

Corrected. We now mention that the profile is discussed later in the paper. We have expanded that discussion (later in the paper).

26) p.53, caption Fig.29: Please add the date.

Done.

27) p.54, l.1196: Please explain what the averaging time for Bz was to avoid averaging out negative time intervals.

Done. We have also added a comment on magnetospheric reaction timescales.

28) p.55, l. 1225: What is meant by a solar filament in this context? Please explain.

Corrected. This filament is the interplanetary manifestation of the Illing and Hundhausen (1986) CME filament. We now mention this in the text.

29) p.31, caption Fig. 31: Please add the year.

Done.

30) p.57, l.1257-1260: I suggest elaborating things not addressed a little bit, see major comments.

Amended. The details follow.

31) Same p., next par.: I suggest adding the role of V, also for CME arrival time predicC4 tions.

Yes. Okay. Very important. Done.

32) p.58, first 2 lines: But what about forecasting with ENLIL?

To address the issue of using physics based computer codes, data based computer codes and machine learning algorithms, we have made some "Final Comments" at the end of the paper. We have added references to many ENLIL based codes but remark that different codes have different strengths in predicting plasma properties and timing, but they do not address the MC magnetic field direction and intensity, the prime point of this paper. The sheath fields are also not well specified nor tested.

33) Same p., last par.: I suggest adding drag modelling here.

Some references had been added in the Final Comments. Basically one of the ENLIL references states that one has to have imaging data to do real-time studies of deceleration and acceleration. We think the eventual goals would be to model the slow solar wind upstream of the CME so that the slow solar wind can be modeled. This has not been done to our knowledge.

34) p. 59, last lines: I suggest to add some more concluding remarks and references to books on space weather, including recently established forecast models and new projects.

Done. We have added a "Final Comments" section at the very end of the paper. Rather than address details on forecasting models and new space projects, we thought it more important to emphasize model predictions of MC fields at 1 AU and testing which has not been done yet. Also many of the space projects typically do not address the fundamental physical problems mentioned here.

35) p.60, l. 1338: wording of sentence

Thank you. Done.

36) p.67, l. 1530: I suggest adding a statement on GNSS. 37) P.75, l. 1746: Solar activity includes many other phenomena, e.g., CMEs, jets, etc. but here only flares are addressed.

Corrected. We changed the title of ‘Solar activity” to “Solar Flares”. CMEs are discussed separately. We have added a section on GNSS.

Interactive comment on "Space Weather Forecasting: What We Know Now and What Are the Current and Future Challenges?" by Bruce T. Tsurutani et al.

Anonymous Referee #2

[Main comments]

In this review paper, the authors summarized observations of space weather phenomena and their physical interpretations. The main topic is about geomagnetic storms and magnetospheric phenomena, which is based on the authors' previous studies, ranging from the arrival of ICMEs and solar wind plasma at the Earth to the resulting geomagnetic and ionospheric storms. Phenomenological understanding is broadly explained, and questions about unresolved problems are described in each section, leading to what to reveal by new space missions like PSP, Solar Orbiter, MMS, Araseand SWARM.

This paper is written not only for space plasma physicists but for non-space plasma readers, like solar physicists and ionospheric scientists. It looks that the authors hope lots of people to read this article and try the unresolved problems with the interdisciplinary cooperation. The terminologies are summarized at the end of the main text, and in each section, histories of the studies are explained, which are useful for beginners and young researchers.

On the other hand, though the title is "Space Weather Forecasting", the manuscript does not cover predictions of solar flares, CMEs, SEPs, GICs and plasma bubbles , as well as social impacts on the infrastructures. The methods using numerical simulations and machine-learning techniques are not well introduced in this paper. It would be more useful for readers if the authors can include the current prediction models and their prediction accuracy in this review paper.

Especially, with a new approach using machine-learning algorithms, probabilistic pre-dictions can be done even if the physical mechanisms are not fully revealed. For accurate forecasting, the full understanding of physical processes are really necessary? If we understand all the nonlinear processes in space weather phenomena, can we forecast them perfectly? It would be also useful for readers if the authors can answer these questions.

We thank the referee for his/her helpful comments in improving this paper. The points that you have raised above are very pertinent and are indeed topics that have not been covered well. To address your specific comment about discussing predictions of solar, interplanetary, magnetospheric and ionospheric phenomena, we have decided to change the tone of the paper to indicate that we are addressing only the knowledge of the physical causes of such phenomena. Our original thought was that we need to know the physical causes before making forecasts/predictions. However the words "forecast/predictions" mean other things to other people (see comments from referee #1) and this can be confusing. We have therefore changed the title of the paper and part of the text to reflect this.

To address some of your other questions about "forecasting" using computer codes and machine learning algorithms, we address it here in detail in a Final Comments section at the end of the paper. Many physics-based codes have been constructed over tens of years.

However most of them have not been tested even using data from past magnetic storms. People has simply assumed that with all the major "physics" put into the codes, that one would be able to predict observations. One of us (BTT) has been involved with a NASA funded project to test the codes for ionospheric total electron content (TEC) data. We have been at this for the last 5 years. We have been using the well-established codes with measured solar wind input and have had the CCMC personnel of the Goddard Space Flight Center run the codes for us. The results have not been good. Basically we are not able to get accurate reproductions of the observations from any of the codes. At this time, we have no idea why we are not getting the predicted results, especially with solar wind, solar and geomagnetic activity index inputs. We have submitted two papers on this topic and as one would expect, the referees are not happy. Well, we are not happy either, but we simply want to report our results so improvements can be made. So to answer one of your questions, the independent reporting on the accuracy of codes in predicting so far is essentially non-existent.

The other referee has mentioned the ENLIL code and related codes. We now reference many of these works. People have tested MC propagation from the Sun to 1 AU but only the solar wind plasma properties and arrival times. The MC itself has not been modelled and tested. This is now stated in the paper.

Concerning machine learning algorithms, that too can be a red herring. Some of us have been studying such applications. Although great claims of success by proponents have been made, actual space weather successes are rare to none. What if the ionosphere is dominated by chaos? Then machine learning will not help. We have added several references to this topic in the Final Comments section (a new section at the end of the paper).

From the above one can see that neither we nor anyone else is really qualified to talk about "forecasting" using computer codes or machine learning algorithms. There have been no tests for the topics addressed in this paper to the knowledge of the authors. On the other hand, we do not wish to put such future studies in a negative light. Perhaps someone will be able to make a verifiable breakthrough. We wish to be positive on this subject. To address the topic of "forecasting", we have made some short comments near the end of the paper.

We are very interested in what atmospheric weather people do and have been following their work closely. They have been diligently working at their problem far longer than space weather people have been. It is interesting to know how they make their predictions. They have many codes at their disposal. They down-select to say the ~25 best ones and then take the mean value! This seems to work well. But why it works leaves a big question? Maybe that is the answer for space weather as well.

We have passed our section of "Final Comments" to the other NASA funded JPL researchers (Xing Meng, Tony Mannucci (P.I.) and Olga Verkhyagladova). They are in agreement with the wording of this section. As mentioned before, we have been examining existing ionospheric TEC codes for the last 5 years.

[Minor comments]

1) [Fig. 7] It looks that the solar image is not from SDO but Yohkoh. SDO does not have a soft X-ray telescope.

We apologize for the error! Thank you very much for the correction. This has been fixed.

2) [Fig. 8] The inner solar image was not taken by a soft X-ray telescope but an EUV telescope of EIT (195A Fe XII). The inner coronal image in the black circle was taken by Mauna Loa coronagraph, while the outer one was by SOHO/LASCO-C2.

Corrected. Thank you. We did not mention the outer coronagraph image previously. We do now.

3) [section 2.4.1] There is a sentence that to determine IMF-Bz component in the sheaths, we need more effort on predicting the slow solar wind plasma and magnetic field, but this statement is obscure. What will be the key to predict the slow solar wind plasma?

Corrected. Thank you. Right now we have no idea on how to determine the properties of the slow solar wind, but as you note this is key to predicting the IMF Bz in sheaths. We have reemphasized this point near the end of the paper.

4) [General comments] There are so many abbreviations like MC, ICME, IMF, CIR,HSS, HCS, HPS, HILDCAA, AE, EIA, EMIC wave, PC wave, RED, PPEF, SSW, SSS, which are difficult for non-space plasma readers to understand.

Yes, we have no solution to this problem other than to put in a Glossary so the reader can go back and forth. Putting in the full spelling of the acronyms will lengthen the paper by a lot.

5) It's better to show the definition of L value.

Corrected. We have inserted a definition in the text and also added this to the Glossary.

The Physics of Space Weather: What We Know Now and What Are the Current and Future Challenges?

Bruce T. Tsurutani[1], Gurbax S. Lakhina[2], Rajkumar Hajra[3]

[1]Pasadena, Calif, USA
[2]Indian Institute for Geomagnetism, Navi Mumbai, India
[3]National Atmospheric Research Laboratory, Gadanki, India

ABSTRACT

Major geomagnetic storms are caused by unusually intense solar wind southward magnetic fields that impinge upon the Earth's magnetosphere (Dungey, 1961). How can we predict the occurrence of future interplanetary events? Do we currently know enough of the underlying physics and do we have sufficient observations of solar wind phenomena that will impinge upon the Earth's magnetosphere? We view this as the most important challenge in Space Weather. We discuss the case for magnetic clouds (MCs), interplanetary sheaths upstream of interplanetary coronal mass ejections (ICMEs), corotating interaction regions (CIRs) and solar wind high-speed streams (HSSs). The sheath- and CIR-related magnetic storms will be difficult to predict and will require better knowledge of the slow solar wind and modeling to solve. For interplanetary space weather, there are challenges for understanding the fluences and spectra of solar energetic particles (SEPs). This will require better knowledge of interplanetary shock properties as they propagate and evolve going from the Sun to 1 AU (and beyond), the upstream slow solar wind and energetic "seed" particles. Dayside aurora, triggering of nightside substorms, and formation of new radiation belts can all be caused by shock and interplanetary ram pressure impingements onto the Earth's magnetosphere. The acceleration and loss of relativistic magnetospheric "killer" electrons and prompt penetrating electric fields in terms of causing positive and negative ionospheric storms are reasonably well understood, but refinements are still needed. The forecasting of extreme events (extreme shocks, extreme solar energetic particle events, and extreme geomagnetic storms ("Carrington" events or greater)) are also

discussed. Energetic particle precipitation into the atmosphere and ozone destruction is briefly discussed. For many of the studies, the Parker Solar Probe, Solar Orbiter, Magnetospheric Multiscale Mission (MMS), Arase, and SWARM data will be useful.

1. INTRODUCTION

1.1. Some Comments on the History of the Physics of Space Weather

Space Weather is a new term for a topic that actually began over a century and a half ago. It is just that with the space age beginning in 1957 (with the launch of Sputnik) and soon thereafter, many scientifically instrumented satellites led to an explosion of knowledge of the physics of Space Weather. However it is useful to review some of the early scientific studies that occurred prior to 1957. Prior to the space age (where we have satellites orbiting the Earth, probing interplanetary space and viewing the Sun in UV, EUV and X-ray wavelengths), it was clearly realized that solar phenomena caused geomagnetic activity at the Earth. For example, Carrington (1859) noted that there was a magnetic storm that followed ~17 h 40 min after the well-documented optical solar flare which he reported. This storm (Chapman and Bartels, 1940) was only more recently studied in detail by Tsurutani et al. (2003) and Lakhina et al. (2012), but the hints of a causal relationship was there in 1859. After Carrington (1959) published his seminal paper, Hale (1931), Newton (1943) and others showed that magnetic storms were delayed by several days from intense solar flares. These types of magnetic storms are now known to be caused by either their associated interplanetary coronal mass ejections (ICMEs) or their upstream sheaths. Details will be discussed later in this review.

Maunder (1904) showed that geomagnetic activity often had a ~27 day recurrence. This periodicity was associated with some mysteriously unseen (by visible light) feature on the Sun. Chree (1905, 1913) showed that these data were statistically significant, thus inventing the Chree "superposed epoch analysis", a scientific data analysis technique which is still used today. The mysteriously unseen solar features responsible for the geomagnetic activity were called "M-regions" by Bartels (1934) where the "M" stood for "magnetically active". It is now known that M-regions are coronal holes (Krieger et al., 1973), solar regions from which solar wind high-speed streams (HSSs) emanate, causing geomagnetic activity at the Earth (Sheeley et al., 1976, 1977; Tsurutani et al.

1995). The current status of geomagnetic activity associated with HSSs and the future work needed to better understand and to predict the various facets of Space Weather events will be discussed later.

With the advent of rockets and satellites, the near-Earth interplanetary medium has been probed by magnetic field, plasma, and energetic particle detectors. The Sun has been viewed in many different wavelengths. The Earth's auroral regions have recently been viewed by UV imagers giving a global view of auroras including the dayside. The ionosphere has been probed by global positioning system (GPS) dual frequency radio signals, allowing a global map of the ionospheric total electron content (TEC) in relatively high spatial and temporal resolution. The purpose of this review article will be to give a reasonably thorough review of some of the major Space Weather effects in the magnetosphere, ionosphere and atmosphere and in interplanetary space, in order to explain what the solar and interplanetary causes are or are expected to be. The most useful part of this review will be to focus on what future advances in Space Weather might be in the next 10 to 25 years. In particular we will mention what outstanding problems the Parker Solar Probe, Solar Orbiter, MMS, Arase, ICON, GOLD, and SWARM data might be useful in solving.

Our discussion will first start with phenomena that occur most frequently during solar maxima (flares, CMEs and ICME-induced magnetic storms). We will explain to the reader what is meant by an ICME and why we distinguish this from a CME. Next, phenomena associated with the declining phase of the solar cycle will be addressed. These include corotating interaction regions (CIRs) and HSSs, which cause high-intensity long-duration continuous AE activity (HILDCAA) events, and the acceleration and loss of magnetospheric relativistic electrons. We will then return to the topic of interplanetary shocks and their acceleration of energetic particles in interplanetary space and also their creating new radiation belts inside the magnetosphere. Interplanetary shock impingement onto the magnetosphere create dayside auroras and also trigger nightside substorms. Prompt penetration electric fields during magnetic storm main phases will be discussed in terms of the consequences of positive and negative ionospheric storms, depending on the local time of the observation and the phase of the magnetic storm. Two relatively new topics, that of supersubstorms (SSSs) and the possibility of precipitating magnetospheric relativistic electrons

affecting atmospheric weather will be discussed. A glossary will be provided to give definition of the terms used in this review article.

There have been some recent books/articles that touch on the many topics of the physics of Space Weather, however not in the same way that we will attempt to do here. We recommend the interested reader: "*From the Sun: Auroras, Magnetic Storms, Solar Flares, Cosmic Rays*" by Suess and Tsurutani (1989), "*Magnetic Storms*" by Tsurutani, Kamide, Gonzalez, Arballo (1997a), "*Storm-Substorm Relationship*" by Sharma, Kamide, Lakhina (2004), "*Recurrent Magnetic Storms: Corotating Solar Wind Streams*" by Tsurutani, McPherron, Gonzalez, Lu, Sobral, Gopalswamy (2006a), "*The Sun and Space Weather*" by Hanslmeier (2007), "*Physics of Space Storms: From the Solar Surface to the Earth*" by Koskinen (2011), and "*Extreme Events in Geospace: Origins, Predictability and Consequences*" by Buzulukova (2018). Because Space Weather is an enormous field/topic, not all facets of it have ever been covered in one book. The present authors are active researchers in the field and will attempt to introduce new viewpoints and topics not covered in the above works.

1.2. Organization of Paper

The concept of magnetic reconnection is introduced first for the non-space plasma reader. Magnetic reconnection is the physical process responsible for transferring solar wind energy into the magnetosphere during magnetic storms. We have organized the rest of the paper by discussing Space Weather phenomena by solar cycle intervals. However it should be mentioned that this is not totally successful since some phenomena span all parts of the solar cycle.

Solar maximum phenomena such as CMEs, ICMEs, fast shocks, sheaths, and the forecasting of geomagnetic storms associated with the above are covered in Subsections 2.1 to 2.4. The Space Weather phenomena associated with the declining phase of the solar cycle are discussed in Section 3.0. Topics such as CIRs, CIR storms, HSSs, embedded Alfvén wave trains within HSSs, HILDCAA events, relativistic magnetospheric electron acceleration and loss, and electron precipitation and ozone depletion are discussed in Subsections 3.1 to 3.6. Although interplanetary shocks are primarily features associated with fast ICMEs and thus primarily a solar maximum

phenomenon, shocks can also bound CIRs (~20% of the time) at 1 AU during the solar cycle declining phase as well. Shocks and the high density plasmas that they create can input ram energy into the magnetosphere. Topics such as solar cosmic ray particle acceleration, dayside auroras, triggering of nightside substorms and the creation of new magnetospheric radiation belts are covered in Subsections 4.1 to 4.4. Solar flares and ionospheric TEC increases is another Space Weather effect causing direct solar-ionospheric coupling not involving interplanetary space nor the magnetosphere. This is briefly discussed in Section 5.0. Prompt penetration electric fields (PPEFs) and ionospheric TEC increases (and decreases) occurs during magnetic storms. Although the biggest effects are observed during ICME magnetic storms (solar maximum), effects have been noted in CIR magnetic storms as well. This is discussed in Section 6.0. The "Carrington" magnetic storm is the most intense magnetic storm in recorded history. The aurora associated with the storm reached 23° from the geomagnetic equator (Kimball, 1960), the lowest in recorded history. Since this event has been used as an example for extreme Space Weather and events of this type are a problem for the U.S. Homeland Security, we felt that there should be a separate section on this topic, Section 7.0. We also discuss the possibility of events even larger than the Carrington storm occurring. In Section 8.0 auroral SSSs are discussed. Why is this topic covered in this paper? It is possible that SSSs which occur within superstorms are the actual causes for the extreme ionospheric currents, geomagnetically induced currents (GICs), that are responsible for potential power grid failures and not the geomagnetic storms themselves. Section 9.0 gives our summary/conclusions for the physics and the possibility of forecasting Space Weather events. Section 10.0 is a glossary of Space Weather terms used by researchers in the field. Most of the definitions were carefully constructed in a previous book (Suess and Tsurutani, 1998). These should be useful for an ionospheric person looking up solar terms, etc. It could be particularly useful for the non-space plasma readership as well.

2. RESULTS: Solar Maximum

2.1. Southward Interplanetary Magnetic Fields, Magnetic Reconnection and Magnetic Storms

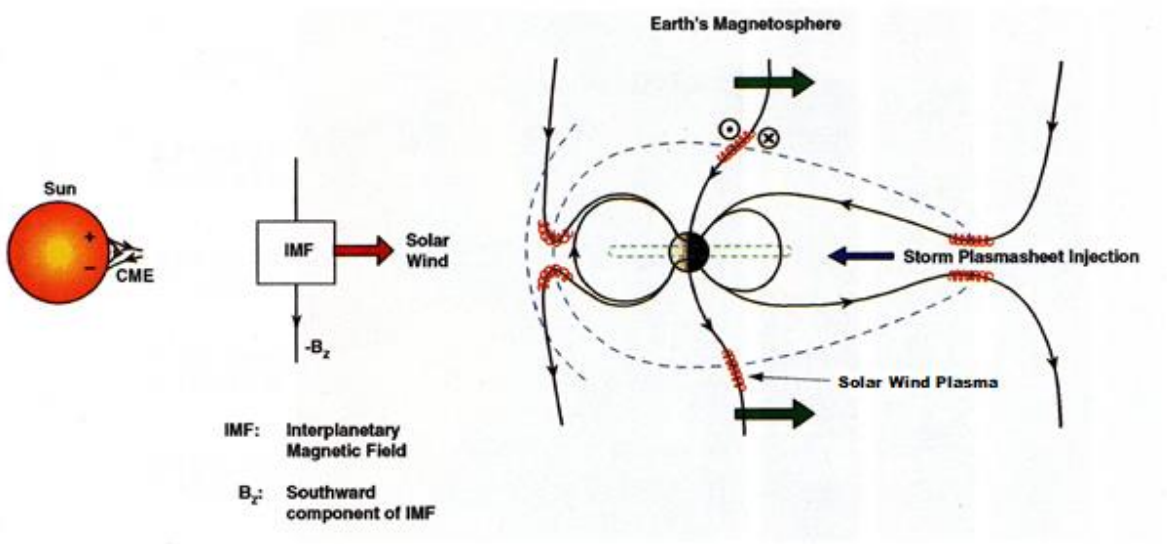

Figure 1. Magnetic reconnection powering geomagnetic storms and substorms. Adapted from Dungey (1961).

Figure 1 shows the Dungey (1961) scenario of magnetic reconnection. A one-to-one relationship between southward interplanetary magnetic fields (IMFs) and magnetic storms has been shown by Echer et al. (2008a) for 90 intense (Dst < -100 nT) magnetic storms that occurred during solar cycle 23. If the IMF is directed southward, it will interconnect with the Earth's magnetopause northward magnetic fields (the Earth's north magnetic pole is located in the southern hemisphere near the south rotational pole). The solar wind drags the interconnected magnetic fields and plasma downstream (in the antisunward direction). The open magnetic fields then reconnect in the tail. Reconnection leads to strong convection of the plasmasheet into the nightside magnetosphere.

What is known by theory and verified by observations is that the stronger the southward component of the IMF and the stronger the solar wind velocity convecting the magnetic field, the stronger the solar wind-magnetospheric system is driven (e.g., Gonzalez et al., 1994). Intense IMF Bsouth in MCs (and sheaths) drive intense magnetic reconnection at the dayside magnetopause and intense reconnection on the nightside. Strong nightside magnetic reconnection leads to strong inward convection of the plasmasheet. The stronger the magnetotail reconnection, the stronger the inward convection. Via conservation of the first two adiabatic invariants (Alfvén, 1950), the greater the convection, the greater the energization of the radiation belt particles.

As the midnight sector plasmasheet is convected inward to lower L, the initially ~100 eV to 1 keV plasmasheet electrons and protons are adiabatically compressed (kinetically energized) so that the perpendicular (to the ambient magnetic field) energy becomes greater than the parallel energy. This leads to plasma instabilities, wave growth and wave-particle interactions (Kennel and Petschek, 1966). The resultant effect is the "diffuse aurora" caused by the precipitation of the ~10 to 100 keV electrons and protons into the upper atmosphere/lower ionosphere. At the same time double layers are formed just above the ionosphere, giving rise to ~1 to 10 keV "monoenergetic" electron acceleration and precipitation in the formation of "discrete auroras" (Carlson et al., 1998).

If the IMF southward component is particularly intense, this can lead to a magnetic storm with Dst < -100 nT. The Dst decrease is caused by strong convection of the plasmasheet into the inner part of the magnetosphere and the formation of an intensified ring current. This ring current produces a diamagnetic field which causes the reduced field strength at surface of the Earth. This is the magnetic storm main phase.

After the southward field decreases or changes orientation to northward fields, the magnetic storm recovers. The recovery is associated with a multitude of physical processes associated with the loss of the energetic ring current particles: charge exchange, Coulomb collisions, wave-particle interactions and convection out the dayside magnetopause (West et al., 1972; Kozyra et al. 1997, 2006a; Jordanova et al., 1998; Daglis et al. 1999). A typical time for storm recovery is ~10 to 24 h (Burton et al., 1975; Hamilton et al., 1988; Ebihara and Ejiri, 1998; O'Brien and McPherron, 2000; Dasso et al., 2002; Kozyra et al., 2002; Wang et al., 2003; Weygand and McPherron, 2006; Monreal MacMahon and Llop, 2008).

2.2. Coronal Mass Ejections (CMEs), Interplanetary Coronal Mass Ejections (ICMEs) and Magnetic Storms

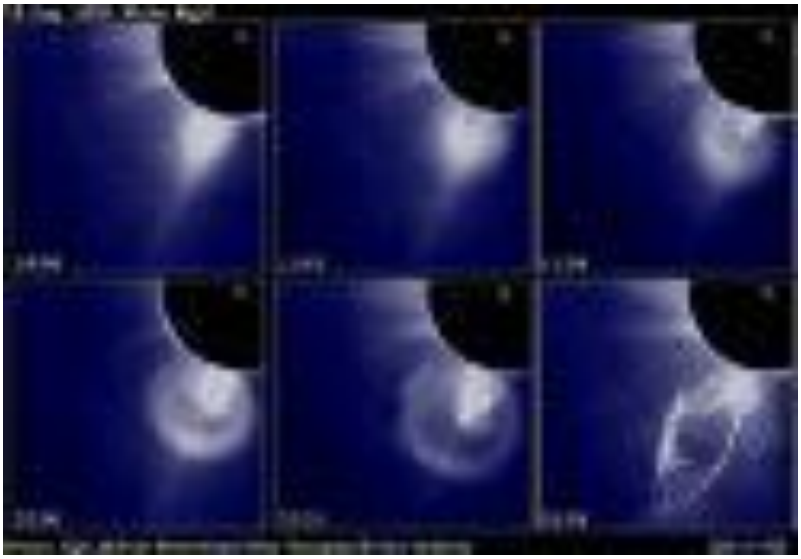

Figure 2. A sequence of images showing the emergence of parts of a CME coming from the Sun. The time sequence starts at the upper left and ends at the lower right. Taken from Illing and Hundhausen (1986).

What are the solar and interplanetary sources of intense IMFs that lead to magnetic reconnection at Earth and intense magnetic storms? What we know from space age observations is that these magnetic fields come from parts of a CME, a giant blob of plasma and magnetic fields which are released from the Sun associated with solar flares and disappearing filaments (Tang et al., 1989). Figure 2 shows the emergence of a CME from behind a solar occulting disc. The time sequence starts at the upper left, goes to the right and then to the bottom left, and ends at the bottom right. The three parts of a CME are best noted in the image on the bottom left. There is a bright outer loop most distant from the Sun, followed by a "dark region", and then closest to the Sun is the solar filament.

2.3. Forecasting Magnetic Storms and Extreme Storms Associated with ICMEs

We will precede ourselves and state here that for the limited number of cases studied to date, the most geoeffective part of the CME is the "dark region". Interplanetary scientists (Burlaga et al., 1981; Choe et al., 1982; Tsurutani and Gonzalez, 1994) have identified this as the low plasma beta region called a magnetic cloud (MC), first identified by Burlaga et al.(1981) and Klein and Burlaga (1982) in interplanetary space by magnetic field and plasma measurements. When there are

223 southward component magnetic fields within the MC (thought to typically be a giant fluxrope), a
224 magnetic storm results (Gonzalez and Tsurutani, 1987; Gonzalez et al. 1994; Tsurutani et al.,
225 1997b; Zhang et al., 2007; Echer et al. 2008a).
226
227 It should be noted that fast CMEs and intense MC fields are relatively rare. The SOHO LASCO
228 instrument has observed > 10,000 CMEs but only ~5% have speeds faster than ~700 km/s. Only
229 very few have speeds > 2,000 km/s and these are coming from coronal regions associated with
230 Active Regions (ARs) (personal communications with referee, 2019).
231
232 Interplanetary and magnetospheric scientists have developed the term ICME or interplanetary
233 CME because it is not currently known (for individual events) how the CME evolves as it
234 propagates from the Sun to the Earth and beyond. Leamon et al. (2004) in comparing interplanetary
235 MCs to associated solar active regions found that there was little or no relationship, compelling
236 the authors to conclude that "MCs are formed during magnetic reconnection and are not simple
237 eruptions of preexisting coronal structures". Yurchyshyn et al. (2007) in a similar study found that
238 "for the majority of interplanetary MCs, the fluxrope axis orientation changed less than 45° going
239 from the Sun to 1 AU". Palmerio et al. (2018) found "for the majority of cases, the flux rope tilt
240 angles rotated several tens of degrees (between the Sun and the Earth) while 35% changed by more
241 than 90°". 3D MHD simulations have shown that CMEs can be severely distorted as they interact
242 with different types of interplanetary structures as they propagate through interplanetary space
243 (Odstrcil and Pizzo, 1999a,b). The latter authors have shown that the CME distortion is
244 substantially different when it interacts with the streamer belt (heliospheric plasma sheet/HPS)
245 than with an HSS. The distortion of the CME can make the ICME unrecognizable at a distance
246 further away from the Sun.
247
248 More detailed topics not covered in Palmerio et al. (2018) or in Odstrcil and Pizzo (1999a,b) are
249 the topics of the fate of the principal features of CMEs as discussed by Illing and Hundhausen
250 (1986). For example, the bright outer loops are seldomly identified at 1 AU (one rare case was
251 identified by Tsurutani et al., 1998) and the filaments are typically not found within the ICME at
252 1 AU. The first filament detection at 1 AU was not reported until 1998 (Burlaga et al., 1998). For
253 more recent observations of filaments at 1 AU, we direct the reader to Lepri and Zurbuchen (2010).

Where have the bright outer loops and filaments gone to? Have they simply detached only to impinge onto the magnetosphere at a later time, or do they go back into the Sun? Or is it possible that many CMEs do not have filaments at their bases? Remote imaging observations from STEREO should be able to answer these questions. New in situ results from Parker Solar Probe, Solar Orbiter and ACE plus ground-based solar observations could perhaps help address the plasma physics of why typical ICMEs do not have attached filaments.

It should be remarked that the high density solar filaments could be extremely geoeffective if they collided with the Earth's magnetosphere (this is covered later in Section 3.2.5). Is it possible for the MC to rotate so that initially southward magnetic fields become northward components? Can the MC fields be compressed or expanded by interplanetary interactions? Can magnetic reconnection be taking place within the ICME between the solar corona and 1 AU as suggested by Manchester et al. (2006) and Kozyra et al., (2013)? If so, how often does this occur and can it be predicted? Modeling and examining the Parker Solar Probe and Solar Orbiter data (for studies on the same ICME) could help us understand whether the MCs evolve as they propagate through interplanetary space.

Of course the most important goal for Space Weather is predicting the southward magnetic fields within the ICME. This extremely difficult task is the holy grail of Space Weather. It is more important than predicting the time of the release of a CME, its speed and its direction.

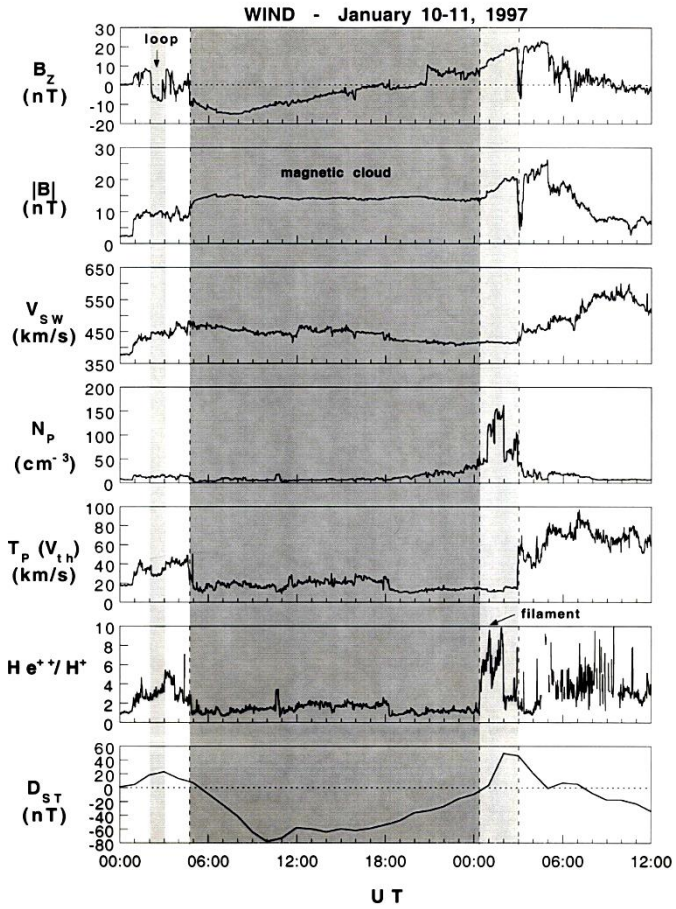

Figure 3. An ICME detected at 1 AU just upstream of the Earth.

Figure 3 shows a rare case of an ICME at 1 AU where all three parts of a CME are detected. The MC is indicated by the shaded region in the figure. The outer loop was identified by Tsurutani et al. (1998) and the filament by Burlaga et al. (1998).

From top to bottom are the IMF Bz component (in geocentric solar magnetospheric/GSM coordinates), the field magnitude, the solar wind velocity, density, temperature and the He^{++}/H^{+} ratio. The bottom panel gives the ground based Dst index whose amplitude is used as an indicator of the occurrence of a magnetic storm. Dst becomes negative when the Earth's magnetosphere is filled with storm-time energetic ~10-300 keV electrons and ions (Williams et al., 1990). Dessler and Parker (1959) and Sckopke (1966) have shown that the amount of magnetic decrease is linearly related to the total kinetic energy of the enhanced radiation belt particles. This is because the

energetic particles which comprise the storm-time ring current, through gradient drift of the charged particles, form a diamagnetic current which decreases the Earth's magnetic field inside the current. We refer the reader to Sugiura (1964) and Davis and Sugiura (1966) for further discussions of the Dst index. The Dst index is a one hr index. More recently a 1 min SYM-H index (Iyemori, 1990; Wanliss and Showalter, 2006) has been developed. This is more useful for high time resolution studies. Both indices are produced by the Kyoto Data Center.

In this example (top panel of Figure 3) the MC fields start with a strong southward (Bz < 0 nT) component and then later turns northward. In the bottom panel, the magnetic storm Dst index becomes negative with very little delay from the southward magnetic fields. The energy transfer mechanism is magnetic reconnection, as discussed earlier in Section 2.1. The high density filament (fourth panel from the top) is present after the MC passage. Values as high as ~160 cm^{-3} have been detected. These values are extreme values (the nominal solar wind density is ~ 3 to 5 cm^{-3}: Tsurutani et al., 2018a). The high densities impinging on the magnetosphere in this case caused compression of the magnetosphere and the Dst index to reach ~+55 nT.

The stronger the southward component of the MC fields, the more intense the magnetic storm at the Earth. In extreme cases storms with intensities of Dst < -250 nT can occur (Tsurutani et al. 1992a; Echer et al. 2008b). An empirical relationship between the speed of the MC at 1 AU and its magnetic intensity has been shown by Gonzalez et al. (1998). A hypothetical explanation is the "melon seed model": squeezing a melon seed will cause it to squirt out, squeezing it harder will make it come out fast. A larger magnetic field will require greater pressure to release it. However a substantial MHD or plasma kinetic model is needed to explain the physics of this empirical relationship in more detail.

Because extremely strong MC magnetic fields are needed to produce extreme magnetic storms like the "Carrington" event (Tsurutani et al., 2003; Lakhina and Tsurutani, 2017), one should focus on extremely fast events for forecasting purposes. The geoeffective interplanetary dawn-to-dusk electric field is Vsw x Bsouth. Because Gonzalez et al (1998) have shown that |B| is empirically proportional to Vsw, the dawn-to-dusk interplanetary electric field has a Vsw^2 dependence. The Carrington ICME took ~17 hr 40 min to go from the Sun to Earth (Carrington, 1859), causing the

largest magnetic storm in history. The minimum Dst has been estimated to be -1760 nT. However the August 1972 event was even faster, taking only ~14 h 40 min to go from the Sun to Earth (Vaisberg and Zastenker 1976; Zastenker et al. 1978). Although the 1972 MC was indeed extreme in speed and magnetic field intensity, the direction of the magnetic field was northward and thus there was geomagnetic quiet following the MC impingement onto the magnetosphere (Tsurutani et al. 1992b). So again, predicting the ICME magnetic field direction is paramount in importance for Space Weather applications.

Modeling ICME propagation in interplanetary space during disturbed AR periods has met only limited success (Echer et al., 2009; Mostl et al., 2015; Hajra et al., 2019). Sometimes it is difficult to even identify to which flare or disappearing filament a detected ICME is related (see Tang et al., 1989; Hajra et al., 2019). Hajra et al. (2019) have noted a halo CME event that did not reach the Earth. The propagation times from the Sun to 1 AU has often been in error by days (Zhao and Dryer, 2014). The additional information provided by the Parker Solar Probe and Solar Orbiter and examination of present ICME propagation codes could help improve the ability to make more accurate forecasts.

2.4. Fast Shocks, Sheaths and Magnetic Storms

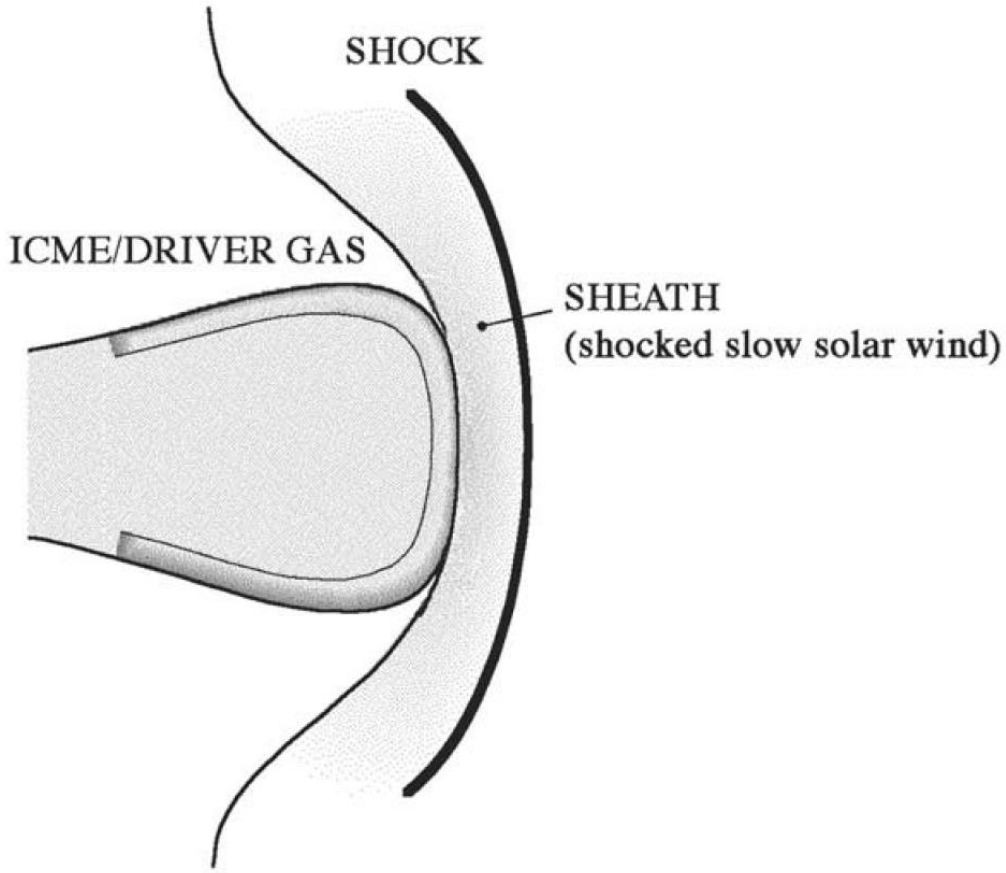

Figure 4. A schematic of an interplanetary sheath antisunward of an ICME. In this diagram the Sun is on the left (not shown).

Figure 4 shows a schematic of a shock and sheath upstream of an ICME. "Fast" CMEs/ICMEs can create upstream fast forward shocks (Tsurutani et al., 1988). By "fast" it is meant that the CME/ICME is moving at a speed higher than the upstream magnetosonic (fast wave mode) speed relative to the upstream plasma and by "forward" we mean that the shock is propagating in the same direction as the "driver gas" or the CME/ICME, antisunward. When a shock is formed, it compresses the upstream plasma and magnetic fields. In this terminology, the upstream direction is the direction in which the shock is propagating (antisunward in this case) and the downstream direction is towards the Sun (see Kennel et al., 1985 and Tsurutani et al., 2011 for details on shocks). The compressed plasma and magnetic fields downstream of the shock is the "sheath". The shock and sheath are not part of the CME/ICME. The origin of this plasma and magnetic fields is the slow solar winaltered by shock compression. This is important to understand if one

wishes to predict magnetic storms caused by interplanetary sheath southward magnetic fields. It should be noted that "slow" ICMEs have been detected at 1 AU (Tsurutani et al., 1994a). These phenomena do not have upstream shocks and sheaths, as expected. However the southward MC magnetic fields still cause magnetic storms.

Kennel et al. (1985) used MHD simulations to show that the plasma densities and magnetic field magnitudes downstream of shocks are roughly related to the shock magnetosonic Mach numbers. This theoretical relationship holds up to a Mach number of ~4. For higher Mach numbers MHD predicts that the compression will remain at a factor of ~4. Since interplanetary shocks detected at 1 AU typically have Mach numbers only of 1 to 3 (Tsurutani and Lin, 1985; Echer et al., 2011; Meng et al. 2019a), 1 to 3 are the typical shock magnetic field and density compression ratios detected at 1 AU. One question for future studies is "does the MHD relationships of magnetic field magnitude and density jumps hold for extreme shocks?" If not, there will be important consequences for extreme Space Weather.

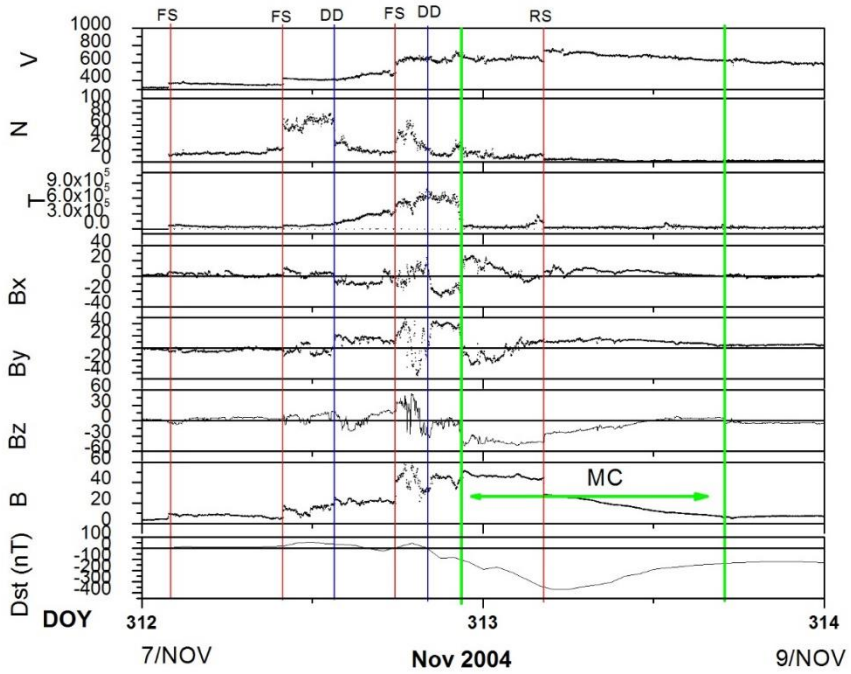

Figure 5. An example of three fast forward shocks pumping up the interplanetary magnetic field intensity. Taken from Tsurutani et al. (2008a).

Figure 5 shows a complex interplanetary event that was selected by the CAWSES II team to study in detail. The full information on this event from the Sun to the atmosphere can be found in the special issue: Large Geomagnetic Storms of Solar Cycle 23 (https://agupubs.onlinelibrary.wiley.com/doi/toc/10.1002/(ISSN)1944-8007.CYCLE231). What is important is that this event was associated with a solar active region (AR) and the results are quite important in terms not only for interplanetary disturbance phenomena but also for geomagnetic activity at the Earth.

From top to bottom in Figure 5 are the solar wind speed, density, and temperature, the IMF Bx, By and Bz components and the magnetic field magnitude in solar magnetospheric (GSM) coordinates. In this coordinate system, **x** points in the direction of the Sun, **y** is $(\Omega \times \mathbf{x})/|\Omega \times \mathbf{x}|$ where Ω is the Earth's south magnetic pole and **z** completes the right hand system. The magnetic storm Dst index is given at the bottom. Fast forward shocks are denoted by the three vertical red lines on 7 November 2004. There are sudden increases in the velocity, density, temperature and magnetic field magnitude at all three events. The Rankine-Hugoniot relationships have been applied to the plasma and magnetic field data and the analysis did determine that they are indeed fast shocks.

The point of showing this interplanetary event is to indicate that each shock pumps up the interplanetary sheath magnetic field by factors of ~2 to 3. The initial magnetic field magnitude started with a value of ~4 nT and at the peak value after the three shocks, it reached a value of ~60 nT. This final value was higher than the MC magnetic field, which was ~45 nT. Details concerning the shocks and compressions can be found in the original paper for readers who are interested. What is important here is how intense interplanetary magnetic fields are created. They can come from the MCs themselves or the sheaths, as shown here. However, in this case the southward magnetic fields that caused the magnetic storm came from the MC and not the sheath.

In the above example it is believed that three fast forward shocks were associated with three ICMEs released from the AR. The longitudinal extent of shocks are, however, wider than the MCs, so

only one MC was detected in the event. A similar situation was found for the August 1972 event discussed earlier.

It should be noted that a fast reverse wave (here by "reverse" we mean that the wave is propagating in the solar direction) was detected during the Figure 5 event. It is identified as the red vertical line on 8 November. In detailed examination of the Rankine-Hugoniot conservation equations, this wave was found to propagate at a speed below the upstream magnetosonic speed and thus was a magnetosonic wave and not a shock. This reverse wave caused a decrease in the MC magnetic field (and the southward component) and thus the start of the recovery phase of the magnetic storm. The reader should note that fast reverse waves and shocks are also important for geomagnetic activity. A detailed discussion of shock and discontinuity effects on geomagnetic activity can be found in Tsurutani et al. (2011).

2.4.1. Forecasting ICME sheath magnetic storms

Determination of the IMF Bz component in the sheaths will be a difficult task. To do this, more effort in understanding the slow solar wind plasma, magnetic fields and their variations will be required. To date, there has been little effort expended in this area. This is, however easy for us to hope for, but in practice is far more difficult to do. Use of data from Solar Probe, Solar Orbiter and a 1 AU spacecraft such as ACE could help in these analyses.

This problem has recently been emphasized by results from Meng et al. (2019a). Meng et al. have shown that superstorms (Dst < -250 nT) that occurred during the space age (1957 to present) are mostly driven by sheath fields or a combination of sheath plus a following magnetic cloud (MC).

Substorms are generated by lower intensity southward magnetic fields with the process of magnetic reconnection being the same as above. However substorm plasmasheet injections only go in to L ~4, the outer part of the magnetosphere (Soraas et al., 2004). The auroras associated with substorms appear in the "auroral zone", 60° to 70° magnetic latitude (MLAT). Magnetic storms associated with much larger IMF Bsouth are detected at subauroral zone latitudes.

3.0. RESULTS: Declining Phase of the Solar Cycle

3.1. Corotating Interaction Region (CIR) Magnetic Storms

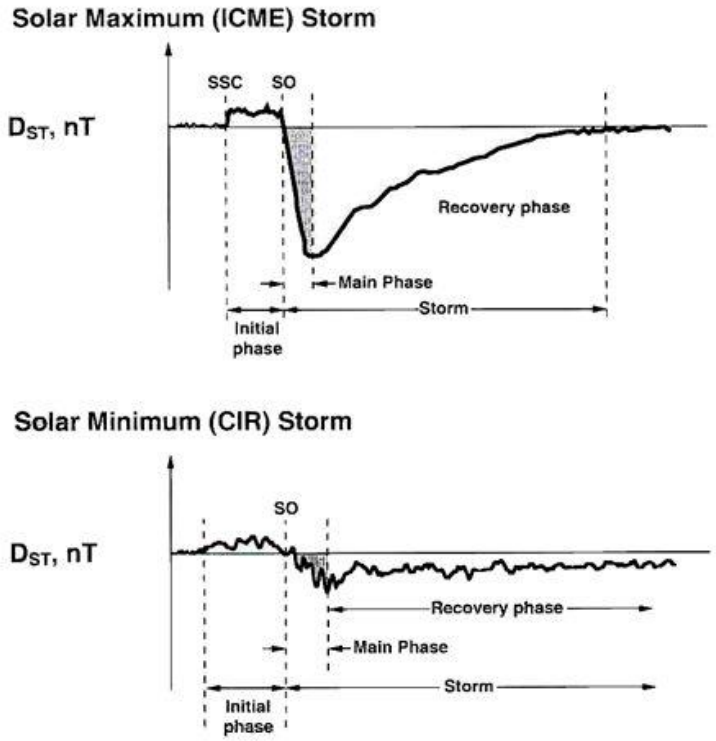

Figure 6. The magnetic Dst profiles of a CIR magnetic storm (bottom) and an ICME magnetic storm (top). Taken from Tsurutani (2000).

During the declining phase of the solar cycle a different type of solar and interplanetary activity dominates the physical cause of magnetic storms, that of Corotating Interaction Regions (CIRs). HSSs emanating from coronal holes (CHs) interact with the slow solar wind and form CIRs at their interaction interfaces. The magnetic storms caused by CIRs are quite different from storms caused by ICMEs and/or their sheaths. Figure 6 shows the difference in profiles of two different types of magnetic storms. The profile of a CIR magnetic storm is shown on the bottom and that of a shock sheath ahead of an ICME MC magnetic storm on top.

The ICME MC magnetic storm Dst profile, discussed briefly earlier (see Figure 3), is reasonably easy to identify (top panel). There is a sudden, ~tens of second duration positive increase in Dst which is caused by the sudden increase in solar wind ram pressure due to the passage of the sheath

high density jump downstream of the shock. This compresses the magnetosphere, creating the sudden impulse (SI^+: see Joselyn and Tsurutani, 1990) detected everywhere on the ground (Araki et al., 2009). Later, in either the sheath or the MC there may be a southward IMF which causes the magnetic storm. If there is a southward component in the MC, it is usually smoothly varying in intensity and direction. This leads to a smooth monochromatic storm main phase as seen in the Dst index (and illustrated in Figures 3 and 6). The loss of the ring current particles is the cause of the storm recovery phase. The details of storm recovery phase durations and causative mechanisms will be an interesting topic for magnetospheric scientists to study in the near future. The Arase mission data will be quite useful for these studies.

The bottom panel of Figure 6 shows the typical profile of a CIR magnetic storm. It is quite different from a sheath-MC magnetic storm profile. There is no SI^+ associated with the beginning of the geomagnetic disturbance. This is because CIRs detected at 1 AU typically are not led by fast forward shocks (Smith and Wolf, 1976; Tsurutani et al. 1995). The positive increase in Dst is associated with the impact of a high density region near the heliospheric current sheet (HCS) (Smith et al., 1978; Tsurutani et al. 2006b) called the heliospheric plasmasheet (HPS; Winterhalter et al., 1994) and/or associated with the compressed plasma at the leading edge of the CIR. These are slow solar wind plasma densities. The most distinguishing feature of the CIR storm main phase is the lack of smoothness, in sharp contrast to the MC magnetic storm. This irregular Dst storm main phase is caused by large Bz fluctuations within the CIR.

CIR magnetic fields have magnitudes of ~20 to 30 nT and typically do not reach the much higher intensities that MC fields typically do. For this reason and also because of the IMF Bz fluctuations, CIR magnetic storms usually have intensities Dst $\geq$ -100 nT (small or no magnetic storms). Extreme magnetic storms with Dst < -250 nT caused by CIRs are rare, if they occur at all (none were found in the Meng et al. 2019a study). However it is clear that compound events involving both CIRs, sheaths ahead of ICMEs and ICMEs could certainly cause extreme magnetic storm events.

CIR related magnetic storms occur most frequently during the declining phase of the solar cycle and ICME magnetic storms typically occur near the maximum phase of the solar cycle. However,

it should be noted that both CIR storms and sheath and/or ICME MC magnetic storms can occur during any phase of the solar cycle. We have simply ordered things by solar cycle so that it will be easier to give the reader the general picture of Space Weather.

3.2 Coronal Holes, High Speed Solar Wind Streams and Geomagnetic Activity

3.2.1. Coronal holes and high speed solar wind streams

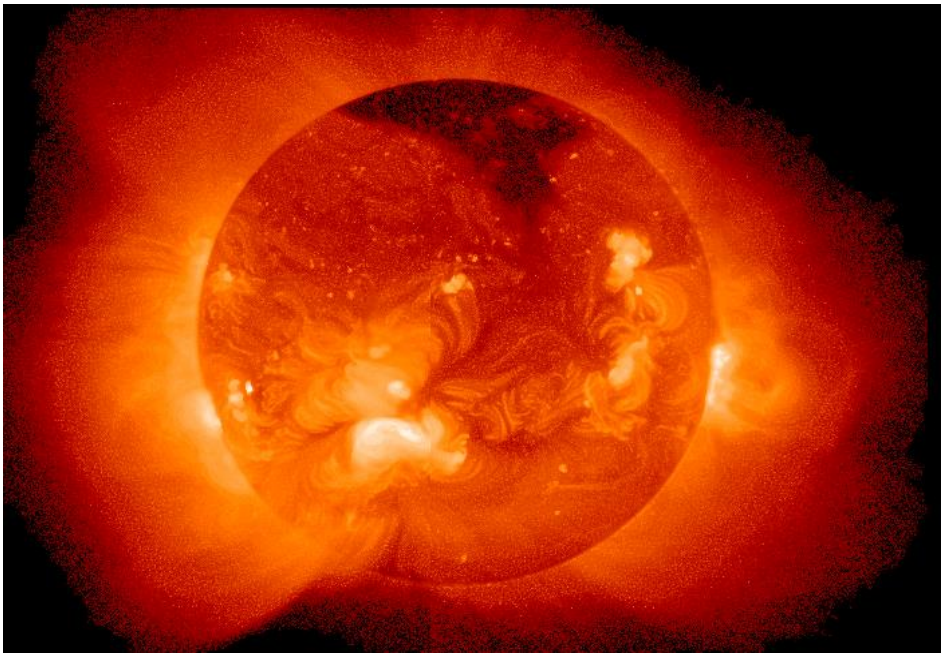

Figure 7. A large coronal hole (the dark region) near the north pole of the Sun. The figure was taken by the soft X-ray telescope (STX) onboard the Yohkoh satellite in 1992.

Figure 7 shows a polar coronal hole at the north pole of the Sun. This image was taken by the soft x-ray telescope (STX) onboard the Yokoh satellite (http://www.spaceweathercenter.org/swop/Gallery/Solar_pics/yohkoh_060892.html). The dark (low temperature) region at the pole is the coronal hole. Large polar coronal holes occur typically in the declining phase of the solar cycle (Bravo and Otaola, 1989; Bravo and Stewart, 1997; Zhang et al., 2005).

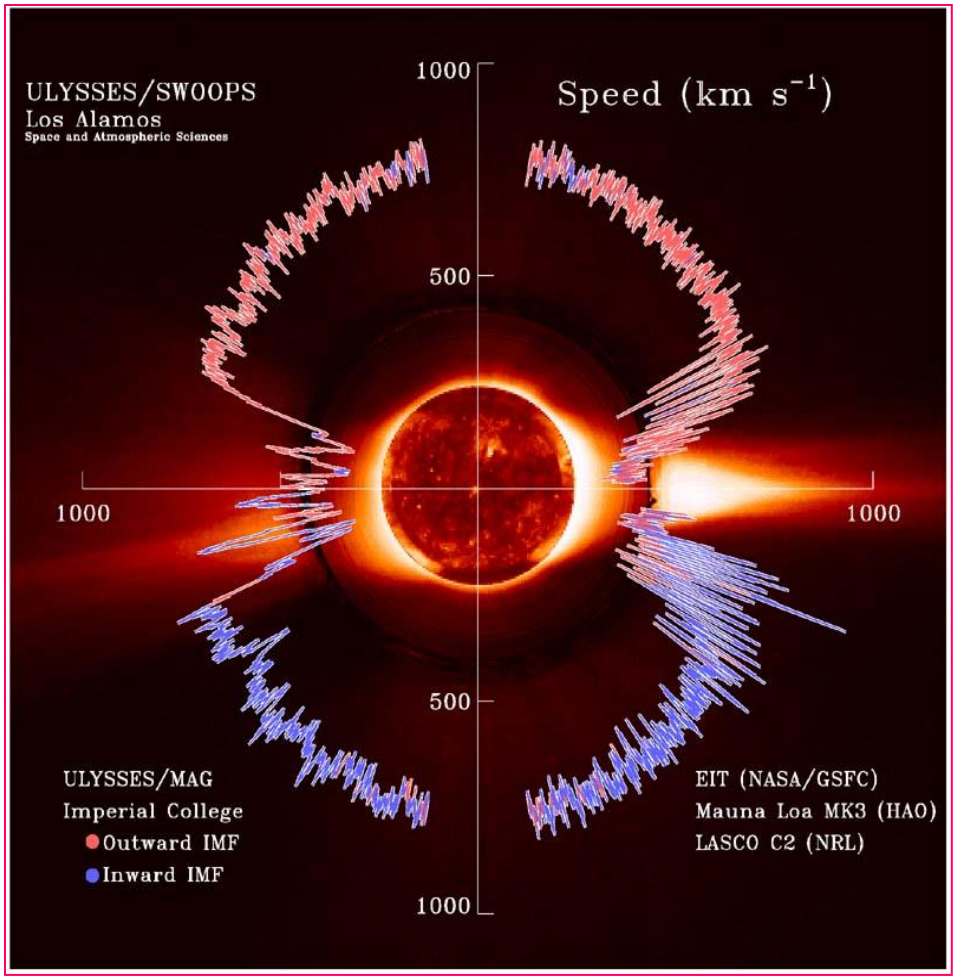

Figure 8. High speed solar wind streams emanating from coronal holes in the north and south solar poles. The figure was taken from Phillips et al. (1995) and McComas et al. (2002).

Figure 8 gives a "dial plot" of the solar wind speed for the first traversal of the Ulysses spacecraft over the Sun's poles. The radius from the center of the Sun to the trace indicates the solar wind speed. The magnetic field polarity is indicated by the color of the trace, red for outward IMFs and blue for inward IMFs. A SOHO EIT soft x-ray image of the Sun is placed at the center of the figure and a High Altitude Observatory Mauna Loa coronagraph image shows the inner corona at that time. The outer corona is an image taken by the SOHO C2 coronagraph.

Two large polar coronal holes are detected at the Sun, one at the north pole and the other at the south pole. It is noted that HSSs of ~750 to 800 km/s are detected at Ulysses when over the polar coronal hole regions. When Ulysses was near the solar equatorial region where helmet streamers

are present, the solar wind speeds are of the slow solar wind variety, Vsw ~ 400 km/s. The reader should note that it took years for Ulysses to make this polar orbit while the solar and coronal images were taken at one point in time. However this composite figure is useful to illustrate the main points about the origins of HSSs.

3.2.2 High speed solar wind streams and the formation of CIRs

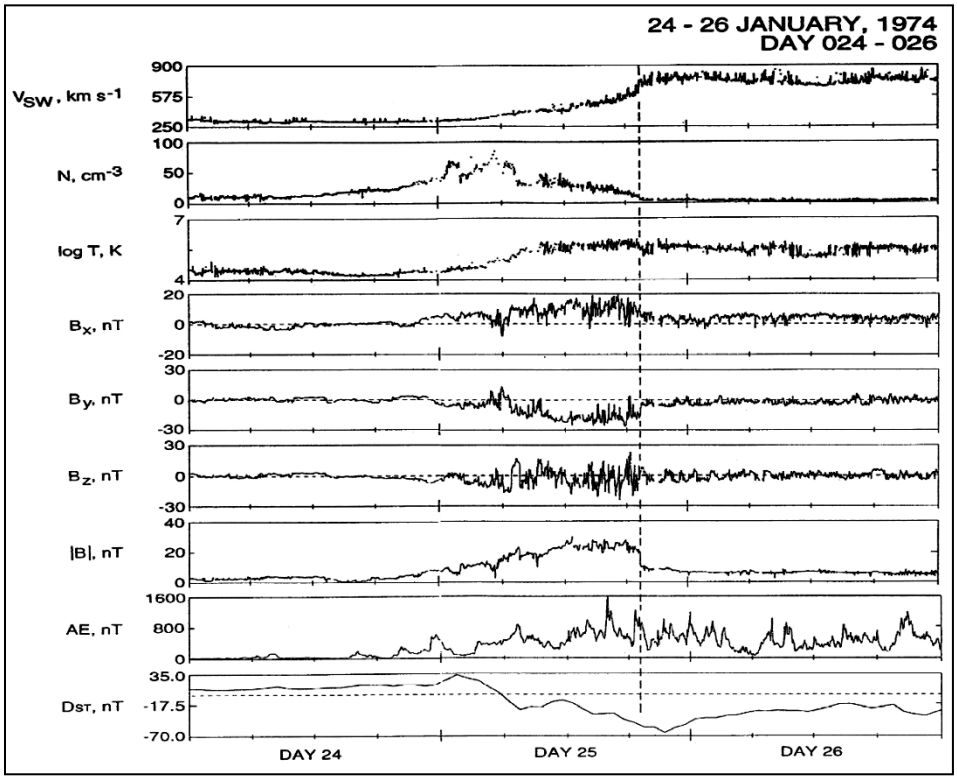

Figure 9. A high speed solar wind stream-slow solar wind interaction and the formation of a CIR during January 1974. The format is the same as in Figure 4 except that the AE index is given in the next to bottom panel. The figure is taken from Tsurutani et al. (2006b).

Figure 9 shows a HSS-slow speed stream interaction during January 1974. The right portion of the top panel on day 26 shows a HSS with speeds of 750-800 km/s at 1 AU. On day 24, the top panel left indicates a solar wind speed of ~300 km/s, or the slow solar wind. The effects of the stream-stream interaction occurs on day 25. This is best seen in the IMF magnitude panel, 7th from the top. The stream-stream interaction creates intense magnetic fields of ~25 nT. The 6th from the top panel is the IMF Bz component (in GSM coordinates). The Bz is highly fluctuating. Magnetic

reconnection between the IMF southward components and the magnetopause magnetic fields leads to the irregularly shaped storm main phase shown in the bottom (Dst) panel.

To be able to forecast a CIR magnetic storm, one would have to first understand the sources of the IMF Bz fields. For example are they compressed upstream Alfvén waves (Tsurutani et al. 1995, 2006c)? Or could they be waves generated by the shock interaction with upstream waves in the slow solar wind? That would be only the first step for forecasting, of course. Then with knowledge of the properties of the slow speed stream, the details of the wave compression/interaction would then have to be calculated/modeled.

Another approach would be to determine if there is an underlying southward component of the IMF within the CIR. This would most likely be caused by the geometry of the HSS-slow speed stream interaction and may be predictable from MHD modeling. If this is correct, then the wave fluctuations can be modeled as being superposed on top of these DC magnetic fields. In (rare) cases of radial alignment, Solar Probe closest to the Sun could characterize sheath fields. The evolution of those fields would be detected by Solar Orbiter. Simulation of further evolution could be applied and predictions of the fields at 1 AU could be tested by ACE data. If there are waves generated by the shock, then the above scenario would not work as well as expected, or at least would be more complicated to apply in a useful manner.

3.2.3. High speed solar wind streams, Alfvén waves and HILDCAAs

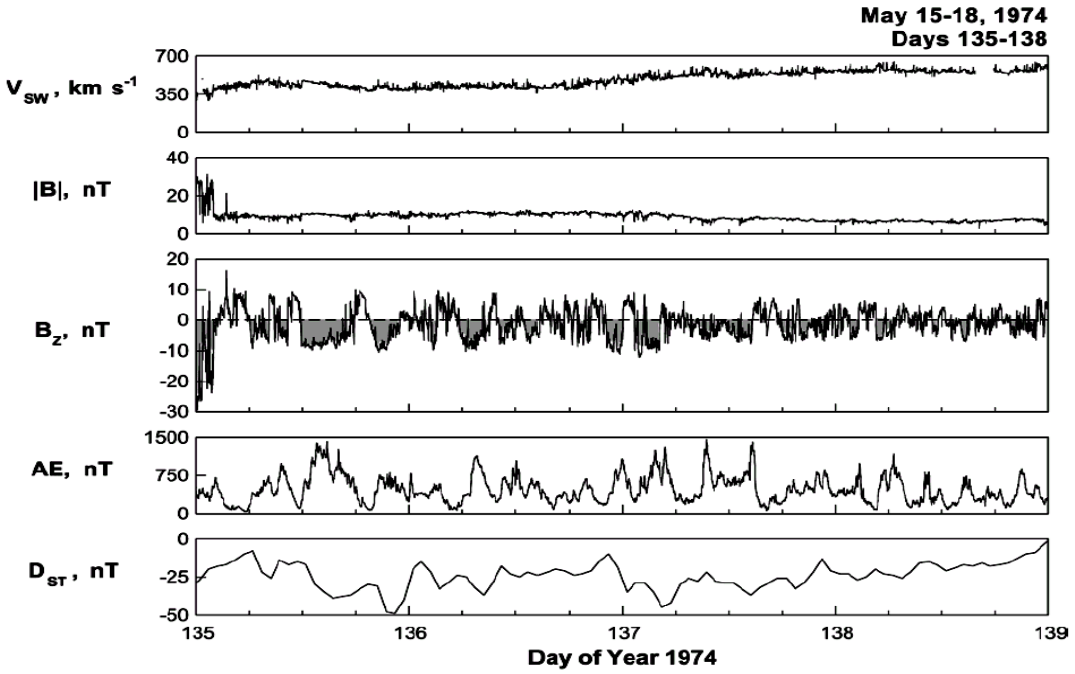

Figure 10. A high-intensity, long-duration continuous AE activity (HILDCAA) event during 1974. Taken from Tsurutani et al. (2006c).

The schematic in Figure 6 showed a long "recovery phase" that trails the CIR magnetic storm main phase (see Tsurutani and Gonzalez, 1987). However we now know that the storm wasn't "recovering" as in the case of an MC magnetic storm recovery but that something else was occurring. This "recovery" can last from days to weeks. Thus processes of charge exchange, Coulomb collisions, etc. for ring current particle losses are not tenable to explain such long "recoveries".

Figure 10 shows the interplanetary cause of this extended geomagnetic activity. It occurs primarily during HSSs independent of whether a CIR magnetic storm occurred prior to it or not (Tsurutani and Gonzalez, 1987; Tsurutani et al., 1995, 2006b; Kozyra et al. 2006b; Turner et al. 2006; Hajra et al. 2013, 2014a, 2014b, 2014c, 2017). From top to bottom are the solar wind speed, the IMF magnitude, the IMF Bz component (in GSM coordinates) and the auroral electrojet (AE) index. The bottom panel is the Dst index.

The interplanetary data were taken from the IMP-8 spacecraft, an Earth orbiting satellite that was located upstream of the magnetosphere in the solar wind at this time. The location was inside 40 Re, where an Re is an Earth radius. The magnetic Bz fluctuations have been shown to be Alfvén waves which are of large nonlinear amplitudes in HSSs (Belcher and Davis, 1971; Tsurutani and Gonzalez, 1987; Tsurutani et al., 2018b). What is apparent from this figure is that every time the IMF Bz is negative (southward), there is an AE increase and a Dst decrease. This has been interpreted as being due to magnetic reconnection between the southward components of the Alfvén waves and the Earth magnetopause. The AE is enhanced by the same magnetic reconnection process that occurs during substorms, and a small parcel of plasmasheet plasma is injected into the nightside magnetosphere causing the Dst index to decrease slightly. It is noted that there are many southward IMF Bz dips in this four day interval of data shown in Figure 10. There are also many corresponding AE increases and Dst decreases. Thus the interpretation of the constant/average Dst value of ~ -25 nT for four days is that continuous plasma injection and decay is occurring. This is clearly not a "recovery phase" where the ring current particles are simply lost, it only appears as a recovery from the Dst trace. Soraas et al. (2004) have shown that particles are injected during these events but only to L values of 4 and greater (The L =4 magnetic field line is the dipole magnetic field that crosses the magnetic equator a distance 4 Earth radii from the center of the Earth). These are shallow injections as suggested above.

These geomagnetic activity events have been named High-Intensity, Long-Duration Continuous AE events or HILDCAAs (Tsurutani and Gonzalez, 1987). This name is simply a description of the events without an interpretation. In 2004 when a detailed examination using Polar EUV auroral imaging was applied, it was found that many phenomena besides simple isolated substorms occurred (Guarnieri, 2006; Guarnieri et al., 2006). Although substorms occur during HILDCAA events, there are AE increases (injection events?) that are not well-correlated with substorm onsets (Tsurutani et al., 2004b). The full extent of HILCAAs is not well understood (see also Souza et al., 2016, 2018; Mendes et al., 2017). By using IMAGE auroral observations and geomagnetic indices to identify convection events which are not classical Akasofu (1964) substorms, the fields and particle data from SWARM, MMS and Arase could be used to characterize the physics properties of these "convection" events.

600 There is also the question of the origin of the interplanetary Alfvén waves? Do they originate at
601 the Sun caused by supergranular circulation, or is that mechanism untenable as argued by Hollweg
602 (2006)? Could the waves be generated locally between the Sun and Earth as speculated by Matteini
603 et al. (2006, 2007) and Hellinger and Travnicek (2008)? Parker Solar Probe could identify Alfvén
604 waves within high speed streams and Solar Orbiter (when radially aligned) could determine the
605 wave evolution.
606
607 The original requirement for identifying a HILCAA event was quite strict. The event had to occur
608 outside of a magnetic storm main phase (Dst was required to be > -50 nT: Gonzalez et al. 1994),
609 the peak AE intensity had to be greater than 1,000 nT (high-intensity), the event had to last longer
610 than 2 days (long-duration), and there could not be any dips in AE less than 200 nT for longer than
611 two hours (continuous). Clearly there are events with the same interplanetary causes and
612 geomagnetic effects as for the strict definition. However the strict definition is useful for further
613 studies using different data sets.
614
615 **3.2.4. HILDCAAs and the Acceleration of Relativistic Magnetospheric Electrons**

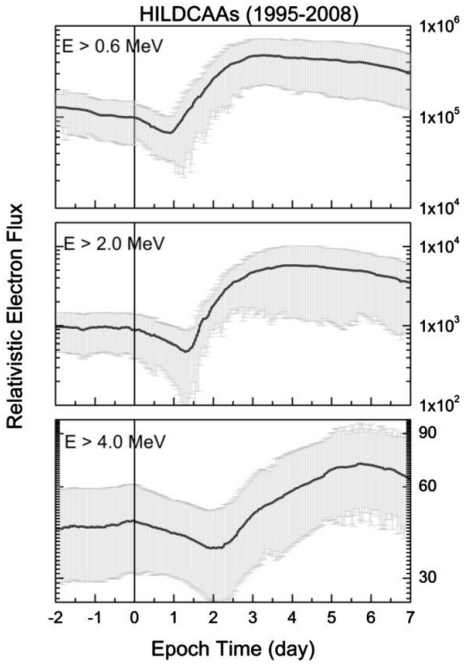

616
617 Figure 11. The relationship between HILDCAAs and relativistic electron acceleration. The figure
618 is taken from Hajra et al. (2015a).
619

One of the consequences of HSSs and HILDCAAs is the acceleration of relativistic (~MeV) electrons. These energetic particles can damage orbiting satellite electronic components (Wrenn, 1995), and thus are known as "killer electrons". Figure 11 shows the relationship between the onset of HILCAA events (vertical line) and relativistic electron fluxes. From top to bottom are the E > 0.6 MeV, the E > 2.0 MeV and the E > 4.0 MeV electron fluxes detected by the GOES-8 and GOES-12 satellites located at L = 6.6. This figure is a superposed epoch analysis (Chree, 1913) result of 35 HILDCAA events in solar cycle 23, from 1995 to 2008, which are not preceded by magnetic storms. This was done to avoid contamination by storm-time particle acceleration (by intense convection/compression). The zero epoch time (vertical line) corresponds to the HILDCAA onset time. Here the "strict" definition of HILDCAAs was used to define the onset times.

The figure shows that the flux enhancement of E > 0.6 MeV electrons is statistically delayed by ~1.0 day from the onset of the HILDCAAs. The E > 4.0 MeV electrons are statistically delayed by ~2.0 days from the HILDCAA onset. It is thus possible that HILCAAs may be used to forecast relativistic electron flux enhancements in the magnetosphere (see Hajra et al., 2015b; Tsurutani et al., 2016a; Hajra and Tsurutani, 2018a; Guarnieri et al., 2018). This however has not been done yet and could be implemented by scientists today.

The physics for electron acceleration to relativistic (~MeV) energies has been well-developed by magnetospheric scientists. Two competing acceleration mechanisms have been developed. In one mechanism, with each injection of plasmasheet particles on the nightside magnetosphere, the anisotropic ~10 to 100 keV electrons generate electromagnetic whistler mode chorus waves (Tsurutani and Smith, 1974; Meredith et al. 2002) by the loss cone/temperature anisotropy instability (Brice, 1964; Kennel and Petschek, 1966; Tsurutani et al., 1979; Tsurutani and Lakhina, 1997). The chorus then interacts with the ~100 keV injected electrons to energize them to ~0.6 MeV energies (Inan et al., 1978; Horne and Thorne, 1998; Thorne et al., 2005, 2013; Summers et al., 2007; Tsurutani et al., 2010; Reeves et al., 2013; Boyd et al., 2014). The lower-frequency part of the chorus in turn interact with the ~0.6 MeV electrons to accelerate them to ~2.0 MeV energies, etc. This bootstrapping mechanism has been suggested by several authors (Baker et al., 1979,

1998; Li et al., 2005; Turner and Li, 2008; Boyd et al., 2014, 2016; Reeves et al., 2016) and has been confirmed by Hajra et al. (2015a) during HILDCAA events.

An alternative scenario is that relativistic electrons are created through particle radial diffusion driven by micropulsations (Elkington et al., 1999, 2003; Hudson et al., 1999; Li et al., 2001, O'Brien et al., 2001; Mann et al.,2004; Miyoshi et al., 2004). However the same general scenario would hold as for chorus acceleration. The substorms and convection events within HILDCAAs would be the sources for the micropulsations and the micropulsations would last from days to weeks in duration. Bootstrapping of energy would still take place.

A few important questions for researchers to ask are: "How high can the relativistic magnetospheric electron energy get?". If there are two HSSs, one from the south pole and another from the north pole so that Earth's magnetosphere is bathed in HSSs for years, as happened during 1973-1975 (Sheeley et al., 1976, 1977; Gosling et al. 1976; Tsurutani et al. 1995), will the energies go above ~10 MeV? What will physically limit the energy range? This answer is important for keeping Earth-orbiting satellites safe during such events.

3.2.5. Solar wind ram pressure pulses and the loss of relativistic electrons

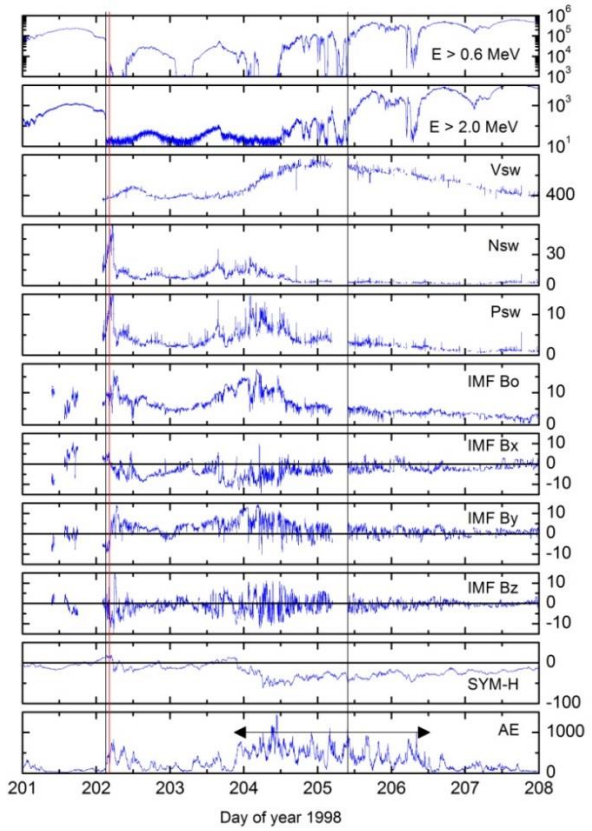

Figure 12. A relativistic electron decrease (RED) event and later acceleration. Taken from Tsurutani et al. (2016b).

Figure 12 shows a relativistic electron decrease (RED) event occurring during 1998. From top to bottom are the E > 0.6 MeV electron fluxes, the E > 2.0 MeV electron fluxes, the solar wind speed, density and ram pressure, and the IMF magnitude, Bx, By and Bz component in the GSM coordinate system. The bottom two panels are the 1 min SYM-H index (a high time resolution Dst index) and the AE index. The relativistic electron measurements were taken at L = 6.6.

At the beginning of day 202, a vertical black line indicates the onset of a high density HPS crossing (Winterhalter et al., 1994) that is identified in the fourth panel from the top. The HPS is by definition located adjacent to the HCS (Smith et al. 1978). The HCS is noted by the reversal in the signs of the IMF Bx and By components (seventh and eighth panels from the top). The onset of the HPS is followed within one hour by the vertical red line, the sudden disappearance of the E > 0.6 MeV (first panel) and E > 2.0 MeV (second panel) relativistic electron fluxes. Tsurutani et al.

(2016b) has shown that for 8 relativistic electron flux disappearance events during solar cycle 23 all of the disappearances were associated with HPS impingements onto the magnetosphere.

Where have the relativistic electrons gone? There are two primary possibilities. One is that the energetic electrons have gradient drifted out of the magnetosphere through the dayside magnetopause, a feature that has been called "magnetopause shadowing" by West et al. (1972). However a second possible mechanism is electron pitch angle scattering by electromagnetic ion cyclotron (EMIC) waves. We think that this second possibility is more intriguing and has far more interesting consequences, if correct. One might ask where the EMIC waves come from and why is pitch angle scattering particularly important? It has been shown by Remya et al. (2015) that when the magnetosphere is compressed, both electromagnetic chorus (electron) waves (Thorne et al., 1974; Tsurutani and Smith, 1974; Meredith et al. 2002) and EMIC (ion) waves (Cornwall, 1965; Kennel and Petschek, 1966; Olsen and Lee, 1983; Anderson and Hamilton, 1993; Engebretson et al., 2002; Halford et al. 2010; Usanova, 2012; Saikin, 2016) are generated. The compression of the magnetosphere causes betatron acceleration of remnant ~10 to 100 keV electrons and protons, and thus plasma instabilities associated with both particle populations occur. What is particularly important is that the EMIC waves are coherent (Remya et al., 2015), leading to extremely rapid pitch angle scattering of ~ 1 MeV electrons by the waves. The scattering rate has been shown to be three orders of magnitude faster than that with incoherent waves (Tsurutani et al., 2016b).

Another possible loss mechanism is associated with possible generation of PC waves by the HPS impingement followed by radial diffusion of the relativistic electrons. Wygant et al. (1998) and Halford et al. (2015) have mentioned that larger loss cone sizes at lower L could be a source of loss to the ionosphere. Rae et al. (2018) has shown that superposition of compressional PC waves and the conservation of the first two adiabatic invariants could enhance particle losses. However one should mention that there are not observations of PC wave generation during HPS impingements and this needs to be tested. It is also uncertain how rapidly the relativistic electrons would be lost by the above processes. It has been shown that the total loss of L >6.6 relativistic electrons occurs in ~1 hour (Tsurutani et al., 2016b).

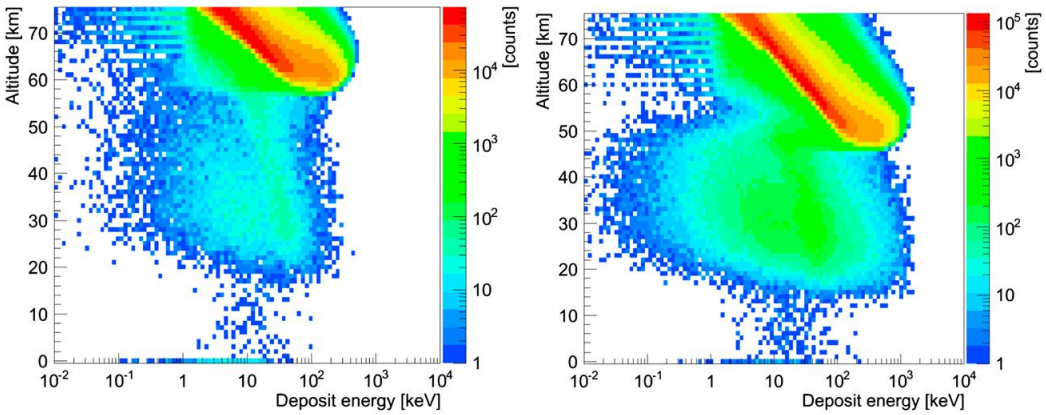

Figure 13. The GEANT4 code run results for the precipitation of E > 0.6 MeV electrons (left panel) and E > 2.0 MeV electrons (right panel). The vertical scale is altitude above the ground and the horizontal scale is energy deposition. The color scheme (legend on the right) gives the amount of counts. Taken from Tsurutani et al. (2016b).

Why can the loss of relativistic electrons to the atmosphere be important? Figure 13 shows the results of the GEometry ANd Tracking 4 (GEANT4) code developed by the European Organization for Nuclear Research (Agostinelli et al., 2003) applied to the relativistic electron disappearance problem. The GEANT4 code takes into account Rayleigh scattering, Compton scattering, photon absorption, gamma ray pair production, multiple scattering, ionization, bremsstrahlung for electrons and positrons and annihilation of positrons (positron formation is not germane for these "low energy" relativistic particles, but the code includes it anyway). A standard atmosphere was used.

Figure 13 shows the GEANT4 Monte Carlo results for the electron shower for E > 0.6 MeV electrons on the left and for E > 2.0 MeV electrons on the right. Two important features should be noticed. First the bulk of energy deposition (the red areas) descends down to ~60 km for the E > 0.6 MeV electron simulation and down to ~50 km for the E > 2.0 MeV electron simulation. This portion of the energy from the incident electrons is due to direct ionization and particle energy cascading. However there is a second region which might be extremely important. That is the blue-green area that goes down to ~20 km for the E > 0.6 MeV simulation and ~16 km for the E > 2.0 MeV simulation. There are also "hits" seen on the ground. This lower altitude energy deposition is due to the relativistic electrons interacting with atmospheric atomic and molecular

nuclei creating bremsstrahlung X-rays and γ-rays. X-rays and γ-rays have very large mean free paths and thus can freely propagate through the dense atmosphere without interactions. They propagate to much lower altitudes where they interact and continue the energy cascading process further.

The reason why this process may be quite an important Space Weather topic is that it might relate to atmospheric weather as well. Wilcox et al. (1973) discovered a correlation between interplanetary HCS crossings and high atmospheric vorticity winds at 300 mb altitude. Over the years a number of different explanations for the physics of the trigger has been offered (Tinsley and Deen, 1991; Lam et al., 2013). Tsurutani et al. (2016b) presented the above relativistic electron precipitation scenario (instead of HCS crossings) for the possible triggers of high atmospheric vorticity winds. Quantitative estimates of potential energy deposition at different atmospheric altitudes were provided in the original paper.

It is noted that the energy deposition should occur in a limited spatial region of the globe (just inside the auroral zone and a small region of the dayside atmosphere) which is more geoeffective than either cosmic ray energy or solar flare particle deposition. The fact that it is relativistic electron precipitation gives an additional advantage that substantial energy is deposited at quite low altitudes.

Advances to this problem can be made in a number of different ways. Simultaneous ground-detected EMIC waves, γ-rays and atmospheric heating/cooling could be sought. Correlation with such events with solar wind pressure pulses like the HPSs or interplanetary shocks (see Hajra and Tsurutani, 2018b) would advance our knowledge of the details of such events.

Atmospheric heating events known as Sudden Stratospheric Warmings (SSWs) (Scherhag, 1960; Harada et al., 2010) occur at subauroral latitudes by unknown causes. They are known to be related to atmospheric wind system changes, perhaps the same phenomenon as the Wilcox et al. (1973) effect. Atmospheric scientists generally assume that SSWs are created by gravity waves propagating from lower atmosphere upward, but so far no one-to-one correlated case has been found. Thus it would be quite interesting to see if Space Weather can have a major impact on

768 atmospheric weather. The connection between these two disciplines could be quite interesting for
769 the next generation of Space Weather scientists.
770
771 **3.2.6. Energetic particle precipitation and ozone depletion**
772

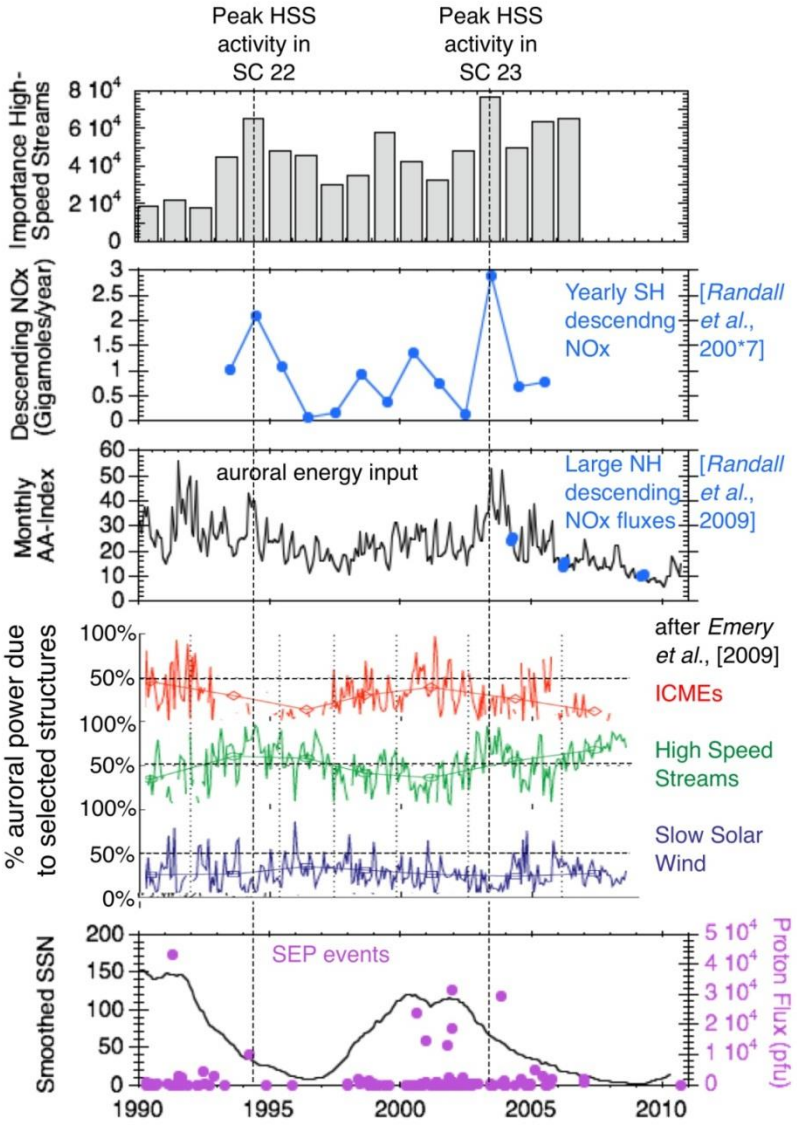

773
774 Figure 14. The dashed vertical lines show the peaks in solar wind high speed streams during SC
775 22 and SC23. These are coincident with the peaks in auroral energy input and the peaks in yearly
776 NOx descent. The authors thank J.U. Kozyra for providing this unpublished figure.
777

Figure 14 shows two solar cycles of data, SC22 and SC23. From top to bottom are the "importance" of high speed streams, the descending NOx, the monthly AA index, the percent auroral power due to three types of solar wind phenomena (ICMEs, HSSs and slow solar wind), and the bottom panel solid line trace is the sunspot number (SSN). Also shown in the bottom panel is the solar energetic particle (SEP) flux.

There are two vertical dashed lines. They correspond to the peaks in HSS activity for SC22 and SC23 (top panel), peaks in auroral energy input (third panel from the top), and peaks in the yearly descending NOx (second panel from the top). It is noted that all three peaks are aligned in time. The bottom panel shows that both dashed vertical lines correspond to times in the descending phase of the solar cycle.

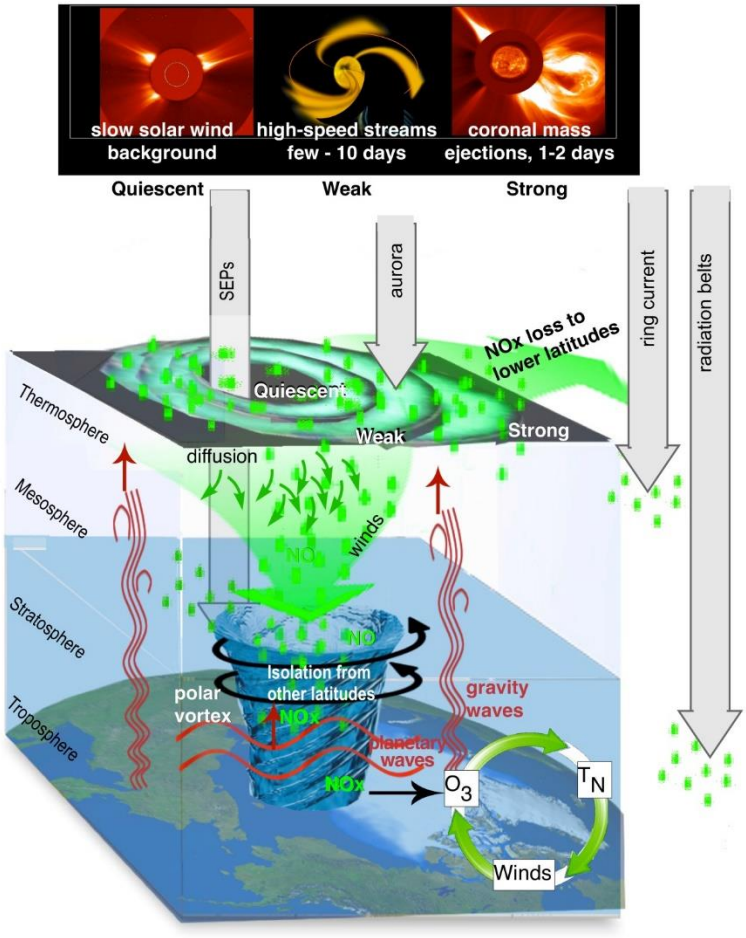

Figure 15. The scenario for polar cap ozone destruction using the observations shown in Figure 14. The authors thank J.U. Kozyra and her colleagues (personal communication, 2019) for this unpublished figure.

Figure 15 shows the Kozyra et al. (2019) scenario for ozone destruction over the polar cap. The top of the Figure shows the various types of solar wind (and associated energetic particles) that can affect atmospheric ozone. The quiet solar wind will lead to quiescence. HSSs lasting a few to ten days have weak effects and ICMEs (and of course shock acceleration of energy particles) can have much stronger effects.

Energetic particles from different sources will precipitate in different regions of the ionosphere. The energetic particles associated with interplanetary CME shock acceleration will be deposited in the polar regions of the both the north and south ionospheres. If the particles are energetic enough with sufficient gyroradii, they can reach to as low latitudes as ~50° magnetic latitude. Precipitating substorm/HILDCAA ~10-100 keV magnetospheric charged particles will deposit their energy on closed auroral zone (~60° to 70°) magnetic field lines.

The energetic particle entering the atmosphere lose a portion of their energy in the dissociation of N^2 into N + N. The nitrogen atoms will attach to oxygen atoms to form NOx. Auroral HILDCAA ~10 -100 kev energy particles will only penetrate to depths of ~75 km above the surface of the Earth. Solar energetic particles with greater kinetic energies can penetrate lower into the atmosphere to ~50 to 60 km. If there is a polar vortex, this vortex can "entrain" the NOx molecules and atmospheric diffusion can bring them down to lower altitudes over months time duration. The NOx can act as a catalyst in the destruction of ozone.

One interesting consequence of extreme ICME shocks is that one would expect extreme Mach numbers to lead to both extreme SEP fluences and also extremely high energies. The former will lead to greater production of NOx at the polar regions and the latter to deeper penetration and thus less loss of NOx as they diffuse downward. Alternatively there is a scenario where radiation belt "killer" relativistic electrons can play an important role. If there are large solar polar coronal holes like in 1973-1975, HSSs could produce extremely intense and energetic relativistic electrons.

Shocks and HPS impingements on the magnetosphere could cause loss of the electrons to the lower atmosphere. This magnetospheric energy pumping and dumping may have important consequences for NOx production. The topic of shock acceleration of energetic particles will be discussed in more details in Section 4.1.

4.0. RESULTS: Interplanetary Shocks

4.1. Interplanetary Shocks and Energetic Charged Particle Acceleration

Interplanetary shocks have a variety of effects both in interplanetary space and to the Earth's magnetosphere. It is important for the reader to note that these Space Weather phenomena can occur with or without the occurrence of magnetic storms. Shock and magnetic storm intensities are related but only in a loose sense. The physical mechanism for energy transfer for different phenomena is different. As one example, interplanetary shock acceleration of energetic charged particles (called "solar cosmic rays") are due to an ICME ram energy driving the fast shocks which then transfers energy to the charged particles. Solar cosmic ray events can occur with or without magnetic storms (Halford et al. 2015, 2016; Mays et al., 2015; Foster et al. 2015). Some of the major extreme Space Weather topics will be addressed below.

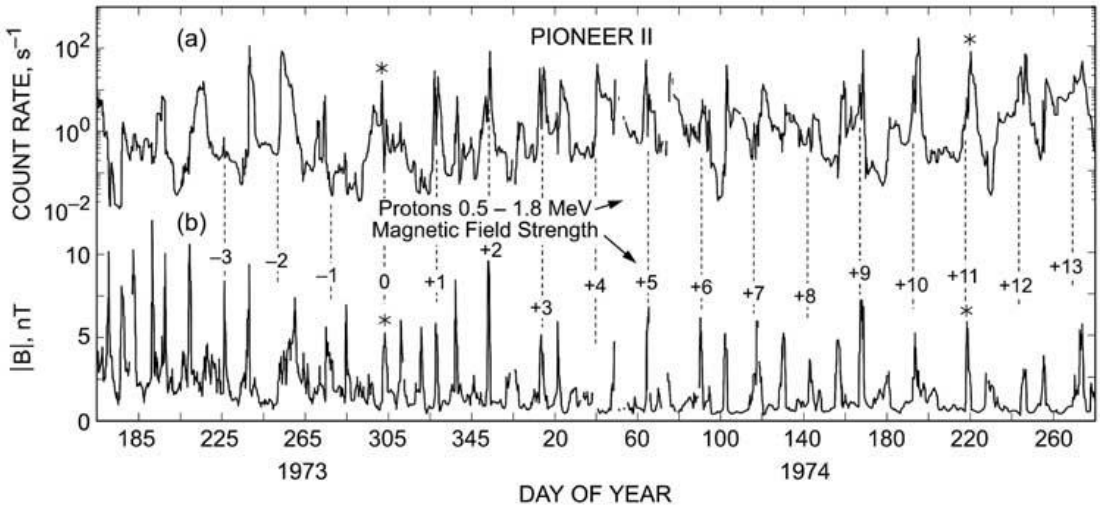

Figure 16. Energetic ~0.5 to 1.8 MeV protons accelerated by interplanetary fast forward and fast reverse shocks. Taken from Tsurutani et al. (1982).

Acceleration of energetic particles in deep space was discovered by Pioneer 11 energetic particle scientists (McDonald et al., 1976; Barnes and Simpson, 1976; Pesses et al., 1978, 1979; Van Hollebeke et al., 1978; Christon and Simpson, 1979). As the Pioneer 11 spacecraft traveled away from the Sun, it was found that the particle fluences kept increasing, contrary to the concept of adiabatic deceleration. The interplanetary magnetic field magnitude decreases with increasing distance from the Sun, so one would expect energetic particle deceleration with distance. Thus it was clear to scientists that something must be accelerating these particles in the interplanetary medium. Figure 16 shows one channel of the Pioneer 11 energetic proton count rate, ~0.5 to 1.8 MeV (see Simpson et al., 1974). The bottom panel is the Pioneer 11 magnetic field (Smith et al., 1975). Some of the peak magnetic fields are numbered, corresponding to a ~25 day recurrence of these magnetic structures. The magnetic magnitude structures are identified as well-developed CIRs (see Smith and Wolfe, 1976), bounded by fast forward and fast reverse shocks.

Tsurutani et al. (1982) identified the shocks and showed statistically that both forward and reverse shocks were related to proton peak count rates. One of the results, which still remains to be solved, is that the proton peaks were generally higher at the reverse shocks. What is the mechanism for greater particle acceleration at fast reverse shocks? This has received little attention and should be addressed in the future.

Reames (1999) has argued that fast forward shocks upstream (anti-solarward) of ICMEs are the most important phenomenon for the acceleration of "solar flare" particle events. Particle acceleration occurs throughout interplanetary space from near the Sun (where the shocks first form) to 1 AU and beyond as the shocks propagate through the heliosphere. Studies of this acceleration as a function of longitudinal distance away from magnetic connection to the flare site (this gives the variations in the shock normal angle and thus dominant mechanism for acceleration—see Lee (2017) and references therein) have been done by Lario (2012). The features of the energetic particles in space have different characteristics depending on these distances and the portion and characteristics of the shock that the particles are being accelerated from.

Forecasting the solar flare/interplanetary shock features such as the fluence, energy, spectra and composition will require knowledge of the upstream seed population, upstream (and downstream) waves, and shock properties such as the magnetosonic Mach number and shock normal angle. This is a very difficult task since knowledge of the entire slow solar wind plasma from the Sun to 1 AU will be required for accurate forecasting. But again, the Parker Solar Probe and Solar Orbiter may help in developing two points of measurements for modeling of specific events.

A more fundamental problem is why measured interplanetary fast forward shock Mach numbers at 1 AU are so low? As previously mentioned, Tsurutani and Lin (1985) from ISEE-3 measurements have found that at 1 AU, the measured magnetosonic Mach numbers were typically only 1 to 3. Tsurutani et al (2014) have identified a shock with Mach number ~9 and Riley et al. (2016) has identified an event with magnetosonic Mach number ~28. The latter event was associated with the SOHO 2012 extreme ICME which did not impact the Earth's magnetosphere. The above are extreme events and little or no events have been detected with intermediate values. A study that is needed is to determine shock Mach numbers at different distances from the Sun. These will give clues as to why 1 AU shock Mach numbers are so low. Is the acceleration of energetic particles causing the dissipation of shock energy as they propagate from the Sun to 1 AU? Data from Parker Solar Probe, Solar Orbiter and ACE could be useful in this regard.

In a related issue, the use of STEREO imaging and MHD modeling could be useful to determine the mass loading of ICME sheaths in causing the deceleration of the ICMEs. This deceleration will also lower the Mach number of the shocks.

4.2. Extreme Interplanetary Shocks and Extreme Interplanetary Energetic Particle Acceleration

Tsurutani and Lakhina (2014) have shown from simple calculations that for CMEs have extreme speeds of 3,000 km/s (Yashiro et al., 2004; Gopalswamy, 2011), shock Mach numbers of ~45 are possible. These Mach numbers are getting close to expected supernova shock values. Why haven't such strong shocks been observed at 1 AU? If such events are possible, what would the energetic particle fluences be? Experts on shock particle acceleration will hopefully answer this complex

question. It is well known that such solar flare particles enter the polar regions of the Earth's atmosphere and cause radio blackouts. Will extreme solar flare particle fluence precipitation cause different ionospheric effects other than those known today? This latter question might be addressed by ionospheric modelers.

It should be noted that although Space Weather is a chain of events/phenomena going from the Sun to interplanetary space to the magnetosphere, ionosphere and atmosphere, there is often not a direct link between different facets of Space Weather. Each feature of Space Weather should be examined separately and it should not be assumed that an extreme flare will cause extreme cascading Space Weather phenomena. We use solar flare particles as an example for the reader. The largest solar flare particle event in the space age occurred in August 1972 (Dryer et al., 1976 and references therein). However there was no magnetic storm caused by the MC impact onto the Earth's magnetosphere (the MC field was directed almost entirely northward, leading to geomagnetic quiet: Tsurutani et al. 1992b). On the other hand, the largest magnetic storm on record is the "Carrington" storm. The storm intensity will be discussed further in Section 7.0. There is little or no evidence of large solar flare particle fluences in Greenland ice core data from that event (Wolff et al., 2012; Schrijver et al., 2012). Usoskin and Kovfaltsov (2012) examining historical proxy data (^{14}C and ^{10}Be) also find a lack of any signature associated with the Carrington flare. Although this is an extreme example, it is useful to mention it to illustrate the point: different facets of Space Weather may have only loose correlations with other facets.

An area that has received a lot of attention lately is ancient solar flares. Miyake et al. (2012) discovered an anomalous 12% rapid increase in ^{14}C content from 774 to 775 AD in Japanese cedar tree rings. Usoskin et al. (2013) have argued that such an extreme radiation event could be associated with an extreme solar energetic particle event (or a sequence of events). The latter authors estimated that the fluence of > 30 MeV particles was ~4.5×10^{10} cm^{-2}. Could such an extreme particle event be associated with an extremely strong interplanetary shock or instead series of strong shocks? Space Weather scientists are currently working on this problem.

4.3. Interplanetary shocks, dayside aurora and nightside substorms

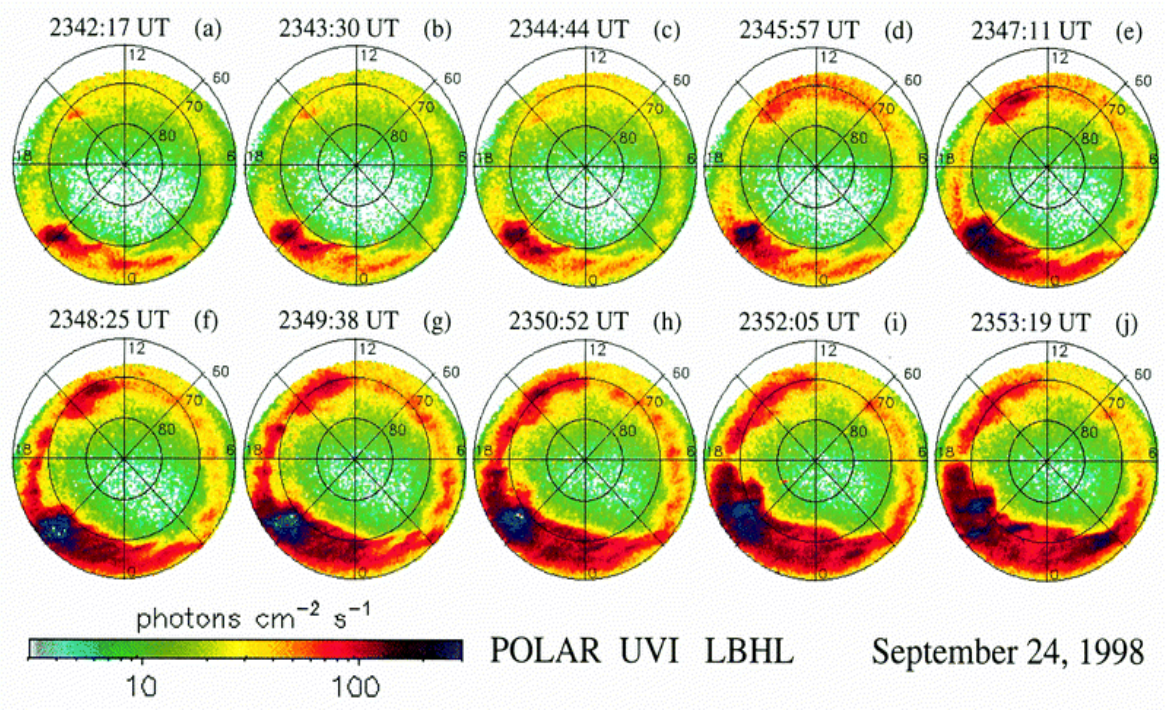

Figure 17. Interplanetary shocks cause dayside auroras and trigger nightside substorms. The images show the northern polar views of polar cap and auroral zones taken in UV wavelengths. Local noon is at the top in each image. The Figure is taken from Zhou and Tsurutani (2001).

Interplanetary shocks can trigger the precipitation of energetic ~10 to 100 keV electrons into the auroral ionosphere (Halford et al. 2015). In fact, low energy (E < 10 keV) electron precipitation can occur as well. Figure 17 shows interplanetary shock impingement auroral UV effects for an event on September 23, 1998. Each image has the north pole at the center and 60° magnetic latitude (MLAT) shown at the outer edge. Noon is at the top and dawn is at the right. The cadence between images is ~1min 13 s. From ACE measurements and propagation calculations it is known that the fast forward shock arrived the magnetosphere between the images c), 2344:44 UT and d), 2345:47 UT. What is apparent in panel d) is the sudden appearance of aurora on the dayside (Zhou and Tsurutani et al., 1999). From further analyses of these shock auroral events, Zhou et al. (2003) have shown that magnetospheric compression of preexisting ~10 to 100 keV electrons and protons will generate both electromagnetic electron and proton plasma waves and diffuse auroras (as discussed previously). Also noted were the generation of field-aligned dayside currents. Compression of the magnetosphere will generate Alfvén waves (Haerendel, 1994) which will

propagate along the magnetic field lines down to the ionosphere. Wave damping could provide substantial ionospheric heating.

The mechanism for energy transfer from the solar wind to the magnetosphere is the absorption of the solar wind ram energy. Dayside auroras occur with shock impingement irrespective of the interplanetary magnetic field Bz direction. Another possible mechanism for the dayside aurora not mentioned above are double layers above the ionosphere (Carlson et al., 1998) with the acceleration of ~1 to10 keV electrons and the formation of discrete dayside auroras. What is the relative importance of these three different auroral energy mechanisms? This would be an excellent topic for the SWARM and Arase satellite missions. Coordinated ground measurements would be useful.

Returning back to Figure 17 panel e) 2347:11UT, there is a substorm intensification centered at ~2100 magnetic local time (MLT). The substorm further intensification and expansion can be noted in the sequence of images. Interplanetary shock triggering of substorms has been known to occur before the advent of imaging polar orbiting spacecraft (Heppner, 1955; Akasofu and Chao, 1980). The AE index had been used to identify these events.

An important fundamental question for substorm physics that has existed for a long time, is where in the tail/magnetosphere does the substorm get initiated and by what physical mechanism? Is it reconnection or plasma instabilities (Akasofu, 1972; Hones, 1979; Lui et al., 1991; Lui, 1996; Baker et al., 1996; Lakhina, 2000)? Where does the energy come from, recent percurser solar wind inputs as suggested by Zhou and Tsurutani (1999), or stored tail energy or even possibly solar wind ram energy (see Hajra and Tsurutani, 2018b)? The rapid response of the magnetosphere to the shock should limit the downstream location of the substorm initiation point. It should be noted that there are probably several different mechanisms for causing substorms. Although this is only the shock triggering case, knowledge of this may help understand other cases, if they are indeed different. The MMS mission will be ideally suited for addressing this question in the tail phase of the mission.

4.4. Interplanetary shocks and the formation of new radiation belts

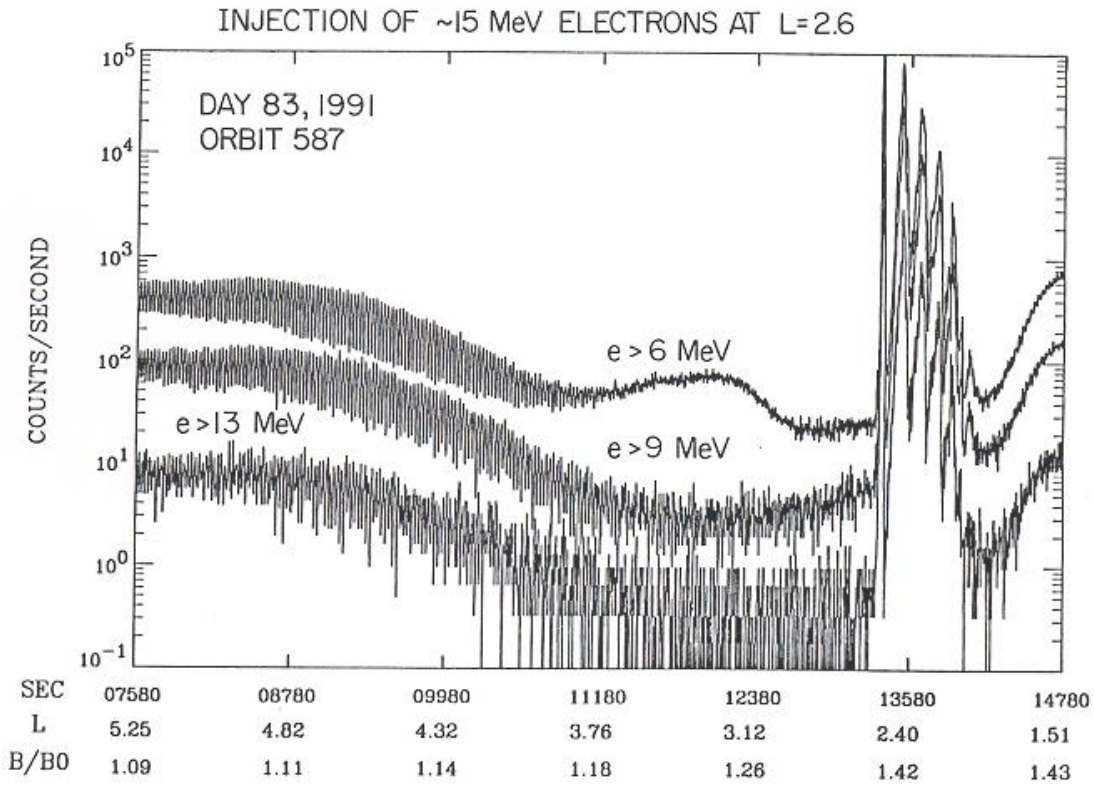

Figure 18. Shock creation of a new relativistic electron radiation belt in the magnetosphere. The three energy channel plots show an abrupt increase in flux at the same time. Recurrence of the flux with decreasing amplitude occurs at least 4 more times. Figure taken from Blake et al. (1992).

Figure 18 shows evidence of a new "radiation belt" triggered by a strong interplanetary shock. The Figure shows three traces, E > 6 MeV, > 9 MeV and > 13 MeV fluences. At the time of the strong and sudden increase in all energy fluxes, the spacecraft was at L = 2.6. This is time-coincident with the shock impingement upon the magnetosphere (not shown). With increasing time, a second, then third, etc., electron flux pulse appear. These are "drift echoes" where the energetic electron "cloud" have gradient drifted around the magnetosphere to return to the satellite location once again.

4.4.1. What is the mechanism to create this new radiation belt?

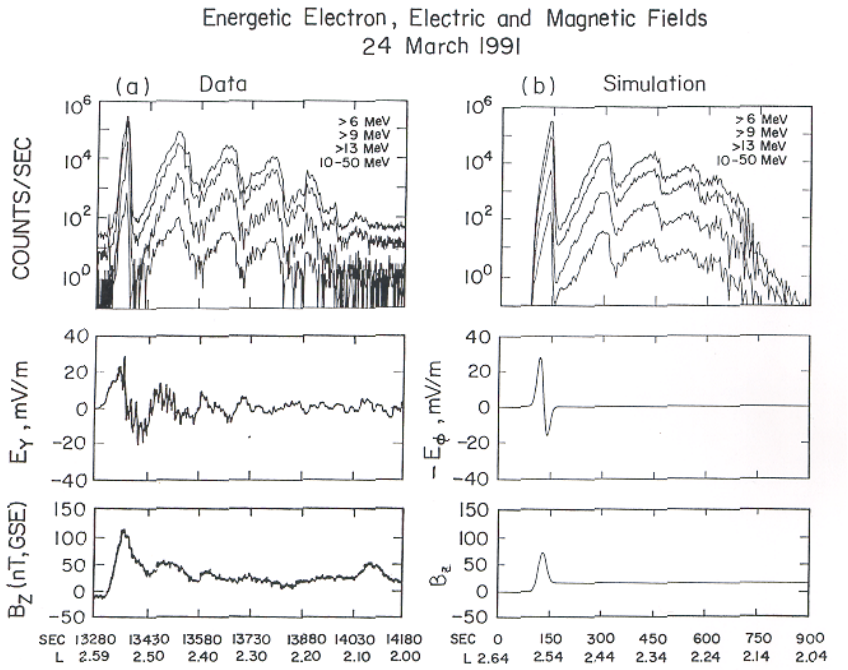

Figure 19. An expanded version of the relativistic electron pulse and measured magnetospheric electric field and magnetic field Bz on the left and simulation results on the right. Taken from Li et al. (1993).

The left hand column of Figure 19 shows an expanded version of Figure 16 on the top with the addition of the ~10 to 50 MeV count rate channel included. Next is the d.c. electric field in the Y direction, and magnetospheric Bz on the bottom. The right hand column bottom shows a magnetic pulse input into the system. This generates a time varying azimuthal electric field (right middle) and the relativistic electron flux at the top right.

Using the input of a single magnetospheric magnetic pulse into the magnetosphere, Li et al. (1993) simulated the acceleration and injection of E > 40 MeV electrons. What is interesting is that the origin of the electrons was L > 6 with energies of only a few MeV. The reader should read Li et al. (1993) for more details concerning the simulation and results. Related works on acceleration of magnetospheric electrons by shock impact on the magnetosphere can be found in Wygant et al. (1994), Kellerman and Shprits, 2012; Kellerman et al., 2014; Foster et al. (2015).

How strong was the interplanetary shock? There were not any spacecraft upstream of the Earth at the time of the event, so no measurements of shock strength can be made. However Araki (2014) has noted that this shock caused a SI^+ of magnitude 202 nT. This is the second largest SI^+ in recorded history. In Tsurutani and Lakhina (2014) with the assumption of a 3,000 km/s CME and only a 10% deceleration from the Sun to 1 AU, they estimated a maximum SI^+ of 234 nT under normal conditions. Could this 1991 shock strength have been close to the M =45 estimate mentioned earlier? One cannot really tell for sure because the shock Mach number strongly depends on the upstream plasma conditions, which can only be estimated in this case.

Tsurutani and Lakhina (2014) estimated a dB/dt six times larger than the one used in the Li et al. (1993) modeling. What would a maximum dB/dt cause in a new radiation belt formation? How much greater could the relativistic electron energy and flux become?

5.0. RESULTS: Solar Flares and Ionospheric Total Electron Content

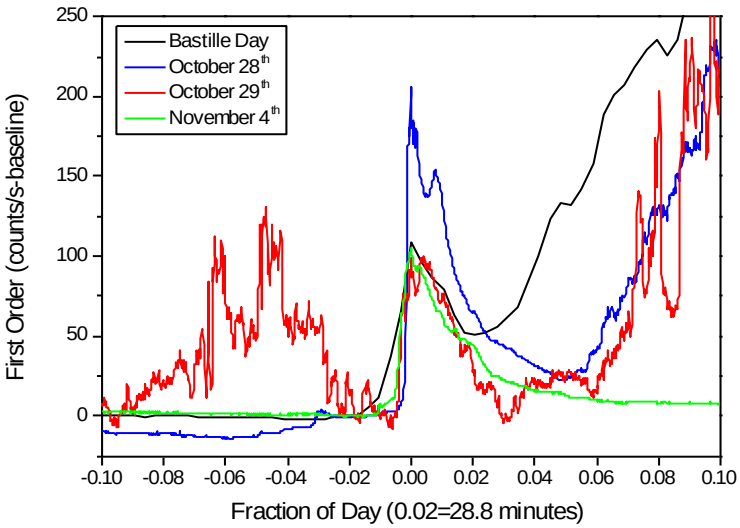

Figure 20. The largest solar EUV flare in recorded history, October 28, 2003. Taken from Tsurutani et al. (2005b).

Figure 20 shows four well-known solar X-ray flare events taken in a narrow band 26-34 nm EUV spectrum. The four flare events are the Bastille day (July 14, 2000) flare and three "Halloween" flares occurring on October 28, 29 and November 4, 2003. The narrow band EUV spectrum is shown because some of the flare X-ray and EUV fluxes were so intense that most spacecraft detectors became saturated (all except the SOHO SEM narrowband EUV detector). The X-ray flare intensities could only be estimated from fitting techniques for the saturated data. Here we use the narrow band channel of the SOHO SEM detector where the four above mentioned flares were not saturated. The four flare count rate profiles were aligned so that they start at time zero. What is particularly remarkable is that the October 28, 2003 flare has the highest EUV peak intensity of all four events and was greater by a factor of ~2. This is the most intense EUV solar flare in recorded history.

After each flare reached a peak intensity and then decreased in count rate, there was often a following increase in count rate. This is particularly notable in the Bastille day (black trace) flare. This increase is contamination due to delayed energetic electrons propagating through space along interplanetary magnetic field lines reaching the spacecraft later in time. The November 4 flare (green) did not have such contamination because it was a limb flare and presumably (magnetic) connection from the flare site to the spacecraft did not occur.

NOAA personnel have estimated the November 4 flare had an intensity of ~X28. This event saturated the detector so this is a conservative estimate. Thomson et al. (2004) using a different technique estimated a value of X45 for this event. NOAA has estimated that the October 28 flare as ~X17. However in EUV fluxes, the October 28 flare was the most intense by far.

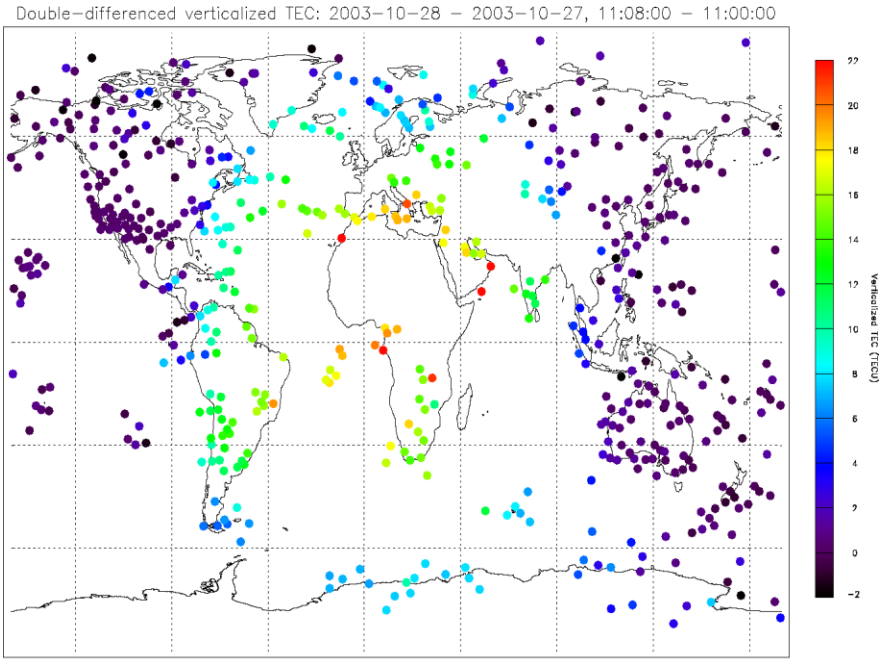

Figure 21. The global TEC during the October 28, 2003 solar flare. The scale is given on the right. The figure is taken from Tsurutani et al. (2005b).

Figure 21 shows the global total electron content (TEC) in the ionosphere after the October 28, 2003 solar flare. The map has been adjusted so Africa, the subsolar point, is in the center of the Figure. The top and bottom of the plot correspond to the Earth's polar regions and the left side and right side edges local midnight. The enhanced TEC area corresponds to the sunlit hemisphere. At the subsolar point the TEC enhancement was ~30%. This is the record for flare-induced ionospheric TEC (Tsurutani et al., 2005b). The nightside hemisphere shows no TEC enhancement, as expected. The TEC enhancement is due to ionization by X-rays, EUV photons and UV photons, all part of the solar flare spectrum.

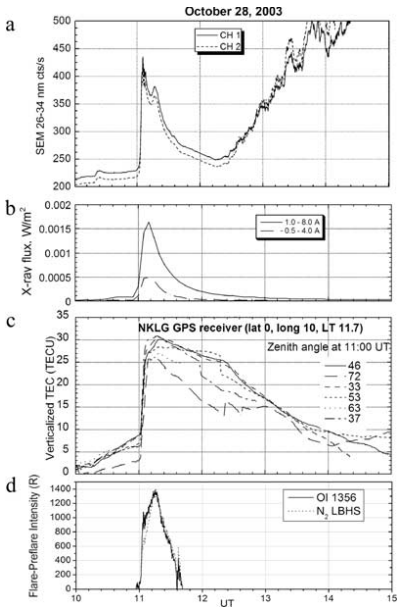

Figure 22. The ionospheric and atmospheric effects of the October 28, 2003 solar flare.

Figure 22 shows the effects of the October 28 solar flare. From top to bottom are the SOHO SEM EUV count rate, the GOES X-ray flux, the Libreville, Gabon TEC data and the GUVI O and N^2 dayglow data. It is noted that the flare profiles in EUV and X-rays last ~tens of mins and are similar in profile to each other. However the TEC over Libreville last hours. This is due to the EUV portion of the solar flare. These photons deposit their energy at ~170 to 220 km altitude where the recombination time scales are ~ 3 to 4 hours. Thus EUV photon ionization has longer lasting ionospheric TEC effects. The X-ray portion of the solar flare spectrum deposit their energy in the ~80 to 100 km altitude range where the recombination time scale is tens of min (Thomson et al., 2005, and references therein). This solar flare example is one where solar energy goes directly from the Sun to the Earth's ionosphere. There is no transfer of energy to interplanetary space and then to the magnetosphere.

Some future Space Weather problems are to understand if the solar flare photon spectrum varies often and why this happens? We have indicated that the 28 October 2003 and the 4 November 2003 flares were significantly different spectra-wise. The question is why and how often does this happen? Ionospheric satellites like the Constellation Observing System for Meteorology, Ionosphere and Climate-2 (COSMIC II) and SWARM can probe for detailed altitude dependence of ionization to work backwards to attempt to identify what spectrum would cause the layered

ionization detected. Solar flare data taken by instrumentation onboard the SORCE and TIMED spacecraft would be useful to understand the details of flare spectral differences but solar physicists are needed to explain what the causes are. Other questions are how large can X-ray and EUV flares become? What will their ionospheric effects be?

6.0. RESULTS: Magnetic Storms and Prompt Penetrating Electric Fields (PPEFs)

For substorms, PPEFs occurring in the ionosphere have been known for a long time, since the beginning of the space age (Nishida and Jacobs, 1962; Obayashi, 1967; Nishida, 1968; Kelley et al. 1979, 2003). In the last 10 years lots of work has been done on PPEFs during magnetic storms. Why didn't people look at storms earlier? Because it was theoretically predicted that the PPEFs would be shielded out. Why doesn't shielding happen? This is a very good question for workers in the field. Right now we don't know the answer.

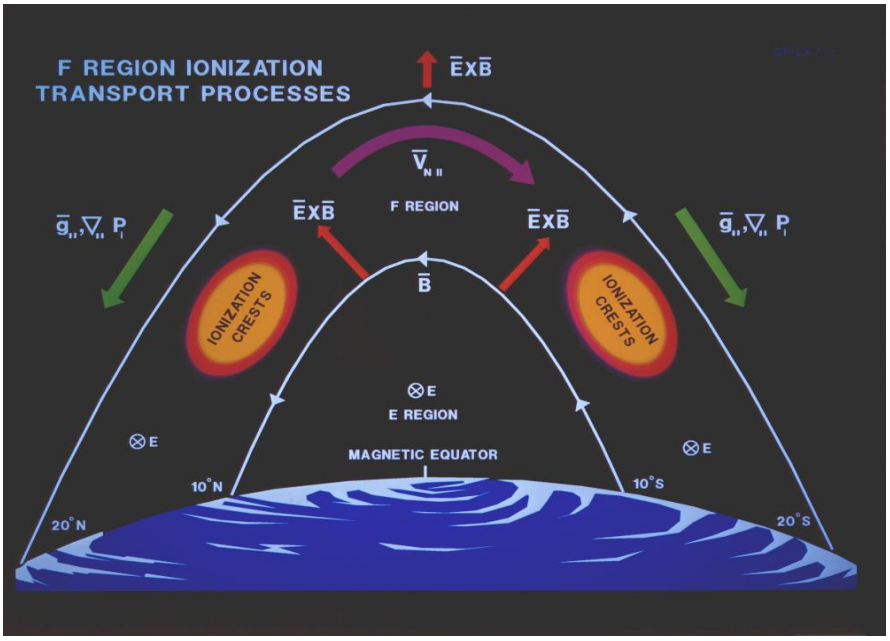

Figure 23. Dayside (near) equatorial ionization anomalies (EIAs) located ~± 10° on both sides of the magnetic equator. The local Earth magnetic field is shown in this schematic. The figure is taken from Anderson et al. (1996).

Figure 23 show the geometry of the Earth's magnetic field near the magnetic equator. It is parallel to the Earth's surface at the equator but where the equatorial ionization anomalies (EIAs) are located, the magnetic field is slanted. The EIAs are standardly located at ~±10° MLAT in the dayside ionosphere. With red arrows, the figure also shows the direction of E x B convection. At exactly the magnetic equator, E x B is in a purely upward direction. At the positions of the EIAs, the E x B direction is both upward and to higher absolute magnetic latitudes.

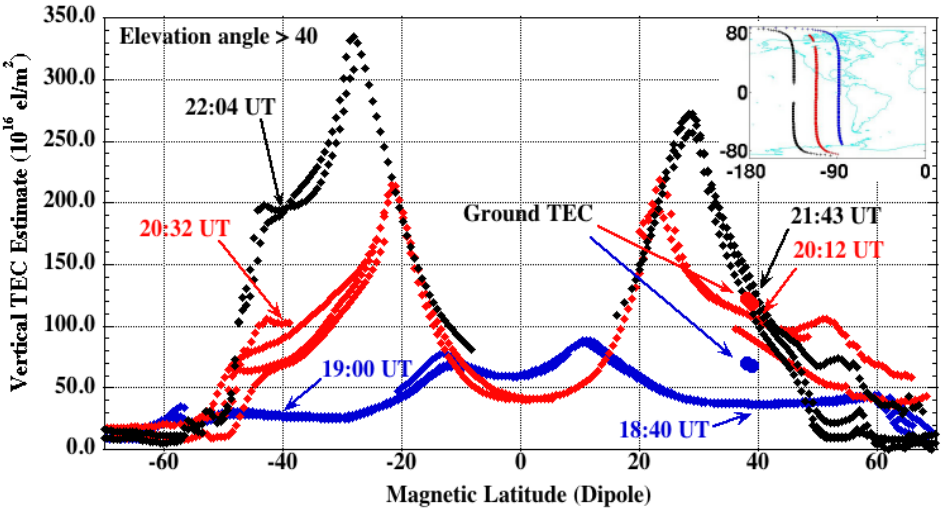

Figure 24. Three passes of the CHAMP satellite measuring the near equatorial and midlatitude TEC during October 30, 2003. CHAMP was at an altitude of ~430 km, so the TEC measured was the total thermal electron column density above that altitude. The figure is taken from Mannucci et al. (2005).

Figure 24 shows three passes of the CHAMP satellite in polar orbit with an altitude of ~430 km at the near equatorial crossings. The three orbits are given in the upper right hand portion of the Figure. The first TEC trace shown in blue is before the onset of the October 30-31 magnetic storm. The two EIAs are identified by the TEC enhancements at ~ ±10° with peak intensities of ~80 TEC units. In the next pass (red trace), the EIAs are located at ~ ±21° MLAT and the peak intensities are ~ 210 TEC units. During the next satellite pass, the EIAs are located near ±30° and the TEC values become as high as ~330 TEC units. This "movement" of the EIAs to higher magnetic

latitudes can be explained by a convective electric field (PPEF) in the east-west direction causing an uplift to both EIAs by E x B convection as explained earlier associated with Figure 23. One might ask why does the TEC increase to such high values?

The answer is as the PPEF removes the plasma from the ionospheric lower F region and brings it to higher altitudes where the recombination time scale is longer (hours), the Sun's EUV photons replace the plasma by photoionization of the upper atmosphere, replacing the lost plasma and thus increasing the "total electron content" of the ionosphere. This is one cause of a "positive ionospheric storm".

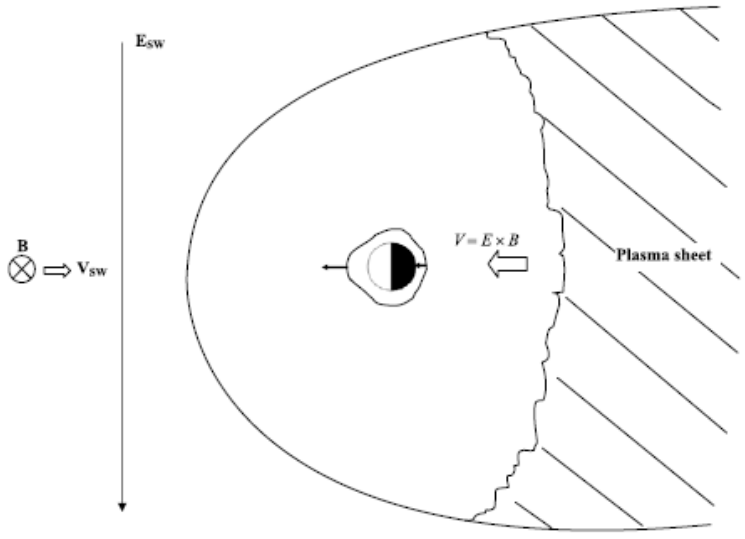

Figure 25. The interplanetary, magnetospheric and equatorial ionospheric electric fields during a PPEF event. The Figure is taken from Tsurutani et al. (2004c; 2008b).

Figure 25 shows the interplanetary motional electric field for southward interplanetary Bz. The electric field will be in the dawn-to-dusk direction. When magnetic reconnection takes place in the nightside plasmasheet, the convective electric field will be in the same direction but with a reduced amplitude. This electric field brings the plasmasheet plasma into the nightside low L region magnetosphere during magnetic storms. The PPEFs penetrate into the dayside equatorial ionosphere (shown in Figure 24) and also the nightside equatorial ionosphere. However significantly different from the dayside case, the E x B convection on the nightside will bring the ionospheric plasma to lower altitudes, leading to recombination and reduction in TEC. This is one

form of a "negative ionospheric storm". See Mannucci et al. (2005, 2008) for discussions of positive and negative ionospheric storms.

There are many important questions about PPEFs which are almost always present during major magnetic storms. As previously mentioned, "why aren't the electric fields shielded out?" What is the mechanism for generating PPEFs, wave propagation from the polar ionosphere as suggested by Kikuchi and Hashimoto (2016) or a more global picture as Figure 25 and Nishida and Jacobs (1962) suggest? Figure 25 is a simple schematic. What are the real local time dependences of the PPEF? Does this vary from storm to storm, and if so, why? Why does the relative PPEF magnitude vary from one storm to the next? Again future spacecraft and ground based studies will be able to help answer these questions.

7.0 RESULTS: The Carrington Storm

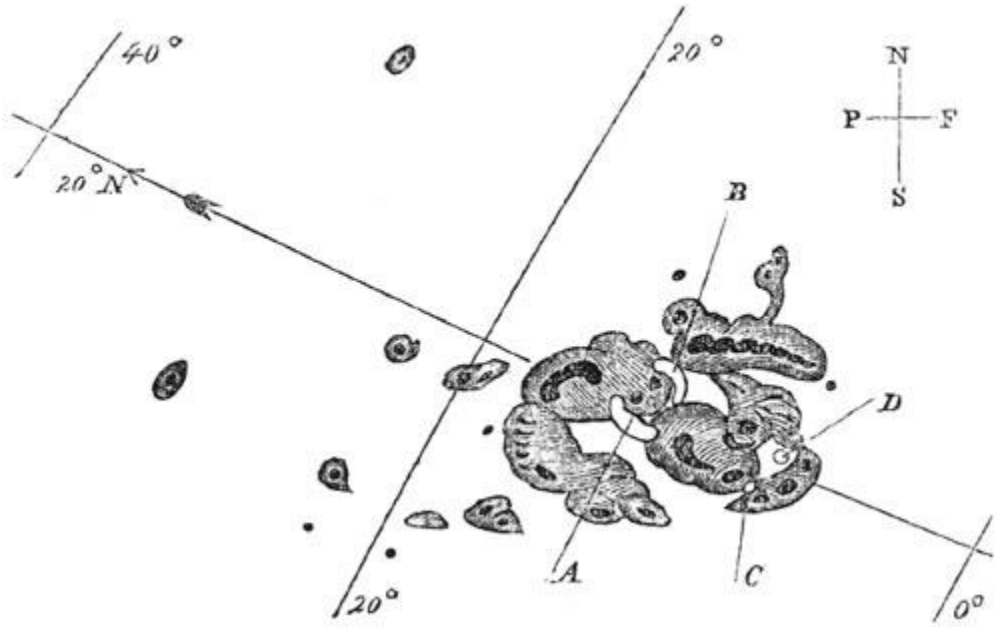

Figure 26. The solar active region during the Carrington 1 September 1859 optical solar flare. The figure is taken from Carrington (1859).

Figure 26 is the active region (AR) that was hand-drawn by Richard Carrington. This was the source of the optical solar flare that he and Hodgson (1859) saw and reported on 1 September

1859. See Cliver (2006) for a nice accounting of the observational activity taken during 1859 flare interval and Kimball (1960) for an accounting of the aurora during the storm. The optical part of the flare lasted only ~ 5 min. Some ~17 hr 40 min later a magnetic storm occurred at Earth (Carrington, 1859).

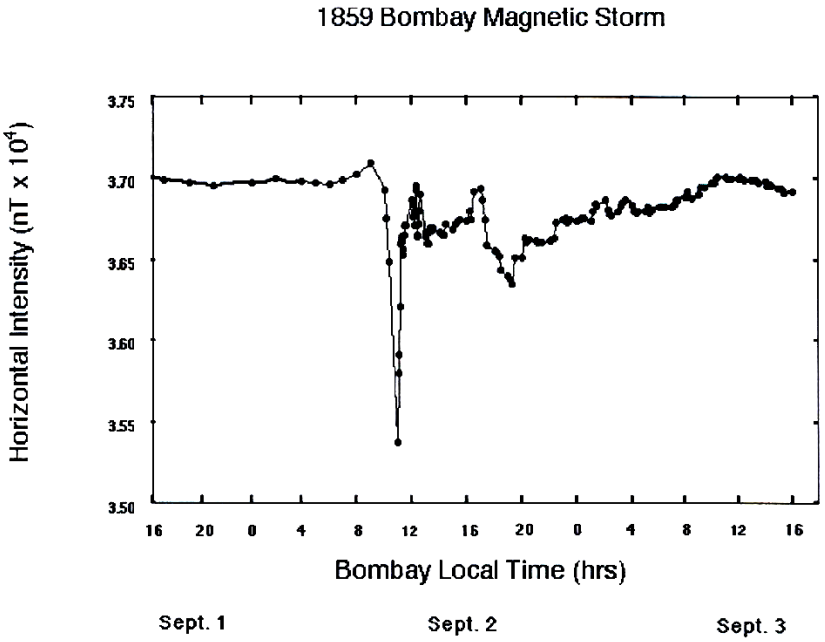

Figure 27. The Carrington storm detected in the Colaba, India magnetometer. The Figure is taken from Tsurutani et al. 2003 and Lakhina et al. 2012.

Figure 27 shows the H-component magnetic field taken by the Colaba magnetic observatory during the "Carrington" magnetic storm. The SI^+ is estimated to be ~ 110 nT and the magnetic decrease ~1600 nT at Colaba (Mumbai, India). The SI^+ and storm main phase has been recently shown to be most likely caused by an upstream solar wind density of 5 particles cm^{-3} and a MC with intensity ~90 nT (pointed totally southward) by Tsurutani et al. (2018a). No particularly unusual solar wind conditions are believed to have been necessary (in contrast to the original conclusions of Ngwira et al., 2014). Ngwira et al. (2018) is now in accord with this more recent assessment of a normal upstream solar wind.

The intensity of the "Carrington" storm was estimated as Dst =-1760 nT (Tsurutani et al., 2003) based on observations of the lowest latitude of red auroras being at ±23° (Kimball, 1960). The

storm intensity was calculated using recent theoretical expressions of magnetospheric potentials needed to convect plasma into such low latitudes. Siscoe (1979) basing his estimate on a model that treats the pressure as a constant along the magnetic flux tube came up with a value of Dst = -2000 nT.

It should be mentioned that some researchers have taken exception with the Colaba magnetogram as an indication of ring current effects (see Comment by Akasofu and Kamide (2005) and Reply by Tsurutani et al. (2005a)). The Colaba magnetic profile is unlike those of ICME magnetic storms discussed in Sections 2.3, 2.4 and 3.1 of this paper. Several researchers have estimated the storm intensity based on the Colaba magnetogram (see articles in a special journal edited by Clauer and Siscoe, 2006; Acero et al. 2018). The Colaba data clearly show that the storm had exceptionally large geomagnetic effects, irregardless of the interpretation of the Colaba data. Possible interpretations of the Colaba profile will be discussed later in the paper.

The most accurate method of estimating a magnetic storm intensity is by using the latitude of the aurora. Red auroras (Stable Auroral Red or SAR arcs) are presumably an indication of the location of the plasmapause (R.M. Thorne, private communication, 2002). Kimball (1960) noted that "red glows" were detected at ±23° from the geomagnetic equator during the Carrington event. In 1960 the term "SAR arc" was not in use, but we can assume that this was what he was reporting. At the present time, this is the most equatorward SAR arcs that have been observed (thus the most intense magnetic storm). That is until researchers find records of even lower latitude red auroras!

Comments on the short duration of the recovery phase has been made by Li et al. (2006). A high density filament was used to explain this unusual feature of the magnetic storm profile. Tsurutani et al. (2018a) have recently proposed another possibility. During extreme events when the storm time convection brings the plasmasheet into very low L, all of the standard ring current loss process rates will be enhanced. There will be greater Coulomb scattering, greater charge exchange loss rates and greater plasma wave growth with consequential greater wave-particle pitch angle scattering and losses to the atmosphere. In Tsurutani et al. (2018a) the authors focused particularly on wave-particle interactions because the size of the loss cone will increase dramatically with decreasing L. This, plus greater energetic particle compression due to the extreme inward

convection, will lead to stronger loss cone/temperature anisotropy instabilities, greater wave growth and thus greater losses. This hypothesis can be easily tested by magnetospheric spacecraft observations during large magnetic storms and by magnetospheric modeling perhaps bringing some light to the unusual Colaba magnetic signature.

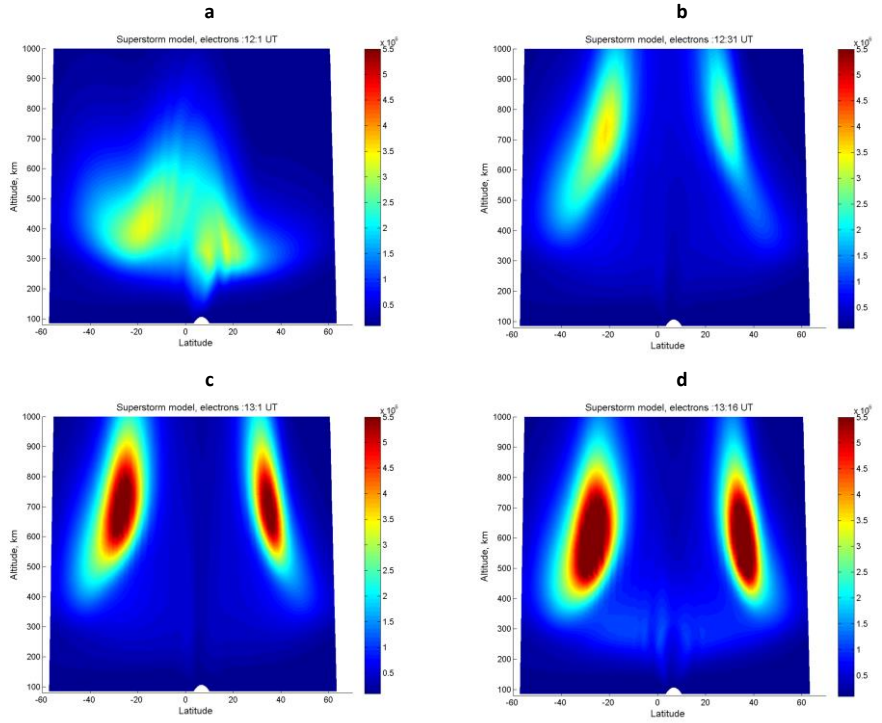

Figure 28. A model of the PPEF effects of the Carrington 1859 storm on the dayside ionosphere. The input electric field was taken from Tsurutani et al. (2003) and the simulation was performed using the Huba et al. (2000, 2002) SAMI2 code. The figure is taken from Tsurutani et al. (2012).

7.1. The Carrington PPEF

One of the concerns for extreme Space Weather in the ionosphere are extremely intense PPEFs and the daytime superfountain effect on the uplift of O^+ ions (positive ionospheric storms). Higher ion densities in the exosphere will lead to the possibility of enhanced low altitude satellite drag. In Tsurutani et al. (2003), the authors used modern theories of the electric magnetospheric potential given by Volland (1973), Stern (1975) and Nishida (1978) to determine the electric field during

the Carrington storm main phase. The former authors obtained an estimate of ~20 mV/m. They then applied this electric field in the SAMI2 model with the results shown in Figure 28.

Figure 28 shows the SAMI2 results of the modeled dayside ionosphere with a ~20 mV/m added to the diurnal variation electric field. The quiet ionosphere is shown at the upper left. The uplift of the O^+ ions both in altitude and MLAT after ~30 min is given on the upper right panel. The maximum time that the electric field was applied was 1 hr. The ionosphere at that time is shown on the lower left. The storm time equatorial ionospheric anomalies (EIAs) are located at |MLAT| ~30° to 40° and an altitude of ~550 to 900 km for the most dense portion of the EIAs. The bottom right panel shows that the EIAs have come down in altitude but to higher latitudes ~15 min after the termination of the PPEF application. Parts of the still intense EIAs are now beyond |MLAT| > 40° and now the bulk of the maximum density portion is at ~400 to 800 km altitude.

It was found that at altitudes of ~700 to 1,000 km, the O^+ densities are predicted to be ~300 times that of the quiet time neutral densities. It has been also been shown by Tsurutani and Lakhina (2014) that in extreme cases, the magnetospheric/ionospheric electric field can be twice as large as the Carrington storm and six times as large as the 1991 event. Even if the magnetospheric radiation belt is saturated (there are other scientific papers that state that magnetospheric beta can be greater than one: Chan et al. 1994; Saitoh et al. 2014; Nishiura et al., 2015), this is a different facet of Space Weather and the electric field may not be saturated. What will be the ionospheric effects of these even larger electric fields?

A fundamental question for the future is "can the upward O^+ ion flow drag sufficient numbers of oxygen neutrals upward so that the oxygen ions plus neutral densities are even higher still?" A short time interval analytic calculation done by Lakhina and Tsurutani (2017) and a mini-Carrington event modeled by Deng et al. (2018) have indicated that the answer is "yes". However a full code needs to be developed and run to answer this question quantitatively. This is an interesting future problem for computer modelers.

8.0 RESULTS: Supersubstorms

Super intense substorms (supersubstorms: SSSs) appear to be externally (solar wind) triggered. Why are they important? They might be the feature within extreme magnetic storms that cause geomagnetically induced currents (GICs)/power outages. This hypothesis needs to be tested.

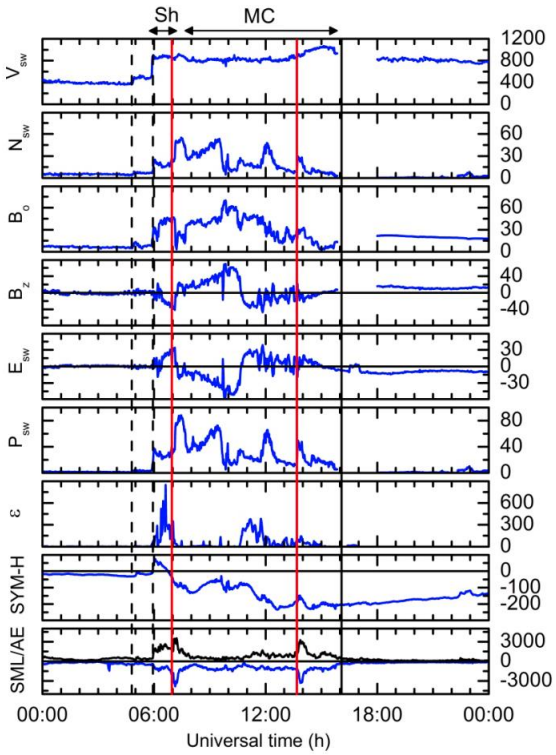

Figure 29. Two supersubstorms (SSSs) that occur during a two-phase magnetic storm on 20 November 2001. The onsets of the supersubstorms are indicated by the vertical red lines. The figure is taken from Tsurutani et al. (2015).

Figure 29 shows the solar wind data during an intense magnetic storm and two SSSs. From top to bottom are the solar wind speed and density, the magnetic field magnitude and Bz component, and the interplanetary motional electric field, ram pressure and Akasofu epsilon parameter (Perreault and Akasofu, 1978). The bottom two parameters are the SYM-H index and the SML index (blue) and AE index (black). An initial forward shock is indicated by a vertical dashed line at ~0500 UT, a second shock at ~0600 UT, and the two SSS onsets by red vertical lines. The criterion for a SSS event was a SML peak value < -2500 nT (an arbitrary number, but chosen to be an extremely high value). At the top of the diagram, the sheath region is indicated by a "Sh" and the magnetic cloud region by "MC". The first storm main phase is caused by southward Bz in the sheath and the

second, more intense main phase by southward Bz in the MC. The interplanetary magnetic field measurement cadence is 1 min. It has been noted that the magnetosphere typically reacts to southward Bz with durations > 10 to 15 min (Tsurutani et al., 1990), so this high rate of cadence is sufficient to identify any causes of geomagnetic response.

It is noted that the SSS events in this case are not triggered at either of the two shocks nor do they occur during the peak negative SYM-H values of the storm main phases. However the first SSS event is collocated with a peak Esw and a peak southward Bz of the sheath plasma. The SSS event is also collocated with a large solar wind pressure pulse which is caused by an intense solar wind density feature. The second SSS event occurred in the recovery phase of the second magnetic storm. The IMF Bz was ~0 nT. The second SSS event was associated with a solar wind pressure pulse associated with a small density enhancement.

A study of SSSs from 1981 to 2012 was conducted by Hajra et al. (2016). In that study a variety of solar wind features were found to be associated with SSS onsets. In that survey it was noted that two SSS events were triggered by fast forward shocks. One of these events will be discussed below.

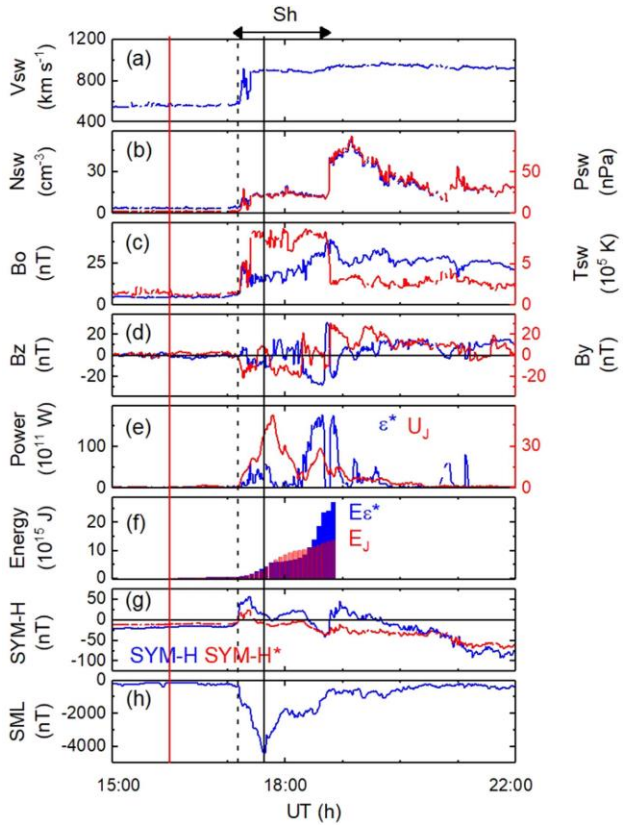

Figure 30. A SSS triggered by an interplanetary shock on 21 January 2005. The dashed vertical line indicates a fast forward shock and the solid black line the peak intensity of the SSS event. The figure is taken from Hajra and Tsurutani (2018b).

Figure 30 shows solar wind/interplanetary parameters and geomagnetic parameters during a SSS event on 21 January 2005. From top to bottom are the solar wind speed, density and ram pressure, the magnetic field magnitude and solar wind temperature (in the same panel), the IMF Bz and By components (GSM coordinates), Joule energy and the Akasofu epsilon pressure corrected parameter ε*, the time-integrated energy input into the magnetosphere and time-integrated joule energy. The next to the bottom panel contains the SYM-H index and the pressure corrected SYM-H index (SYM-H*). The bottom panel is the SML index. A dashed vertical line denotes the occurrence of a fast forward shock. A vertical solid line indicates the peak of the SSS event.

The SSS event onset at 1711 UT coincided with a shock with magnetosonic Mach number of ~5.5 with a shock normal angle of 81°. The high density sheath sunward of the shock causes a SI^+ of ~57 nT. The solar feature associated with this event was an X7 class flare that occurred at ~0700

UT January 20 (Bombardieri et al., 2008; Saldanha et al., 2008; Pérez-Peraza et al., 2009; Wang et al., 2009; Firoz et al., 2012; Bieber et al., 2013; Tan, 2013). The IMF Bz turned abruptly southward at the time of the shock so this is part of the energy driving the event. When the IMF Bz turned abruptly northward at ~1738 UT, the SSS began a recovery phase. This was followed by an interplanetary solar filament (Kozyra et al., 2013), but the latter was not geoeffective in this case. This high plasma density, high magnetic field intensity feature was interpreted by Kozyra et al. (2013) as the interplanetary manifestation of the Illing and Hundhausen (1986) most sunward portion of the 3 parts of a CME discussed earlier.

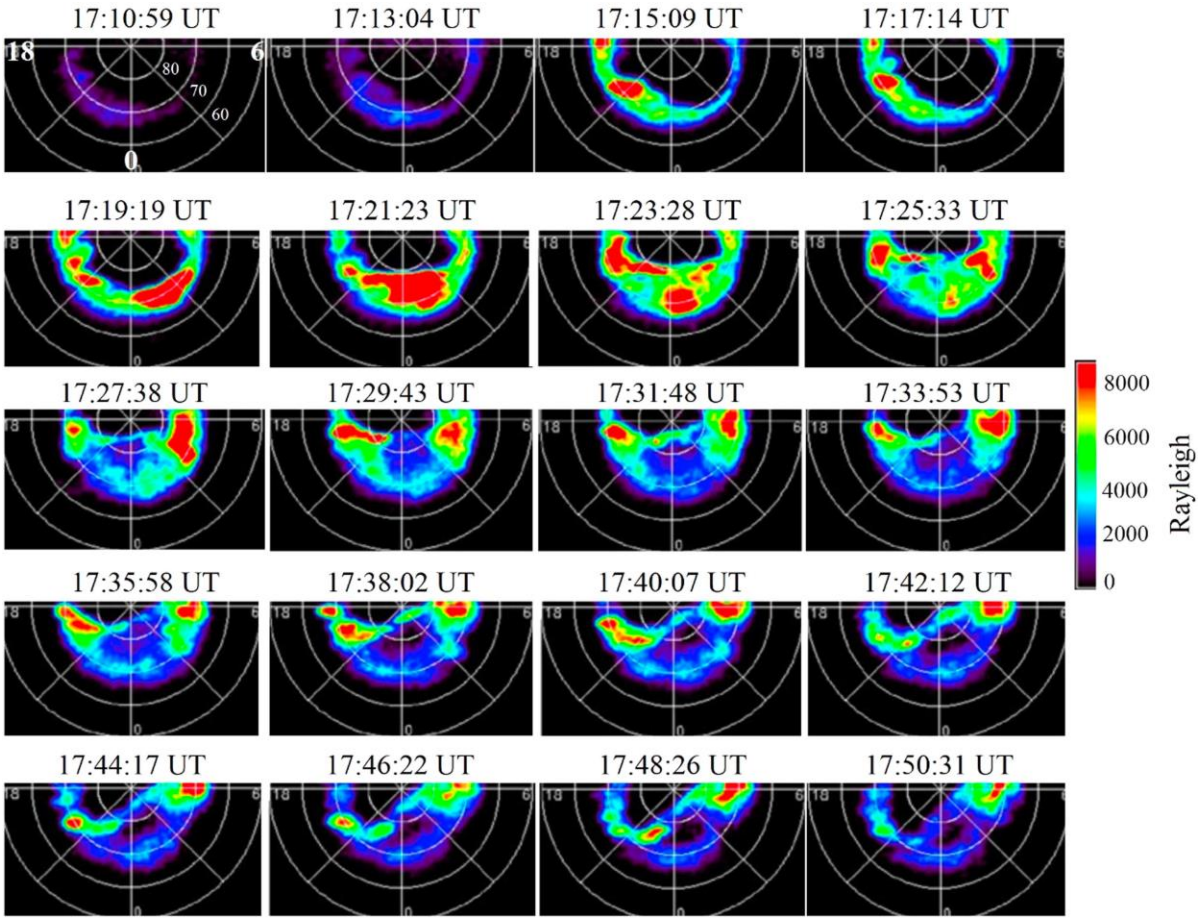

Figure 31. IMAGE-FUV images taken from ~1711 UT to ~1751 UT on January 21, 2005. These selected auroral images correspond to the SSS event in Figure 30.

Figure 31 contains the Imager for Magnetopause-to-Aurora global Exploration (IMAGE) far ultraviolet images for the SSS event in Figure 30. At ~1713 UT there was a small brightening at

~68° MLAT, which was a very small substorm or pseudobreakup (Elvey, 1957; Tsurutani et al., 1998; Aikio et al., 1999). At ~1715 UT, 2 min later there was a ~2100 MLT premidnight brightening of the aurora at ~68° to 75°. At ~1719 UT the most intense aurora was located at ~68° to 72° in the postmidnight/morning sector, ~0000 to 0400 MLT. The aurora moved from a dominant premidnight location to a postmidnight location in ~4 min.

By ~1726 UT there was almost no aurora of significant intensity at local midnight. At the peak of the SML value at ~1738 UT until ~1751, there were both intense premidnight and postmidnight auroras.

The SSS event did not exhibit the Akasofu (1964) standard model of a substorm with an intensification at midnight and then expansion to the west, east and north. The changes in the location of intense auroras were too rapid to track with the IMAGE cadence of ~2 min.

The SSS events display rapid auroral movements which may entail the appearance of sudden local field-aligned currents. Even smooth motion of auroral forms will cause strong dB/dt effects over local ground stations. SSS events may be features that can cause GIC effects that have been attributed to "magnetic storms". Thus it might be the SSS events within magnetic storms which are the real cause. SWARM satellites are excellently instrumented spacecraft that can study the SSS events in detail and possible resultant GIC effects. However as noted in the auroral images, there is a need for even higher time resolution global images than is present today. Therefore, it is important to development and fly auroral UV imagers that can be operated at ~1 s cadence in intense auroral substorm events.

8.0. CONCLUSIONS: The Physics of Space Weather and Possible Forecasting

We have discussed the current knowledge about various facets of the physics of Space Weather. There are others which we have not touched upon because of limited time and knowledge. The reader should know that other areas of Space Weather exist which may be equally important.

The most critical area for forecasting magnetic storms, either during solar maximum or the declining phase of the solar cycle is the prediction of the magnetic field Bz and the speed of the convected fields at 1 AU. For CME/MC storms (primarily during solar maximum), this is identifying MC Bz fields near the Sun and understanding the evolution of the MC as it propagates from the Sun to Earth. This major challenge will be applicable for the prediction of extreme magnetic storms and hopefully great progress will be made in the next 5 to 10 years. It was shown that for simple MCs for extreme storms one need to focus on events where the transit time from the Sun to the Earth is less than ~24 hours.

For sheaths upstream of ICMEs during solar maximum and CIRs during the declining phase (CIRs are double sheath structures), the problem is different. Detailed knowledge of the slow solar wind in the space between the Sun and Earth are needed to accurately describe and predict the IMF Bz that impacts the Earth. So far little work has been applied towards predicting the slow solar wind (plus verification). Effort needs to be placed in this area to be able to forecast intense to moderate magnetic storms. It was shown that sheath magnetic fields are extremely important for the generation of super intense (Dst < -250 nT) magnetic storms (Meng et al., 2019b).

A great deal of knowledge presently exists for establishing SEP events, those energetic particles associated with acceleration at ICME shock fronts (see Luhmann et al., 2017). What is needed for better forecasting is to understand the Mach number of the shocks, the shock normal angles and possibly upstream "seed" particles. The upstream seed particle population is similar to the sheath Bz problem in that this component of the slow solar wind needs to be modeled carefully and accurately. Three spacecraft in the solar wind at different distances from the Sun should help a lot.

The appearance of HSSs at 1 AU is a very tractable problem. That is if the coronal hole boundaries in the photosphere can be established firmly and the HSS propagation to 1 AU can be done accurately. However the most difficult task again is the IMF Bz. If Alfvén waves are generated in the interplanetary medium, this will make the task even more difficult. One solution is to measure the interplanetary magnetic field at 1 AU and use filtering techniques (Guarnieri et al. 2018) or again have large apogee Earth orbiters like the IMP-8 spacecraft again. Another

possibility is developing some type of statistical IMF Bz generator. Of course this technique will only give a ~30 min to 1 hour advanced warning.

Predicting the interplanetary shock Mach numbers and ram pressure jumps will allow foreknowledge of new radiation belt formation, SI^+ effects and magnetospheric and ionospheric dB/dt effects. Dayside auroral intensities and nightside substorm triggering will also be enhanced by predicting incoming shocks.

Several spacecraft missions have been mentioned in relationship to some forecasting problems. However the reader should note that the missions and/or their data alone will not solve these problems. It will be the scientists either on these missions or perhaps totally independent scientists who will make the most progress on these problems. An example is magnetic storms caused by interplanetary shocks/sheaths and CIRs. How long will it take scientists to be able to accurately forecast the time of occurrence of the storm (the easiest part) and the intensity (the hardest part)? Here we will not make an estimate of how long this will take. Shock acceleration of solar flare particles is clearly a fundamental part of Space Weather. How long will it scientists to be able to predict the fluence and spectral shape at a variety of distances away from the Sun? This is a fundamental problem which space agencies are not currently directly addressing.

Final Comments

A great amount of effort has been put into developing Space Weather models with the appropriate physics and chemistry included. Some models even use solar and solar wind data and geomagnetic indices that might be useful for short time-duration predictions (Gopalswamy et al., 2001; Srivastava, 2005; Cho et al., 2010; Kim et al.,2010; Kim et al., 2014; Schrijver et al., 2015; Savani et al., 2015). However in most cases, the usefulness of such models for predictive purposes has not been independently and objectively tested. This needs to be done so that missing physics and chemistry can be applied. When done (testing), surprises might result. Meng et al. (2019b) have tested the applicability of two well-known ionospheric codes to predict ionospheric TEC. It was found that the predictability was not so good, even though interplanetary plasma and field data, the solar F10.7 flux, and the geomagnetic Kp indices were used. The causes of this lack of good

representation of the ionospheric TEC data is not understood at this time. It is now being realized that not only the predictibility of various models need improvement, but also the level of uncertainty of prediction needs to be assessed as well (Knipp et al., 2018; Savani et al., 2017).

CME propagation through the interplanetary medium using ENLIL-based codes are making good progress in estimating arrival times of ICMEs at 1 AU and have had varying success in predicting the solar wind parameters as well (Falkenberg et al., 2010; Davis et al., 2011; Pizzo et al. 2015; Jackson et al., 2015; Jian et al. 2015, 2016). However the fundamental issue of space weather prediction for magnetic storms is the direction and intensity of the magnetic field both in the MC and upstream sheath. These topics still remain a challenge.

Another new approach, the application of machine learning algorithms, is quite hopeful. For this application, the physics and chemistry need not be known to be applied. Rather the reverse, finding good correlations between solar and interplanetary parameters and magnetospheric observations (for magnetic storms as an example) could lead to the understanding of the physics, the topic of this paper. But again one should test these approaches and carefully and objectively assess their accuracy and reliability in making predictions (see Wing et al., 2005, 2016; Reikard, 2015, 2018).

We have one final comment on a third type of approach at predicting Space Weather. For atmospheric weather forecasts, the experts downselect to ~25 of their best codes, and run each of the codes with the same input data. The codes produce ~25 different predictions. The weather service uses the average of the values. Why this scheme works reasonably well is not understood. This may be the final path of Space Weather forecasting.

Our hope is that the paper is stimulating to the reader in a positive sense: that they will be energized to attack some of the interesting problems in our field of Space Weather. On the other hand if the reader finds statements/topics that they disagree with, please send us email comments and we will try to answer them the best that we can. And if you have disagreements that should see print, Nonlinear Processes in Geophysics has a “Comment” and “Reply” format for discussions of this type.

10.0 GLOSSARY

Partially taken from: *"From the Sun: Auroras, Magnetic Storms, Solar Flares, Cosmic Rays"* (Suess and Tsurutani, 1998, AGU Press)

Adiabatic Invariant: In a nearly collisionless, ionized gas, electrically charged particles orbit around magnetic lines of force. Certain physical quantities are approximately constant for slow (adiabatic) changes of the magnetic field in time or in space and these quantities are called *adiabatic invariants*. For example, the magnetic moment of a charged particle, $\mu=mV_{\perp}^2/(2B)$, is such a constant where $V_{\perp}$ is the velocity of the particle perpendicular to the magnetic field, B is the magnetic field strength, and m is the particle mass. In a converging field such as in approaching the pole of a dipole magnetic, the field strength increases and therefore $V_{\perp}$ increases as well because μ has to remain constant.

Aeronomy: The science of the (upper) regions of atmospheres, those regions where dissociation of molecules and ionization are present.

Alfvén Wave (magnetohydrodynamic shear wave): A transverse wave in magnetized plasma characterized by a change of direction of the magnetic field with no change in either the intensity of the field or the plasma density.

Anisotropic Plasma: A Plasma whose properties vary with direction relative to the ambient magnetic field direction. This can be due, for example, to the presence of a magnetic or electric field. See also Isotropic Plasma; Plasma.

Arase satellite, formerly called Exploration of energization and Radiation in Geospace or **ERG**: a scientific satellite developed by the Institute of Space and Astonautical Science (ISAS) of the Japanese Aerospace Exploration Agency (JAXA) to study the Van Allen radiation belts.

Astronomical Unit (AU): The mean radius of the Earth's orbit, 1.496 $x10^{13}$ cm.

Aurora: A visual phenomenon that occurs mainly in the high-latitude night sky. Auroras occur within a band of latitudes known as the auroral oval, the location of which is dependent

on the intensity of geomagnetic activity. Auroras are a result of collisions between precipitating charged particles (mostly electrons) and atmospheric atoms and molecules, exciting the atmospheric constituents. The charged particles come from the outer parts of the magnetosphere and guided by the geomagnetic field. Each gas (oxygen and nitrogen molecules and atoms) emits its own characteristic radiation when bombarded by the precipitating particles. Since the atmospheric composition varies with altitude, and the faster precipitating particles penetrate deeper into the atmosphere, certain auroral colors originate preferentially from certain heights in the sky. The auroral altitude range is 80 to 500 km, but typical auroras occur 90 to 250 km above the ground. The color of the typical aurora is yellow-green, from a specific transition line of atomic oxygen. Auroral light from lower levels in the atmosphere is dominated by blue and red bands from molecular nitrogen and molecular oxygen. Above 250 km, auroral light is characterized by a red spectral line of atomic oxygen. To an observer on the ground, the combined light of these three fluctuating, primary colors produces an extraordinary visual display. Auroras in the Northern Hemisphere are called the aurora borealis or "northern lights". Auroras in the Southern Hemisphere are called aurora australis. The patterns and forms of the aurora include quiescent "arcs", rapidly moving "rays" and "curtains," "patches," and "veils."

Auroral Electrojet (AE): See Electrojet.

Auroral Oval: An elliptical band around each geomagnetic pole ranging from about 75 degrees magnetic latitude at local noon to about 67 degrees magnetic latitude at midnight under average conditions. It is the locus of those locations of the maximum occurrence of auroras, and widens to both higher and lower latitudes during the expansion phase of a magnetic substorm.

Beta (e.g., low-beta plasma)**:** The ratio of the thermal pressure to the magnetic 'pressure' in a plasma - $p/ (B^2/(8\pi))$ in centimeter-gram-second (c.g.s.)

Bow Shock (Earth, heliosphere): A collisionless shock wave in front of the magnetosphere arising from the interaction of the supersonic solar wind with the Earth's magnetic field. An analogous shock is the heliospheric bow shock which exists in front of the

heliosphere and is due to the interaction of the interstellar wind with the solar wind and the inter planetary magnetic field.

Charge Exchange: An interaction between a charged particle and a neutral atom wherein the charged particle becomes neutral and the neutral particle becomes charged through the exchange of an electron.

Cloud (magnetic): see Magnetic Cloud.

Collisional (de-) **Excitation**: Excitation of an atom or molecule to a higher energy state due to a collision with another atom, molecule, or ion. The higher energy state generally refers to electrons in higher energy around atoms. Deexcitation is the reduction of a higher electron energy state to a lower one, usually accomplished by a collision with another atom, molecule or ion.

Convection (magnetospheric, plasma, thermal): The bulk transport of plasma (or gas) from one place to another, in response to mechanical forces (for example, viscous interaction with the solar wind) or electromagnetic forces. Thermal convection, due to heating from below and the gravitational field, is what drives convection inside the Sun. Magnetospheric convection is driven by the dragging of the Earth's magnetic field and plasma together by the solar wind when the magnetic field becomes attached to the magnetic field in the solar wind.

Coriolis Force: In the frame of a rotating body (such as the Earth), a force due to the bodily rotation. All bodies that are not acted upon by some force have the tendency to remain in a state of rest or of uniform rectilinear motion (Newton's First Law) so that this force is called a "fictitious" forces. It is a consequence of the continuous acceleration which must be applied to keep a body at rest in a rotating frame of reference.

Corona: The outermost layer of the solar atmosphere, characterized by low densities ($<10^9$ cm^{-3} or 10^{15} m^{-3}) and high temperatures ($>10^6$ K).

Coronal Hole: An extended region of the solar corona characterized by exceptionally low density and in a unipolar photospheric magnetic field having "open" magnetic field topology. Coronal holes are largest and most stable at or near the solar poles, and are a

source of high speed (700-800 km/s) solar wind. Coronal holes are visible in several wavelengths, most notably solar x-rays visible only from space, but also in the He 1083 nm line which is detectable from the surface of the Earth. In soft x-ray images (photon energy of ~0.1-1.0 keV or a wavelength of 10-100 Å), these regions are dark, thus the name "holes".

Coronal Mass Ejection (CME): A transient outflow of plasma from or through the solar corona. CMEs are often but not always associated with erupting prominences, disappearing solar filaments, and flares.

Corotation (with the Earth): A plasma in the magnetosphere of the Earth is said to be corotating with the Earth if the magnetic field drags the plasma with it and together they have a 24 hour rotation period.

Cosmic Ray (galactic, solar): Extremely energetic (relativistic) charged particles or electromagnetic radiation, primarily originating outside of the Earth's magnetosphere. Cosmic rays usually interact with the atoms and molecules of the atmosphere before reaching the surface of the Earth. The nuclear interactions lead to formation of daughter products, and they in turn to granddaughter products, etc. Thus there is a chain of reactions and a "cosmic ray shower". Some cosmic rays come from outside the solar system while others are emitted from the Sun in solar flares. See also Anomalous Cosmic Ray; Energetic Particle; Solar Energetic Particle (SEP) Event.

Constellation Observing System for Meteorology, Ionosphere and Climate-2 (COSMIC II): A joint Taiwan National Space Organization (NSPO)-U.S. National Oceanic and Atmospheric Administration (NOAA) mission of six satellites in low-inclination orbit to study the Earth's ionosphere.

Corotating Interaction Region (CIR): An interplanetary region of high magnetic fields and plasma densities created by the interaction of a high speed solar wind stream with the upstream slow solar wind. The antisunward portion of the CIR is compressed slow solar wind plasma and magnetic fields, and the sunward portion is compressed fast solar wind plasma and magnetic fields. The two regions of the CIR are separated by a tangential discontinuity.

Cyclotron Frequency: When a particle of charge q moves in a magnetic field B, the particle orbits, or gyrates around the magnetic field lines. The cyclotron frequency is the frequency of this gyration, and is given by $\omega_c = q|\mathbf{B}|/mc$, where m is the mass of the particle, and c is the velocity of light (in centimeter-gram-second (c.g.s.) units).

Cyclotron Resonance: The frequency at which a charged particle experiences a Doppler-shifted wave at the particle's cyclotron frequency. Because the particle and wave may be traveling at different speeds and in different directions, there is usually a Doppler shift involved.

D Region: A daytime region of the Earth's ionosphere beginning at approximately 40 km, extending to 90 km altitude. Radio wave absorption in this region can be significantly increased due to increasing ionization associated with the precipitation of solar energetic particles through the magnetosphere and into the ionosphere.

Diffusion: The slow, stochastic motion of particles.

Diffusive Shock Acceleration: Charged particle acceleration at a collisionless shock due to stochastic scattering processes caused by waves and plasma turbulence. See also Shock Wave (collisionless).

Dipole Magnetic Field: A magnetic field whose intensity decreases as the cube of the distance from the source. A bar magnet's field and the magnetic field originating in the Earth's core are both approximately dipole magnetic fields.

Drift (of ions/electrons): As particles gyrate around magnetic field lines, their orbits may "drift" perpendicular to the local direction of the magnetic field. This occurs if there is a force also perpendicular to the field - e.g. an electric field, curvature in the magnetic field direction, or gravity.

Driver Gas: A mass of plasma and entrained magnetic field that is ejected from the Sun, that has a velocity higher than the upstream plasma, and which "drives" a (usually collisionless) shock wave ahead of itself. The magnetic cloud within an ICME is the same thing as a driver gas.

Dst Index: A measure of variation in the geomagnetic field due to the equatorial ring current. It is computed from the H-components at approximately four near-equatorial stations at hourly intervals. At a given time, the Dst index is the average of variation over all longitudes; the reference level is set so that Dst is statistically zero on internationally designated quiet days. An index of -50 nT (nanoTesla) or less indicates a storm-level disturbance, and an index of -200 nT or less is associated with middle- latitude auroras. Dst is determined by the World Data Center C2 for Geomagnetism, Kyoto University, Kyoto, Japan.

Dynamo (solar magnetospheric): The conversion of mechanical energy (rotation in the case of the Sun) into electrical current. This is the process by which magnetic fields are amplified by the induction of plasmas being forced to move perpendicular to the magnetic field lines. See also Mean Field Electro-Dynamics.

E-Region: A daytime region of the Earth's ionosphere roughly between the altitudes of 90 and 160 km. The E-region characteristics (electron density, height, etc.) depend on the solar zenith angle and the solar activity. The ionization in the E layer is caused mainly by x-rays in the range 0.8 to 10.4 nm coming from the Sun.

Ecliptic Plane: The plane of the Earth's orbit about the Sun. It is also the Sun's apparent annual path, or orbit, across the celestial sphere.

Electrically Charged Particle: Electrons and protons, for example, or any atom from which electrons have been removed to make it into a positively charged ion. The elemental charge of particles is 4.8×10^{-10} esu. An electron and proton have this charge. Combined (a hydrogen atom), the charge is zero. Ions have multiples of this charge, depending on the number of electrons which have been removed (or added).

Electrojet: (1) Auroral Electrojet (AE): A current that flows in the ionosphere at a height of ~100 km in the auroral zone. (2) Equatorial Electrojet: A thin electric current layer in the ionosphere over the dip equator at about 100 to 115 km altitude.

Electron Plasma Frequency/Wave: The natural frequency of oscillation of electrons in a neutral plasma (e.g., equal numbers of electrons and protons).

Electron Volt (eV): The kinetic energy gained by an electron or proton being accelerated in a potential drop of one Volt.

ESA: European Space Agency

Extreme Ultraviolet (EUV): A portion of the electromagnetic spectrum from approximately 10 to 100 nm.

Extremely Low Frequency (ELF): That portion of the radio frequency spectrum from 30 to 3000 Hz.

Fast Mode (wave/speed): In magnetohydrodynamics, the fastest wave speed possible. Numerically, this is equal to the square root of the sum of the squares of the Alfvén speed and plasma sound speed.

Field Aligned Current: A current flowing along (or opposite to) the magnetic field direction.

Filament: A mass of gas suspended over the chromosphere by magnetic fields and seen as dark ribbons threaded over the solar disk. A filament on the limb of the Sun seen in emission against the dark sky is called a prominence. Filaments occur directly over magnetic-polarity inversion lines, unless they are active.

Flare: A sudden eruption of energy in the solar atmosphere lasting minutes to hours, from which radiation and energetic charged particles are emitted. Flares are classified on the basis of area at the time of maximum brightness in H alpha.

Importance 0 (Subflare): < 2.0 hemispheric square degrees

Importance 1: 2.1-5.1 square degrees

Importance 2: 5.2-12.4 square degrees

Importance 3: 12.5-24.7 square degrees

Importance 4: >= 24.8 square degrees

[One square degree is equal to (1.214 x 10^4 km) squared = 48.5 millionths of the visible solar hemisphere.] A brightness qualifier F, N, or B is generally appended

to the importance character to indicate faint, normal, or brilliant (for example, 2B).

Flux Rope: A magnetic phenomenon which has a force-free field configuration.

Force Free Field: A magnetic field which exerts no force on the surrounding plasma. This can either be a field with no flowing electrical currents or a field in which the electrical currents all flow parallel to the field.

Free Energy (of a plasma): When an electron or ion distribution is either non-Maxwellian or anisotropic, they are said to have free energy" from which plasma waves can be generated via instabilities. The waves scatter the particles so they become more isotropic, reducing the free energy.

Frozen-in Field: In a tenuous, collisionless plasma, the weak magnetic fields embedded in the plasma are convected with the plasma. i.e., they are "frozen in."

Galactic Cosmic Ray (GCR): See Cosmic Ray.

Gamma Ray: Electromagnetic radiation at frequencies higher than x-rays.

Geomagnetic Storm: A worldwide disturbance of the Earth's magnetic field, distinct from regular diurnal variations. A storm is precisely defined as occurring when D_{sT} becomes less than -50 nT (See geomagnetic activity).

Main Phase: Of a geomagnetic storm, that period when the horizontal magnetic field at middle latitudes decreases, owing to the effects of an increasing magnetospheric ring current. The main phase can last for hours, but typically lasts less than 1 day.

Recovery Phase: Of a geomagnetic storm, that period when the depressed northward field component returns to normal levels. Recovery is typically complete in one to two days.

Geomagnetically Induced Currents (GICs): Currents flowing along electric power transmission systems and other electrically conducting instrastructures are produced by naturally induce geoelectric fields during geomagnetic disturbances.

Geosynchronous Orbit: Term applied to any equatorial satellite with an orbital velocity equal to the rotational velocity of the Earth. The geosynchronous altitude is near 6.6 Earth radii

(approximately 36,000 km above the Earth's surface). To be geostationary as well, the satellite must satisfy the additional restriction that its orbital inclination be exactly zero degrees. The net effect is that a geostationary satellite is virtually motionless with respect to an observer on the ground.

GeV: 10^9 electron Volts (Giga-electron Volt).

Global Navigation Satellite System (GNSS): GNSS receivers use the orbiting satellite Global Positioning System (GPS) transmitted signals to obtain the geographic location of a user's receiver anywhere in the world.

Global Positioning System (GPS): is a global navigation satellite system that provides geolocation and time information to a GPS receiver anywhere on or near the Earth where there is an unobstructed line of sight to four or more GPS satellites.

Global-scale Observations of the Limb and Disk (GOLD): a NASA mission to " investigate the dynamic intermingling of space and Earth's uppermost atmosphere"

Heliosphere: The magnetic cavity surrounding the Sun, carved out of the galaxy by the solar wind.

Heliospheric Current Sheet (HCS): This is the surface dividing the northern and southern magnetic field hemispheres in the solar wind. The magnetic field is generally one polarity in the north and the opposite in the south so just one surface divides the two polarities. However, the Sun's magnetic field changes over the 11-year solar sunspot cycle and reverses polarity at solar maximum. The same thing happens in the magnetic field carried away from the Sun by the solar wind so the HCS only lies in the equator near solar minimum. It is called a "current sheet" because it carries an electrical current to balance the oppositely directed field on either side of the surface. It is very thin on the scale of the solar system - usually only a few proton gyroradii, or less than 100,000 km.

Helmet Streamer: See Streamer.

High Frequency (HF): That portion of the radio frequency spectrum between 3 and 30 MHz.

Heliospheric Plasma Sheet (HPS): A high density slow solar wind region that is located adjacent to the heliospheric current sheet (HCS).

High Speed Solar Wind (HSS): A solar wind with speeds of 750 to 800 km/s emanating from solar coronal holes. The HSS is characterized by embedded, particularly large amplitude Alfvén waves. At the edges of HSSs, the velocities can be less due to superradial expansion effects.

Instability: When an electron or ion distribution is sufficiently anisotropic, it becomes unstable (instability), generating plasma waves. The anisotropic distribution provides a source of free energy for the instability. A simple analog is a stick, which if stood on end is "unstable," but which if laid on its side is "stable." In this analog, gravity pulls on the stick and provides a source of free energy when the stick is stood on end.

Interplanetary Magnetic Field (IMF, Parker spiral): The magnetic field carried with the solar wind and twisted into an Archimedean spiral by the Sun's rotation.

Interplanetary Medium: The volume of space in the solar system that lies between the Sun and the planets. The solar wind flows in the interplanetary medium.

Interplanetary Coronal Mass Ejection (ICME): The evolutionary part of a CME as it propagates through interplanetary space. Typically after the CME has propagated 1 AU from the Sun, the ICME only contains the magnetic cloud (MC) portion of the initial three parts of a CME. The MC may also have been compressed/expanded or rotated by the time it reaches 1 AU.

Interplanetary Shock: A fast forward shock is characterized by a sharp increase in solar wind speed, plasma density, plasma temperature and magnetic field magnitude. The shock reduces the upstream plasma from a supermagnetosonic state to a subsonic state, much as an airplane wing sonic shock reduces the relative flow of air from a supersonic speed (relative to the airplane) to a subsonic speed. A fast (magnetosonic) forward (propagating in the direction of the “piston”, in this case the propagation of the ICME in the antisolar direction) shock is detected upstream (antisolarward) of fast ICMEs. A reverse shock propagates in the direction of the Sun. Planetary bow shocks are reverse shocks. There are other types of shocks not discussed in this paper: slow shocks and intermediate shocks.

Interstellar (gas, neutral gas, ions, cosmic rays, wind, magnetic field, etc.) Literally, between the stars. In practical terms, it is anything beyond the outer boundary of the solar wind (the "heliopause") yet within the Milky Way.

Ion: (1). An electrically charged atom or molecule. (2). An atom or molecular fragment that has a positive electrical charge due to the loss of one or more electrons; the simplest ion is the hydrogen nucleus, a single proton.

Ionization State: The number of electrons missing from an atom.

Ionosphere: The region of the Earth's upper atmosphere containing free (not bound to an atom or molecule) electrons and ions. This ionization is produced from the neutral atmosphere by solar ultraviolet radiation at very short wavelengths (<100 nm) and also by precipitating energetic particles.

Ionospheric Storm: A positive ionospheric storm is where the ionospheric total electron content (TEC) increases. A negative ionospheric storm is an event where the ionospheric TEC decreases.

Ionospheric Connection Explorer (ICON): is a NASA 2-year mission that will give new views of the boundary between our atmosphere and space, where planetary weather and Space Weather meet.

Irradiance: Radiant energy flux density on a given surface (e. g. ergs $cm^{-2}s^{-1}$).

keV: 1000 electron Volts (kiloelectron Volt). See electron Volt. See also Anisotropic Plasma; Plasma.

L value: For a dipole magnetic field, the field line that crosses the magnetic equator at a L value equal to the number in Earth radii.

Loop (solar-loop prominence system): A magnetic loop is the flux tube which crosses from one polarity to another. A loop prominence bridges a magnetic inversion line across which the magnetic field changes direction. See also Magnetic Foot Point; Prominence.

Loss Cone: A small cone angle about the ambient magnetic field direction where magnetospheric charged particles with velocity vectors within the cone will mirror at

sufficiently low altitudes such that the particle will have collisions with atmospheric atoms and molecules and will be “lost” from returning to the magnetosphere.

Loss Cone Instability: An instability generated by a plasma anisotropy where the temperature perpendicular to the magnetic field is greater than the temperature parallel to the field. This instability gets its name because this condition exists in the Earth's magnetosphere and the "loss cone" particles are those that are lost into the upper atmosphere.

Magnetic Cloud: A region in the solar wind of about 0.25 AU or more in radial extent in which the magnetic field strength is high and the direction of one component of the magnetic field changes appreciably by means of a rotation nearly parallel to a plane. Magnetic clouds may be parts of the driver gases (coronal mass ejections) in the interplanetary medium.

Magnetic Foot Point: For the Earth’s magnetic field lines, where the magnetic field enters the surface of the Earth.

Magnetic Mirror: Char particles moving into a region of converging magnetic flux (as at the pole of a magnet) will experience "Lorentz" forces that slow the particles and "mirror" them by eventually reversing their direction if the particles are initially moving slowly enough along the field line. See also Mirror Point.

Magnetic Reconnection: The act of interconnection between oppositely directed magnetic field lines. Magnetic reconnection is recognized as a basic plasma process, which converts magnetic energy into plasma kinetic energy accompanied by topological changes in the magnetic field configuration. It does not allow an excessive buildup of magnetic energy in the current sheets.

Magnetic Storm: see Geomagnetic Storm.

Magnetopause: The boundary surface between the solar wind and magnetosphere, where the pressure of the magnetic field of the object effectively equals the ram pressure of the solar wind plasma.

Magnetosheath: The region between the bow shock and the magnetopause, characterized by very turbulent plasma. This plasma has been heated (shocked) and slowed as it passed

through the bow shock. For the Earth, along the Sun-Earth axis, the magnetosheath is about 3 Earth radii thick.

Magnetosonic Speed (acoustic speed): The speed of the fastest low frequency magnetic waves in a magnetized plasma. It is the equivalent of the sound speed in a neutral gas or non-magnetized plasma.

Magnetosphere: The magnetic cavity surrounding a magnetized planet, carved out of the passing solar wind by virtue of the planetary magnetic field, which prevents, or at least impedes, the direct entry of the solar wind plasma into the cavity.

Magnetospheric Multiscale Mission (MMS): A NASA mission designed to spend extensive periods in locations where magnetic reconnection at the magnetopause/magnetotail is expected to occur. The critical electron diffusion region will be studied. The mission consists of 4 spacecraft flown in a tetrahedron configuration.

Magnetotail: The extension of the magnetosphere in the anti-sunward direction as a result of interaction with the solar wind. In the inner magnetotail, the field lines maintain a roughly dipolar configuration. But at greater distances in the anti-sunward direction, the field lines are stretched into northern and southern lobes, separated by a plasmasheet. There is observational evidence for traces of the Earth's magnetotail as far as 1000 Earth radii downstream, in the anti-solar direction.

Maxwellian Distribution: The minimum energy particle distribution for a given temperature. It is also the equilibrium distribution in the absence of losses due to radiation, collisions, etc.

Mean Free Path: The statistically most probably distance a particle travels before undergoing a collision with another particle or interacting with a wave.

Mesosphere: The region of the Earth's atmosphere between the upper limit of the stratosphere (approximately 30 km altitude) and the lower limit of the thermosphere (approximately 80 km altitude).

MeV: One million electron Volts (Megaelectron Volt). See also Electron Volt.

Mirror Point: The point where the charged particles reverse direction (mirrors). At this point, all of the particle motion is perpendicular to the local ambient magnetic field. See also Magnetic Mirror.

Parker Solar Probe: a NASA robotic spacecraft to probe the outer corona of the Sun. It will approach to within 9.9 solar radii (6.9 million kilometers or 4.3 million miles from the center of the Sun and will travel, at closest approach, as fast as 690,000 km/h (430,000 mph).

Photosphere: The lowest visible layer of the solar atmosphere; corresponds to the solar surface viewed in white light. Sunspots and faculae are observed in the photosphere.

Pickup Ion: An ion which has entered the solar system as a neutral particle and then becomes ionized either through charge exchange or photoionization. It is called a pickup ion because as soon as the neutral atom is ionized, it becomes attached to the magnetic field carried by the solar wind and so is "picked up" by the solar wind.

Pitch Angle: In a plasma, the angle between the instantaneous velocity vector of a charged particle and the direction of the ambient magnetic field.

Plasma (ions, electrons): A gas that is sufficiently ionized so as to affect its dynamical behavior. A plasma is a good electrical conductor and is strongly affected by magnetic fields. See also Anisotropic Plasma; Isotropic Plasma.

Plasma Instability (ion, electron): When a plasma is sufficiently anisotropic, plasma waves grow, which in turn alter the distribution via wave-particle interactions. The plasma is "unstable."

Plasma Sheet: A region in the center of the magnetotail between the north and south lobes. The plasma sheet is characterized by hot, dense plasma and is a high beta plasma region, in contrast to the low beta lobes. The plasma sheet bounds the neutral sheet where the magnetic field direction reverses from Earthward (north lobe direction) to anti-Earthward (south lobe direction).

Plasma Wave (electrostatic/electromagnetic): A wave generated by plasma instabilities or other unstable modes of oscillation allowable in a plasma. “Chorus” and “Plasmasheric Hiss”

are whistler wave modes. These are electromagnetic waves with frequencies below the electron cyclotron frequency. Electromagnetic ion cyclotron (EMIC) waves are ion cyclotron waves with frequencies below the proton cyclotron frequency.

Polar Cap Absorption Event (PCA): An anomalous condition of the polar ionosphere whereby HF and VHF (3-300 MHz) radio waves are absorbed, and LF and VLF (3-300 kHz) radio waves are reflected at lower altitudes than normal. The cause is energetic particle precipitation into the ionosphere/atmosphere. The enhanced ionization caused by this precipitation leads to cosmic radio noise absorption and attenuation of that noise at the surface of the Earth. PCAs generally originate with major solar flares, beginning within a few hours of the event (after the flare particles have propagated to the Earth) and maximizing within a day or two after onset. As measured by a riometer (relative ionospheric opacity meter), the PCA event threshold is 2 dB of absorption at 30 MHz for daytime and 0.5 dB at night. In practice, the absorption is inferred from the proton flux at energies greater than 10 MeV, so that PCAs and proton events are simultaneous. However, the transpolar radio paths may still be disturbed for days, up to weeks, following the end of a proton event, and there is some ambiguity about the operational use of the term PCA.

Prominence: A term identifying cloud-like features in the solar atmosphere. The features appear as bright structures in the corona above the solar limb and as dark filaments when seen projected against the solar disk. Prominences are further classified by their shape (for example, mound prominence, coronal rain) and activity. They are most clearly and most often observed in H alpha. See also Loop.

Radiation Belt: Regions of the magnetosphere roughly 1.2 to 6 Earth radii above the equator in which charged particles are stably trapped by closed geomagnetic field lines. There are two belts. The inner belt’s maximum proton density lies near 5000 km above the Earth's surface. Inner belt protons (10s of MeV) and electrons (100s of keV) and originate from the decay of secondary neutrons created during collisions between cosmic rays and upper atmospheric particles. The outer belt extends on to the magnetopause on the sunward side (10 Earth radii under normal quiet conditions) and to about 6 Earth radii on the nightside. The altitude of maximum proton density is near 16,000-20,000 km. Outer belt protons

and electrons are lower energy (about 200 eV to 1 MeV). The origin of the particles (before they are energized to these high energies) is a mixture of the solar wind and the ionosphere. The outer belt is also characterized by highly variable fluxes of energetic electrons. The radiation belts are often called the “Van Allen radiation belts" because they were discovered in 1958 by a research group at the University of Iowa led by Professor J. A. Van Allen. See also Trapped Particle.

Ram Pressure: Sometimes called “dynamic pressure”. The pressure exerted by a streaming plasma upon a blunt object.

Reconnection: A process by which differently directed field lines link up allowing topological changes of the magnetic field to occur, determining patterns of plasma flow, and resulting in conversion of magnetic energy to kinetic and thermal energy of the plasma. Reconnection is invoked to explain the energization and acceleration of the plasmas/energetic particles that are observed in solar flares, magnetic substorms and storms, and elsewhere in the solar system.

Relativistic: Charged particles (ions or electrons) which have speeds comparable to the speed of light.

Ring Current: In the magnetosphere, a region of current that flows near the geomagnetic equator in the outer belt of the two Van Allen radiation belts. The current is produced by the gradient and curvature drift of the trapped charged particles of energies of 10 to 300 keV. The ring current is greatly augmented during magnetic storms because of the hot plasma injected from the magnetotail and upwelling oxygen ions from the ionosphere. Further acceleration processes bring these ions and electrons up to ring current energies. The ring current (which is a diamagtic current) causes a worldwide depression of the horizontal geomagnetic field during a magnetic storm.

Solar Energetic Particle (SEP): An energetic particle of solar flare/interplanetary shock origin.

Sheath: The plasma and magnetic fields in the downstream subsonic region after collisionless shocks. See Shock Wave.

Shock Wave: A shock wave is characterized by a discontinuous change in pressure, density, temperature, and particle streaming velocity, propagating through a compressible fluid or plasma. Fast collisionless shock waves occur in the solar wind when fast solar wind overtakes slow solar wind with the difference in speeds being greater than the magnetosonic speed. Collisionless shock thicknesses are determined by the proton and electron gyroradii rather than the collision lengths. See also Diffusive Shock Acceleration; Solar Wind Shock.

Solar Corona: See Corona.

Solar Cycle: The approximately 11 year quasi-periodic variation in the sunspot number. The polarity pattern of the magnetic field reverses with each cycle. Other solar phenomena, such as the 10.7-cm solar radio emission, exhibit similar cyclical behavior. The solar magnetic field reverses each sunspot cycle so there is a corresponding 22 year solar magnetic cycle.

Solar Energetic Particle (SEP) Event: A high flux event of solar (low energy) cosmic rays. This is commonly generated by larger solar flares or CME shocks, and lasts, typically from minutes to days. See also Cosmic Ray.

Solar Flares: Transient perturbations of the solar atmosphere as measured by enhanced x-ray emission (see x-ray flare class), typically associated with flares. Five standard terms are used to describe the activity observed or expected within a 24-h period:

Very low - x-ray events less than C-class.

Low - C-class x-ray events.

Moderate - isolated (one to 4) M-class x-ray events.

High - several (5 or more) M-class x-ray events, or isolated (one to 4).

M5 or greater x-ray events.

Very high - several (5 or more) M5 or greater x-ray events.

Solar Maximum: The month(s) during the sunspot cycle when the smoothed sunspot number reaches a maximum.

Solar Minimum: The month(s) during the sunspot cycle when the smoothed sunspot number reaches a minimum.

Solar Orbiter: A European Space Agency-led (ESA) mission intended to perform detailed measurements of the inner heliosphere and nascent solar wind to answer the question "How does the Sun create and control the heliosphere?" The mission will make observations of the Sun from an eccentric orbit moving as close as ~60 solar radii (R_S), or 0.284 astronomical units (AU) from the Sun.

Solar Wind: The outward flow of solar particles and magnetic fields from the Sun. Typically at 1 AU, solar wind velocities are 300-800 km/s and proton and electron densities of 3-7 per cubic centimeter (roughly inversely correlated with velocity). The total intensity of the interplanetary magnetic field is nominally 3-8 nT.

SORCE: Solar Radiation and Climate Experiment. A NASA mission that measures electromagnetic radiation produced by the Sun and the power per unit area of that energy on the Earth's surface.

Space Weather: Dynamic variations at the Sun, in interplanetary space, in the Earth's and planetary magnetospheres, ionospheres and atmospheres associated with space phenomena.

Stratosphere: That region of the Earth's atmosphere between the troposphere and the mesosphere. It begins at an altitude of temperature minimum at approximately 13 km and defines a layer of increasing temperature up to about 30 km.

Streamer: A feature of the white light solar corona (seen in eclipse or with a coronagraph) that looks like a ray extending away from the Sun out to about 1 solar radius, having an arch-like base containing a cavity usually occupied by a prominence.

Substorm: A substorm corresponds to an injection of charged particles from the magnetotail into the nightside magnetosphere. Plasma instabilities lead to the precipitation of the particles

into the auroral zone ionosphere, producing intense aurorae. Potential drops along magnetic field lines lead to the acceleration of ~1 to 10 keV electrons with brilliant displays of aurora as the electrons impact the upper atmosphere. Enhanced ionospheric conductivity and externally imposed electric fields lead to the intensification of the auroral electrojets.

Sudden Impulse (SI): An abrupt (10s of seconds) jump in the Earth's surface magnetic field. The positive sudden impulses (SI^+s) are caused by fast forward shock impingement onto the magnetosphere.

Sunspot: An area seen as a dark spot, in contrast with its surroundings, on the photosphere of the Sun. Sunspots are concentrations of magnetic flux, typically occurring in bipolar clusters or groups. They appear dark because they are cooler than the surrounding photosphere. Larger and darker sunspots sometimes are surrounded (completely or partially) by penumbrae. The dark centers are umbrae. The smallest, immature spots are sometimes called pores.

Supersubstorm: Defined as an event with SML < -2500 nT. These auroral zone events appear to have different evolutionary properties than the standard (Akasofu, 1964) auroral substorms.

SWARM: A European Space Agency (ESA) mission originally instrumented to study the Earth's magnetic field. The current goals are to study magnetospheric-ionospheric coupling and auroral Space Weather problems.

Telsa: A unit of magnetic flux density (Weber/m^2). A nanoTesla (nT) is 10^{-9} Teslas.

Termination Shock: The shock wave in the solar wind which is caused by the abrupt deceleration of the solar wind as it runs into the local interstellar medium (LISM). It is thought to lie somewhere between 70 and 150 AU from the Sun.

Thermal Speed (ion, electron): The random velocity of a particle associated with its temperature.

Thermosphere: That region of the Earth's atmosphere where the neutral temperature increases with height. It begins above the mesosphere at about 80-85 km and extends upward to the exosphere.

TIMED: Thermosphere Ionosphere Mesosphere Energetics and Dynamics (TIMED). A NASA mission to investigate and understand the energetics of the Earth's mesosphere and lower thermosphere/ionosphere.

Total Electron Content (TEC): The column density of electrons in the Earth's ionosphere.

Trapped Particle: Particles gyrating about magnetic field lines (e.g., in the Earth's magnetosphere). See also Magnetic Mirror and Pitch Angle.

Troposphere: The lowest layer of the Earth's atmosphere, extending from the ground to the stratosphere, approximately 13 km altitude. In the troposphere, temperature decreases with height.

Ultraviolet (UV): That part of the electromagnetic spectrum between 5 and 400 nm.

Ultra Low Frequency (ULF): 1 milliHertz to 1 Hertz.

Very High Frequency (VHF): That portion of the radio frequency spectrum from 3 to 300 MHz.

Very Low Frequency (VLF): That portion of the radio frequency spectrum from 3 to 300 kHz.

Van Allen Radiation Belt: See Radiation Belt.

REFERENCES

Acero, F.J., Vaquero, J.M., Gallego, M.C., and Garcia, J.A.: A limit for the values of the Dst geomagnetic index, *Geophys. Res. Lett.*, *45*, doi.org/10.1029/2018GL079676, 2018.

Agostinelli, S., et al.: GEANT4-A simulation toolkit, *Nucl. Instr. Meth. In Phys. Res. Sect. A, 506*, 250, doi:10.1016/S0168-9002(03)01368-8, 2003.

Aikio, A. T., Sergeev, V. A., Shukhtina, M. A., Vagina, L. I., Angelopoulos, V., and Reeves, G. D.: Characteristics of pseudobreakups and substorms observed in the ionosphere, at the

2017 geosynchronous orbit, and in the midtail, *J. Geophys. Res., 104*, 12263-12287, doi:
2018 10.1029/1999JA900118, 1999.
2019 Akasofu, S.-I.: The development of the auroral substorm, *Plan. Spa. Phys., 12*, 273-282, 1964.
2020 Akasofu, S.-I.: Magnetospheric substorms, a model, in *Solar Terrestrial Physics, Part III*, edited
2021 by D. Dyer, p. 131, D. Reidel Publ., Norwell, Mass, 1972.
2022 Akasofu, S.-I., and Chao, J. K.: Interplanetary shock waves and magnetospheric substorms,
2023 *Planetary and Space Science, 28*, 381-385, 1980.
2024 Akasofu, S.-I., and Kamide, Y.: Comment on "The extreme magnetic storm of 1-2 September
2025 1859" by B.T. Tsurutani, W.D. Gonzalez, G.S. Lakhina and S. Alex, *J. Geophys. Res., 110,*
2026 A09226, doi:10.1029/2005JA011005, 2005.
2027 Alfvén, H.: *Cosmical Electrodynamics*, Oxford at the Clarendon Press, 1950.
2028 Anderson, B. J., and Hamilton, D.C.: Electromagnetic ion cyclotron waves stimulated by modest
2029 magnetospheric compressions, *J. Geophys. Res., 98*, A7, 11369, 1993.
2030 Anderson, D. N., Decker, D. T., and Valladares, C. E.: Global theoretical ionospheric model
2031 (GTIM) in *Solar-Terrestrial Energy Program: Handbook of Ionospheric Models*, Natl. Oceanic
2032 and Atmos. Admin, Boulder, CO, 133-152, 1996.
2033 Araki, T., Tsunomura, S., and Kikuchi, T.: Local time variation of the amplitude of geomagnetic
2034 sudden commencements (SC) and SC-associated polar cap potential, *Earth Plan. Spa., 61*, e13-
2035 e16, 2009.
2036 Araki, T.: Historically largest geomagnetic sudden commencement (SC) since 1868, *Earth, Plan.*
2037 *Spa., 66*:164, http://www.earth-planets-space.com/66/1/164, 2014.
2038 Baker, D.N., Higbie, P.R., Belian, R.D., and Hones Jr., E.W.: Do Jovian electrons influence the
2039 terrestrial outer radiation zone?, *Geophys. Res. Lett., 6*, 531-534,
2040 https://doi.org/10.1029/GL006i006p00531, 1979.
2041 Baker, D.N., Pulkkinen, T.I., Angelopoulos, V., Baumjohann, W., McPherron, R.L.: Neutral line
2042 model of substorms: Past results and present view, *J. Geophys. Res., 101*, 12975-13010, 1996.
2043 Baker, D.N., Li, X., Blake, J.B., and Kanekal, S.: Strong electron acceleration in the Earth's
2044 magnetosphere, *Adv. Space Res., 21*, 609-613, 1998.
2045 Barnes, C.W., and Simpson, J.A.: Evidence for interplanetary acceleration of nucleons in
2046 corotating interaction regions, *Astrophys. J., 210,* L91, 1976.

2047 Bartels, J.: Terrestrial-magnetic activity in the years 1931 and 1932, *Terrestrial Magnetism and*
2048 *Atmospheric Electricity*, *39*, 1-4, 1934.
2049 Belcher, J.W., and Davis Jr., L.: Large-amplitude Alfvén waves in the interplanetary medium, 2,
2050 *J. Geophys. Res.*, *76*, 16, 3534-3563, 1971.
2051 Bieber, J. W., Clem, J., Evenson, P., Pyle, R., Sáiz, A., and Ruffolo, D.: *Astrophys. J.*, *771*, 92,
2052 2013.
2053 Blake, J.B., Kolasinski, W.A., Filius, R.W., and Mullen, E.G.: Injection of electrons and protons
2054 with energies of tens of MeV into L < 3 on March 24, 1991, *Geophys. Res. Lett.*, *19*, 821, 1992.
2055 Bombardieri, D. J., Duldig, M. L., Humble, J. E., and Michael, K. J.: An improved model for
2056 relativistic solar proton acceleration applied to the 2005 January 20 and earlier events,
2057 *Astrophysical J.*, *682*, 1315-1327, 2008.
2058 Boyd, A.J., Spence, H.E., Claudepierre, S.G., Fennell, J.F., Blake, J.B., Baker, D.N., Reeves, G.D.,
2059 and Turner, D.L.: Quantifying the radiation belt seed population in the March 17, 2013 electron
2060 acceleration event, *Geophys. Res. Lett.*, *41*, 2275-2281, https://doi.org/10.1002/2014GL059626,
2061 2014.
2062 Boyd, A.J., Spence, H.E., Huang, C.L., Reeves, G.D., Baker, D.N., Turner, D.L., Claudepierre,
2063 S.G., Fennell, J.F., Blake, J.B., and Shprits, Y.Y.: Statistical properties of the radiation belt seed
2064 population, *J. Geophys. Res. 121*, 7636-7646, https://doi.org/10.1002/2016JA022652, 2016.
2065 Bravo, S., and Otaola, J.A.: Polar coronal holes and the sunspot cycle. A new method to predict
2066 sunspot numbers, *Sol. Phys. 122*, 335. https://doi.org/10.1007/BF00913000, 1989.
2067 Bravo, S., and Stewart, G. A.: Fast and Slow Wind from Solar Coronal Holes, *Astrophys. J. 489*,
2068 992-999. https://doi.org/10.1086/304789, 1997.
2069 Brice, N.: Fundamentals of very low frequency emission generation mechanisms, *J. Geophys. Res.*,
2070 *69*, 4701, 1964.
2071 Buzulukova, N., *Extreme Events in Geospace, Origins, Predictability and Consequences*, Elsevier,
2072 Wash. D.C., 2018.
2073 Burlaga, L., Sittler, E., Mariani, F., and Schwenn, R.: Magnetic loop behind an interplanetary
2074 shock: Voyager, Helios and IMP 8 observations, *J. Geophys. Res.*, *86*, A8, 6673-6684, 1981.
2075 Burlaga, L., Fitzenreiter, R., Lepping, R., et al.: A magnetic cloud containing prominence material:
2076 January, 1997, *J. Geophys. Res.*, *103*, A1, 77-285, 1998.

2077 Burton, R. K., McPherron, R. L., and Russell, C. T.: An empirical relationship between
2078 interplanetary conditions and Dst, *J. Geophys. Res.*, *80*, 4204-4214, 1975.
2079 Carlson, C. W., McFadden, J. P., Ergun, R. E., Temerin, M., Peria, W., Mozer, F. S., Klumpar, D.
2080 M., Shelley, E. G., Peterson, W. K., Moebius, E., Elphic, R., Strangeway, R., Cattell, C., and Pfaff,
2081 R.: FAST observations in the downward auroral current region: Energetic upgoing electron beams,
2082 parallel potential drops, and ion heating, *Geophys. Res. Lett.*, *25*, 2017-2020, 1998.
2083 Carrington, R.C: Description of a singular appearance seen in the Sun on September 1, 1859, *Mon.*
2084 *Not. R. Astron. Soc.*, *XX*, 13, 1859.
2085 Chan, A.A., Xia, M., and Chen, L.: Anisotropic Alfvén-ballooning modes in Earth's
2086 magnetosphere, *J. Geophys. Res., 99*, 17351-17366, 1994.
2087 Chapman, S., and Bartels, J.: *Geomagnetism, vol. 1*, Oxford Univ. Press, New York, 1940.
2088 Cho, K.S., Bong, S.C., Moon, Y.J., Dryer, M., Lee, S.E. and Kim, K.H.: An empirical relationship
2089 between coronal mass ejection initial speed and solar wind dynamic pressure, *J. Geophys. Res.*,
2090 *115*, A10111, https://doi.org/10.1029/2009JA015139, 2010.
2091 Choe, G.S., LaBelle-Hamer, N., Tsurutani, B.T., and Lee, L.C.: Identification of a driver gas
2092 boundary layer, *EOS Trans. AGU*, 73, 485, 1992.
2093 Chree, C.: Review of Maunder's recent investigations on the causes of magnetic disturbances,
2094 *Terr. Mag.*, *10*, 9-14, 1905.
2095 Chree, C.: Some phenomena of sunspots and of terrestrial magnetism at Kew Observatory,
2096 *Philosophical Transactions of the Royal Society A, 212*, 75-116, 1913.
2097 Christon, S.P., and Simpson, J.A.: Separation of corotating nucleon fluxes from solar flare fluxes
2098 by radial gradients and nuclear composition, *Astrophys. J. Lett., 227*, L49, 1979.
2099 Clauer, C.R., and Siscoe, G.: The great historical geomagnetic storm of 1859: A modern look,
2100 Adv. Space Res. 38, 117-118. https://doi.org/10.1016/j.asr.2006.09.001, 2006.
2101 Cliver, E.W.: The 1859 space weather event : Then and now, *Adv. Spa. Res.*, *38*, 119-129, 2006.
2102 Cornwall, J.M.: Cyclotron instabilities and electromagnetic emission in the ultra low frequency
2103 and very low frequency ranges, *J. Geophys. Res., 70*, 61-69, doi:10.1029/JA0761004p00900,
2104 1965.
2105 Daglis, I. A., Thorne, R.M., Baumjohann, W., and Orsini, S.: The terrestrial ring current: origin,
2106 formation and decay, *Rev. Geophys.*, *37*, 4, 407-438, 1999.

2107 Dasso, S., Gómez, D., and Mandrini, C. H.: Ring current decay rates of magnetic storms: A
2108 statistical study from 1957 to 1998, J. Geophys. Res., 107(A5), 1059, doi:10.1029/2000JA000430,
2109 2002.
2110 Davis, T. N., and Sugiura, M.: Auroral electrojet activity index AE and its universal time
2111 variations, Journal of Geophysical Research, 71, 785-801,
2112 https://doi.org/10.1029/JZ071i003p00785, 1966.
2113 Davis, C.J., de Koning, C.A., Davies, J.A., Biesecker, D., Milward, G., Dryer, M., Deehr, C.,
2114 Webb, D.F., Schenk, K., Freeland, S.L., Mostl, C., Farrugia, C.J., and Odstrcil, D.: A comparison
2115 of space weather analysis techniques used to predict the arrival of the Earth-directed CME and its
2116 shock wave launched on 8 April 2010, *Space Weather 9,* S01005,
2117 https://doi.org/10.1029/2010SW00620, 2011.
2118 Deng, Y., Sheng, C., Tsurutani, B.T., and Mannucci, A.J.: Possible influence of extreme magnetic
2119 storms on the thermosphere in the high latitudes, *Space Weath*er 16,
2120 https://doi.org/10.1029/2018SW001847, 2018.
2121 Dessler, A.J., and Parker, E.N.: Hydromagnetic theory of magnetic storms, *J. Geophys. Res.*, *64*,
2122 2239, 1959.
2123 Dryer, M., Smith, Z. K., Steinolfson, R. S., Mihalov, J. D., Wolfe, J. H., and Chao, J.-K.:
2124 Interplanetary disturbances caused by the August 1972 solar flares as observed by Pioneer 9, *J.*
2125 *Geophys. Res.*, *81*, 4651-4663, doi: 10.1029/JA081i025p04651, 1976.
2126 Dungey, J.W.: Interplanetary magnetic field and the auroral zones, *Phys. Rev. Lett.*, *6*, 47, 1961.
2127 Ebihara, Y., and Ejiri, M.: Modeling of solar wind control of the ring current buildup: A case study
2128 of the magnetic storms in April 1997, Geophys. Res. Lett., 25(20), 3751–3754,
2129 doi:10.1029/1998GL900006, 1998.
2130 Echer, E., Gonzalez, W.D., Tsurutani, B.T., and Gonzalez, A.L.C.: Interplanetary conditions
2131 causing intense geomagnetic storms (Dst ≤-100 nT) during solar cycle 23 (1996-2006), *J.*
2132 *Geophys. Res.*, *113*, A05221, doi:10.1029/2007JA012744, 2008a.
2133 Echer, E., Gonzalez, W.D., and Tsurutani, B.T.: Interplanetary conditions leading to superintense
2134 geomagnetic storms (Dst ≤ -250 nT) during solar cycle 23, *Geophys. Res. Lett.*, *35*, L06S03,
2135 doi:10.1029/2007GL031755, 2008b.
2136 Echer, E., Tsurutani, B.T., and Guarnieri, F.L.: Solar and interplanetary origins of the November
2137 2004 superstorms, *Adv. Spa. Res.*, *44*, 615-620, 2009.

2138 Echer, E., Tsurutani, B.T., Guarnieri, F.L., and Kozyra, J.U.: Interplanetary fast forward shocks
2139 and their geomagnetic effects: CAWSES events, *J. Atmosph. Sol.-Terr. Phys., 73*, 1330-1338,
2140 2011.
2141 Elkington, S.R., Hudson, M.K., and Chan, A.A.: Acceleration of relativistic electrons via drift-
2142 resonant interaction with toroidal-mode Pc-5 ULF oscillations, *Geophys. Res. Lett., 26*, 3273,
2143 1999.
2144 Elkington, S.R., Hudson, M.K., and Chan, A.A.: Resonant acceleration and diffusion of outer zone
2145 electrons in an asymmetric geomagnetic field, *J. Geophys. Res., 108*, doi: 10.129/2001JA009202,
2146 2003.
2147 Elvey, C. T.: Problems in auroral morphology, *Proceedings of the National Academy of Sciences*
2148 *Jan 1957, 43* (1) 63-75; DOI: 10.1073/pnas.43.1.63, 1957.
2149 Emery, B.A., Richardson, I.G., Evans, D.S., Rich, F.J.: Solar wind structure sources and
2150 periodicities of auroral electron power over three solar cycles, *J. Atmos. Sol. Terr. Phys. 71*, 1157-
2151 1175. https://doi.org/10.1016/j.jastp.2008.08.005, 2009.
2152 Engebretson, M.J., Peterson, W.K., Posch, J.L., Klatt, M.R., Anderson, B.J., Russell, C.T., Singer,
2153 H.J., Arnoldy, R.L., and Fukunishi, H.: Observations of two types of Pc 1-2 pulsations in the outer
2154 dayside magnetosphere, *J. Geophys. Res. 107*, A12, 1415, doi:10.1029/2001JA00198, 2002.
2155 Falkenberg, T.V., Vrsnak, B., Taktakishvili, A., Odstrcil, D., MacNeice, P., Hesse, M.:
2156 Investigations of the sensitivity of a coronal mass ejection model (ENLIL) to solar input
2157 parameters, *Space Weather 8*, S06004. https://doi.org/10.1029/2009SW000555, 2010.
2158 Firoz, K. A., Gan, W. Q., Moon, Y.-J., and Li, C.: An interpretation of the possible mechanisms
2159 of two ground-level enhancement events, *Astrophys. J., 758*, 119, 2012.
2160 Foster, J.C., Wygant, J.R., Hudson, M.K., Boyd, A.J., Baker, D.N., Erikson, P.J., and Spence,
2161 H.E.: Shock-induced prompt relativistic electron acceleration in the inner magnetosphere, *J.*
2162 *Geophys. Res. Spa. Phys., 120*, 1661-1674, doi:10.1002/2014JA020642, 2015.
2163 Gonzalez, W.D., and Tsurutani, B.T.: Criteria of interplanetary parameters causing intense
2164 magnetic storms (Dst < -100 nT), *Planet. Spa. Sci., 35*, 1101, 1987.
2165 Gonzalez, W.D., Joselyn, J.A., Kamide, Y., Kroehl, H.W., Rostoker, G., Tsurutani, B.T., and
2166 Vasyliunas, V.M.: What is a geomagnetic storm?, *J. Geophys. Res., 99*, A4, 5571-5792, 1994.

2167 Gonzalez, W.D., Gonzalez, A.L.C., Dal Lago, A., Tsurutani, B.T., Arballo, J.K., Lakhina, G.S.,
2168 Buti, B., Ho, C.M., and Wu, S.-T.: Magnetic cloud field intensities and solar wind velocities,
2169 *Geophys. Res. Lett., 25*, 963-966, 1998.
2170 Gopalswamy, N., Lara, A., Yashiro, S., Kaiser, M., and Howard, R.A.: Predicting the 1-AU arrival
2171 times of coronal mass ejections, *J. Geophys. Res. 106*, 29207-29217, 2001.
2172 Gopalswamy, N.: Coronal mass ejections and their heliospheric consequences, in First Asia-
2173 Pacific Sol. Phys. Meet, vol. 2, edited by A. Choudhuri and D. Banerjee, *Astron. Soc. India Conf.*
2174 *Series*, pp. 241–258, 21024 Mrach, Bengaluru, India, 2011.
2175 Gosling, J.T., Bame, S.J., and Feldman, W.C.: Solar wind speed variations: 1962, *J. Geophys.*
2176 *Res., 81*, 5061, 1976.
2177 Guarnieri, F. L.: The nature of auroras during high-intensity long-duration continuous AE activity
2178 (HILDCAA) events: 1998–2001, in *Recurrent Magnetic Storms: Corotating Solar Wind Streams*,
2179 Geophys. Monogr. Ser., vol. *167*, edited by B. T. Tsurutani et al., pp. 235–243, AGU, Washington,
2180 D.C., 2006.
2181 Guarnieri, F. L., Tsurutani, B. T., Gonzalez, W. D., Echer, E., Gonzalez, A. L. C., Grande, M., and
2182 Soraas, F.: ICME and CIR storms with particular emphasis on HILDCAA events, *ILWS Workshop*
2183 2006, Goa, 2006.
2184 Guarnieri, F.L., Tsurutani, B.T., Vieira, L.E.A., Hajra, R., Echer, E., Mannucci, A.J., and
2185 Gonzalez, W.D.: A correlation study regarding the AE index and ACE solar wind data for Alfvénic
2186 intervals using wavelet decomposition and reconstruction, *Nonl. Proc. Geophys. 25*, 67-76,
2187 https://doi.org/10.5194/npg-25-67-2018, 2018.
2188 Haerendel, G.: Acceleration from field-aligned potential drops, *Astrophys. J. Suppl. Ser., 90*, 765,
2189 1994.
2190 Hajra, R., Echer, E., Tsurutani, B.T., and Gonzalez, W.D.: Solar cycle dependence of high-
2191 intensity long-duration continuous AE activity (HILDCAA) events, relativistic electron
2192 predictors?, *J. Geophys. Res. Spa. Phys., 118*, doi:10.1002/jgra.50530, 2013.
2193 Hajra, R., Echer, E., Tsurutani, B.T., and Gonzalez, W.D.: Solar wind-magnetosphere energy
2194 coupling efficiency and partitioning: HILDCAAs and preceding CIR storms during solar cycle 23,
2195 *J. Geophys. Res. Spa. Phys., 119*, 2675-2690, 2014a.

2196 Hajra, R., Echer, E., Tsurutani, B. T., and Gonzalez, W. D.: Superposed epoch analyses of
2197 HILDCAAs and their interplanetary drivers: solar cycle and seasonal dependences, *J. Atmos. Sol.*
2198 *Ter. Phys.*, *121*, 24-31, 2014b.
2199 Hajra, R., Tsurutani, B. T., Echer, E., and Gonzalez, W. D.: Relativistic electron acceleration
2200 during high-intensity, long-duration, continuous AE activity (HILDCAA) events: solar cycle
2201 phase dependences, *Geophys. Res. Lett.*, *41*, 1876-1881, 2014c.
2202 Hajra, R., Tsurutani, B.T., Echer, E., Gonzalez, W.D., and Santolik, O.: Relativistic (E > 0.6, >2.0,
2203 and > 4.0 MeV) electron acceleration at geosynchronous orbit during high-intensity long-duration
2204 continuous AE activity (HILDCAA) events, *Ap. J.*, *799:*39, doi:10.1088/0004-637X/799/1/39,
2205 2015a.
2206 Hajra, R., Tsurutani, B. T., Echer, E., Gonzalez, W. D., Brum, C. G. M., Vieira, L. E. A., and
2207 Santolik, O.: Relativistic electron acceleration during HILDCAA events: are precursor CIR
2208 magnetic storms important?, *Earth, Planets and Space, 67*, 109, doi:10.1186/s40623-015-0280-5,
2209 2015b.
2210 Hajra, R., Tsurutani, B.T., Echer, E., Gonzalez, W.D., and Gjerloev, J.W.: Supersubstorms (SML
2211 < -2500 nT): Magnetic storm and solar cycle dependences, *J. Geophys. Res. Spa. Phys.*, *121*, 7805-
2212 7816, doi:10.1002/2015JA021835, 2016.
2213 Hajra, R., Tsurutani, B. T., Brum, C. G. M., and Echer, E.: High-speed solar wind stream effects
2214 on the topside ionosphere over Arecibo: a case study during solar minimum, *Geophys. Res. Lett.*,
2215 *44*, 7607-7617, doi:10.1002/2017GL073805, 2017.
2216 Hajra, R., and Tsurutani, B. T.: Magnetospheric "killer" relativistic electron dropouts (REDs) and
2217 repopulation: a cyclical process, in *Extreme Events in Geospace: Origins, Predictability, and*
2218 *Consequences*, N. Buzulukova (Eds), pages 373-400, Elsevier, https://doi.org/10.1016/B978-0-
2219 12-812700-1.00014-5, 2018a.
2220 Hajra, R., and Tsurutani, B. T.: Interplanetary shock inducing magnetospheric supersubstorms
2221 (SML < -2500 nT): Unusual auroral morphologies and energy flow, *Astrophys. J.*, *858*:123,
2222 https://doi.org/10.3847/1538-4357/aabaed, 2018b.
2223 Hajra, R., Tsurutani, B.T., and Lakhina, G.S.: The complex space weather events of September
2224 2017, submitted to *J. Geophys. Res.*, 2019.
2225 Hale, G.E.: The spectrohelioscope and its work Part III. Solar eruptions and their apparent
2226 terrestrial effects, *Astrophys. J.*, 73:379-412, 1931.

2227 Halford, A.J., Fraser, B.J., and Morley, S.K.: EMIC wave activity during geomagnetic storm and
2228 nonstorm periods: CRRES results, *J. Geophys. Res.*, *115*, A12248, doi:10.1029/2010JA015716,
2229 2010.
2230 Halford, A.J., McGregor, S.L., Murphy, K.R., Millan, R.M., Hudson, M.K., Woodger, L.A.,
2231 Cattel, C.A., Breneman, A.W., Mann, I.R., Kurth, W.S., Hospodarsky, G.B., Gkioulidou, M., and
2232 Fennel, J.F.: BARREL observations of an ICME-shock impact with the magnetosphere and the
2233 resultant radiation belt electron loss, *J. Geophys. Res. Spa. Phys.*, *120*, 2557-2570, 2015.
2234 Halford, A.J., McGregor, S.L., Hudson, M.K., Milan, R.M., and Kress, B.T.: BARREL
2235 observations of a solar energetic electron and solar energetic proton event, *J. Geophys. Res. Spa.*
2236 *Phys.*, *121*, 4205-4216, doi:10.1002/2016JA022462, 2016.
2237 Hamilton, D. C., Gloeckler, G., Ipavich, F. M., Stüdemann, W., Wilken, B., and Kremser, G.: Ring
2238 current development during the great geomagnetic storm of February 1986, *J. Geophys. Res.*,
2239 *93*(A12), 14343-14355, doi:10.1029/JA093iA12p14343, 1988.
2240 Hanslmeier, A., *The Sun and Space Weather* (2007), Springer Netherlands, edition 2.
2241 https://doi.org/10.1007/978-1-4020-5604-8.
2242 Harada, Y., Goto, A., Hasegawa, H., Fujikawa, N., Naoe, H., and Hirooka, T.: A major
2243 stratospheric sudden warming event in January 2009, *J. Atmos. Sci.*, *67*, 2052,
2244 doi:10.1175/2009JA53310.1, 2010.
2245 Hellinger, P., and Travnicek, P.M.: Oblique proton fire hose instability in the expanding solar
2246 wind: Hybrid simulations, *J. Geophys. Res.*, *113*, A10109, https://doi.org/10.1029/2008JA013416,
2247 2008.
2248 Heppner, J.P.: Note on the occurrence of world-wide SSCs during the onset of negative bays at
2249 College, Alaska, *J. Geophys. Res.*, *60*, 29, 1955.
2250 Hodgson, R.: On a curious appearance seen in the Sun, *Mon. Not. R. Astron. Soc.*, *XX*, 15, 1859.
2251 Hollweg, J.V.: The solar wind: Then and now, in *Recurrent Magnetic Storms: Corotating Solar*
2252 *Wind Streams* (Vol. 167, pp. 19-27), edited by B.T. Tsurutani, R.L. McPherron, W.D. Gonzalez,
2253 G. Lu, J.H.A. Sobral and N. Gopalswamy, AGU Press, Wash D.C., 2006.
2254 Hones, E.W. Jr.: Transient phenomena in the magnetotail and their relation to substorms, *Spa. Sci.*
2255 *Rev.*, *23*, 393-410, 1979.

2256 Horne, R. B., and Thorne, R. M.: Potential waves for relativistic electron scattering and stochastic
2257 acceleration during magnetic storms, *Geophys. Res. Lett., 25,* 3011-3014,
2258 https://doi.org/10.1029/98GL01002, 1998.
2259 Huba, J.D., Joyce, G., and Fedder, J.A.: Sami2 is another model of the ionosphere (SAMI2): A
2260 new low-latitude ionosphere model, *J. Geophys. Res., 105* (A10), 23035, 2000.
2261 Huba, J.D., Dymond, K.F., Joyce, G., Budzien, S.A., Thonnard, S.E., Fedder, J.A., and McCoy,
2262 R.P.: Comparison of O+ density from ARGOS LORAAS data analysis and SAMI2 model results,
2263 *Geophys. Res. Lett., 29* (7), 6-1, doi:10.1029/2001GL013089, 2002.
2264 Hudson, M.K., Elkington, S.R., Lyon, J.G., Goodrich, C.C., and Rosenberg, T.J.: Simulations of
2265 radiation belt dynamics driven by solar wind variations, in *Sun-Earth Plasma Connections*, edited
2266 by J. Burch, R.L Carovillano, and S.K. Antiochos, Amer. Geophys. Un. Press, Wash. D.C., 171,
2267 1999.
2268 Illing, R.M.E. and Hundhausen, A.J.: Disruption of a coronal streamer by an eruptive prominence
2269 and coronal mass ejection, *J. Geophys. Res., 91,* A10, 10,951-10,960, 1986.
2270 Inan, U.S., Bell, T.F., and Helliwell, R.A.: Nonlinear pitch angle scattering of energetic electrons
2271 by coherent VLF waves in the magnetosphere, *J. Geophys. Res., 83,* 3235-3253, 1978.
2272 Iyemori, T.: Storm-time magnetspheric currents inferred from midlatitude geomagnetic field
2273 variations, *J. Geomag. Geoelectr. 42,* 1249, 1990.
2274 Jackson, B.V., Odstrcil, D., Yu, H.S., Hick, P.P., Buffington, A., Mejia-Ambriz, J.C., Kim, J.,
2275 Hong, S., Kim, Y., Han, J., and Tokumaru, M.: The UCSD kinematic IPS solar wind boundary
2276 and its use in the ENLIL 3-D MHD prediction model, *Space Weather 13*, 104-115, 2015.
2277 Jian, L.K., MacNeice, P.J., Taktakishvili, A., Odstrcil, D., Jackson, B., Yu, H.S., Riley, P.,
2278 Sokolov, I.V., and Evans, R.M.: Validation of solar wind prediction at Earth: Comparison of
2279 coronal and heliospheric models installed at the CCMC, *Space Weather 13*, 316-338, 2015.
2280 Jian, L.K., MacNeice, P.J., Mays, M.L., Taktakishvili, A., Odstrcil, D., Jackson, B., Yu, H.S.,
2281 Riley, P., and Sokolov, I.V.: Validation for global solar wind prediction using Ulysses comparison:
2282 Multiple coronal and heliospheric models installed at the Community Coordinated Modeling
2283 Center, *Space Weather 14*, 592-611, 2016.
2284 Jordanova, V. K., Farrugia, CJ., Janoo, L., Quinn, J.M., Torbert, R.B., Ogilvie, K.W., and Belian,
2285 R.D.: October 1995 magnetic cloud and accompanying storm activity: Ring current evolution, *J.*
2286 *Geophys. Res., 103,* 79-92, https://doi.org/10.1029/97JA02367, 1998.

2287 Joselyn, J. A., and Tsurutani, B. T.: Geomagnetic sudden impulses and storm sudden
2288 commencements, A note of terminology, *EOS, 71*, 47, 1808-1809, 1990.
2289 Kellerman, A.C., and Shprits, Y.Y.: On the influence of solar wind conditions on the outher-
2290 electron radiation belts, *J. Geophys. Res., 117*, A05127, doi:0.1029/2011JA017253, 2012.
2291 Kellerman, A.C., Shprits, Y.Y., Kondrashov, D., Subbotin, D., Makarevich, R.A., Donovan, E.,
2292 and Nagal, T.: Three-dimensional data assimilation and reanalysis of radiation belt electrons:
2293 Observations of a four-zone structure using five spacecraft and the VERB code, *J. Geophys. Res.*
2294 *Spa. Phys., 119*, doi:10.1002/2014JA020171, 2014.
2295 Kelley, M.C., Fejer, B.G., and Gonzales, C.A.: An explanation for anomalous equatorial
2296 ionospheric electric field associated with a northward turning of the interplanetary magnetic field,
2297 *Geophys. Res. Lett., 6*(4), 301, 1979.
2298 Kelley, M.C., Makela, J.J., Chau, J.L., and Nicolls, M.J.: Penetration of the solar wind electric
2299 field into the magnetsphere/ionosphere system, *Geophys. Res. Lett., 30*(4), 1158,
2300 doi:10.1029/2002GL016321, 2003.
2301 Kennel, C.F., and Petschek, H.E.: Limit of stably trapped particle fluxes, *J. Geophys. Res. 71*, 1-
2302 28, 1966.
2303 Kennel, C.F., Edmiston, J.P., and Hada, T.: A quarter century of collisionless shock research in
2304 Collisionless *Shocks in the Heliosphere: A Tutorial Review*, Geophys. Mon. Ser., vol. *34*, 1, AGU,
2305 Wash. D.C., 1985.
2306 Kikuchi, T., and Hashimoto, K.K.: Transmission of the electric fields to the low latitude
2307 ionosphere in the magnetosphere-ionosphere current circuit, *Geosc. Letts.*, 3:4,
2308 doi:10.1186/s40562-016-0035-6, 2016.
2309 Kim, R.S., Cho, K.S., Moon, Y.J., Dryer, M., Lee, J., Yi, Y., Kim, K.H., Wang, H., Park, Y.D.,
2310 and Kim, Y.H.: An empirical model for prediction of geomagnetic storms using initially observed
2311 CME parameters at the Sun, *J. Geophys. Res. 115*, A12108,
2312 https://doi.org/10.1029/2010JA015322, 2010.
2313 Kim, R.S., Moon, Y.J., Gopalswamy, N., Park, Y.D., and Kim, Y.H.: Two-step forecast of
2314 geomagnetic storm using coronal mass ejection and solar wind condition, *Space Weather 12*, 246-
2315 256. https://doi.org/10.1002/2014SW001033, 2014.
2316 Kimball, D.S.: A study of the aurora of 1859, *Sci. Rept. 6, UAG-R109*, Univ. of Alaska, Fairbanks,
2317 Alaska, 1960.

2318 Klein, L.W., and Burlaga, L.F.: Interplanetary magnetic clouds at 1 AU, *J. Geophys. Res.*, *87*, 613,
2319 1982.
2320 Knipp, D. J., Hapgood, M.A., and Welling, D.: Communicating uncertainty and reliability in space
2321 weather data, models, and applications. *Space Weath*er *16*, 1453-1454.
2322 https://doi.org/10.1029/2018SW002083, 2018.
2323 Koskinen, H., *Physics of Space Storms: From the Solar Surface to the Earth* (2011), Springer-
2324 Verlag, Berlin, Edition 1. https://doi.org/10.1007/978-3-642-00319-6.
2325 Kozyra, J.U., Jordanova, V.K., Horne, R.B., and Thorne, R.M.: Modeling of the contribution of
2326 electromagnetic ion cyclotron (EMIC) waves to stormtime ring current erosion, in *Magnetic*
2327 *Storms*, Geophys. Mon. Ser., *98*, edited by B.T. Tsurutani et al., 187-202, 1997.
2328 Kozyra, J. U., Liemohn, M. W., Clauer, C. R., Ridley, A. J., Thomsen, M. F., Borovsky, J. E.,
2329 Roeder, J. L., Jordanova, V. K., and Gonzalez, W. D.: Multistep Dst development and ring current
2330 composition changes during the 4-6 June 1991 magnetic storm, *J. Geophys. Res.*, *107*(A8), 1224,
2331 doi:10.1029/2001JA000023, 2002.
2332 Kozyra, J.U., Nagy, A.F., Slater, D.W.: High-altitude energy source(s) for stable auroral red arcs,
2333 *Rev. Geophys.*, *35*, 155-190, 2006a.
2334 Kozyra, J. U., Crowley, G., Emery, B. A., Fang, X., Maris, G., Mlynczak, M. G., Niciejewski, R.
2335 J., Palo, S. E., Paxton, L. J., Randal, C. E., Rong, P. P., III Russell, J. M., Skinner, W., Solomon,
2336 S. C., Talaat, E. R., Wu, Q., and Yee, J. H.: Response of the upper/middle atmosphere to coronal
2337 holes and powerful high-speed solar wind streams in 2003, in *Recurrent Magnetic Storms:*
2338 *Corotating Solar Wind Streams*, Geophys. Monogr. Ser., vol. 167, edited by B. T. Tsurutani et al.,
2339 pp. 319, AGU, Washington, D.C., doi: 10.1029/167GM24, 2006b.
2340 Kozyra, J.U., Manchester IV, W.B., Escoubet, C.P. et al.: Earth's collision with a solar filament
2341 on 21 January 2005: Overview, *J. Geophys. Res. Spa. Phys.*, *118*, doi:10.1002/jgra.50567, 2013.
2342 Krieger, A.S., Timothy, A.F., and Roelof, E.C.: A coronal hole and its identification as the source
2343 of a high velocity solar wind stream, *Sol. Phys. 23*, 123, 1973.
2344 Lakhina, G.S.: Magnetic reconnection, *Bull. Astr. Soc. India*, *28*, 593-646, 2000.
2345 Lakhina, G.S., Alex, S., Tsurutani, B.T., and Gonzalez, W.D.: Supermagnetic storms: Hazards to
2346 society, in *Extreme Events and Natural Hazards: The Complexity Perspective*, Geophys. Mon.,
2347 196, 267-278, 2012.

Lakhina, G.S., and Tsurutani, B.T.: Satellite drag effects due to uplifted Oxygen neutrals during super magnetic storms, *Nonl. Proc. Geophys. 24*, 745-750. https://doi.org/10.5194/npg-24-745-2017, 2017.

Lakhina, G.S., and Tsurutani, B.T.: Supergeomagnetic storms: Past, present and future, Chapter 7 in *Extreme Events in Geospace*, *157*, edited by N. Buzulokova, Elsevier, 2018.

Lam, M.M., Chisham, G., and Freeman, M.P.: The interplanetary magnetic field influences mid-latitude surface atmospheric pressure, *Env. Res. Lett., 8*, doi:10.1088/1748-9326/8/4/045001, 2013.

Lario, D.: Estimation of the solar flare neutron worst-case fluxes and fluences for missions traveling close to the Sun, *Space Weather, 10,* S03002, doi: 10.1029/2011SW000732, 2012.

Leamon, R.J., Canfield, R.C., Jones, S.L., Lambkin, K., Lundberg, B.J., and Pevtsov, A.A.: Helicity of magnetic clouds and their associated active regions, *J. Geophys. Res. 109*, A05106. https://doi.org/10.1029/2003JA010324, 2004.

Lee, K. H.: Generation of parallel and quasi-perpendicular EMIC waves and mirror waves by fast magnetosonic shocks in the solar wind, *J. Geophys. Res., 122*, 7307-7322, 2017.

Lepri, S.T., and Zurbuchen, T.H.: Directo observational evidence of filament material within interplanetary coronal mass ejections, *Astrophys. J. Lett., 723*, L22-L27. https://doi.org/10.1088/2041-8205/723/1/L22, 2010.

Li, X., Roth, I., Temerin, M., Wygant, J.R., Hudson, M.K., and Blake, J.B.: Simulation of the prompt energization and transport of radiation belt particles during the March 24, 1991 SSC, *Geophys. Res. Lett., 20*, 22, 2423-2426, 1993.

Li, X.-L., Temerin, M., Baker, D.N., Reeves, G.D., and Larson, D.: Quantitative prediction of radiation belt electrons at geostationary orbit based on solar wind measurements, *Geophys. Res. Lett., 28*, 1887, 2001.

Li, X., Baker, D.N., Temerin, M., Reeves, G., Friedel, R., and Shen, C.: Energetic electrons, 50 keV to 6 MeV, at geosynchronous orbit: their responses to solar wind variations, *Space Weather, 3*. S04001. https://doi.org/10.1029/2004SW000105, 2005.

Li, X., Temerin, M., Tsurutani, B.T., and Alex, S.: Modeling of 1-2 September 1859 super magnetic storm, *Adv. Spa. Res., 38*(2), 273-279, https://doi.org/10.1016/jasr.2005.06.070, 2006.

Lui, A.T.Y, Chang, C.-L., Mankofsky, A., Wong, H.-K., and Winske, D.: A cross-field current instability for substorm expansions, *J. Geophys. Res., 96*, 11389, 1991.

2379 Lui, A.T.Y.: Current disruption in the Earth's magnetosphere: Observations and models, *J.*
2380 *Geophys. Res.*, *101*, 13067-13088, doi:10.1029/96JA00079, 1996.
2381 Luhmann, J. G., Mays, M.L., Odstrcil, D., Li, Y., Bain, H., Lee, C.O., Galvin, A.B., Mewaldt,
2382 R.A., Cohen, C.M.S., Leske, R.A., Larson, D., and Futaana, Y.: Modeling solar energetic particle
2383 events using ENLIL heliosphere simulations, *Space Weather 15*, 934-954, 2017.
2384 Manchester, W.B. IV, Ridley, A.J., Gombosi, T.I., and Dezeeuw, D.L.: Modeling the Sun-to-Earth
2385 propagation of a very fast CME, *Adv. Space Res.*, *38*, 253-262, 2006.
2386 Mann, I.R., O'Brien, T.P., and Milling, D.K.: Correlations between ULF wave power, solar wind
2387 speed, and relativistic electron flux in the magnetosphere: solar cycle dependence, *J. Atmosph.*
2388 *Solar-Terr. Phys.*, *66*, 187, 2004.
2389 Mannucci, A.J., Tsurutani, B.T., Iijima, B.A., Konjathy, A., Saito, A., Gonzalez, W.D., Guarnieri,
2390 F.L., Kozyra, J.U., and Skoug, R.: Dayside global ionospheric response to the major interplanetary
2391 events of October 29-30, 2003 "Halloween storms", *Geophys. Res. Lett.*, *32*, L12S02,
2392 doi:10.1029/2004GL021467, 2005.
2393 Mannucci, A.J., Tsurutani, B.T., Abdu, M.A., Gonzalez, W.D., Komjathy, A., Echer, E., Iijima,
2394 B.A., Crowley, G., and Anderson, D.: Superposed epoch analysis of the dayside ionospheric
2395 response to four intense geomagnetic storms, *J. Geophys. Res.*, *113*, A00A02,
2396 doi:10.1029/2007JA012732, 2008.
2397 Matteini, L., Landi, S., Hellinger, P., and Velli, M.: Parallel proton fire hose instability in the
2398 expanding solar wind: Hybrid simulations, *J. Geophys. Res.*, *111*, A10101,
2399 https://doi.org/10.1029/2006JA011667, 2006.
2400 Matteini, L., Landi, S., Hellinger, P., Pantellini, F.G., Maksimovic, M., Velli, M., et al.: The
2401 evolution of the solar wind proton temperature anisotropy from 0.3 to 2.5 AU, *Geophys. Res. Lett.*,
2402 *34*, L20105, https://doi.org/10.1029/2007GL030920, 2007.
2403 Maunder, E. W.: Magnetic Disturbances, 1882 to 1903, as recorded at the Royal Observatory,
2404 Greenwich, and their Association with Sun-spots, *Monthly Notices of the Royal Astronomical*
2405 *Society*, *65*, 2-18, https://doi-org.insu.bib.cnrs.fr/10.1093/mnras/65.1.2, 1904.
2406 Mays, M. L., Thompson, B.J., Jian, L.K., Colaninno, R.C., Odstrcil, D., Mostl, C., Temmer, M.,
2407 Savani, N.P., Collinson, G., Taktakishvili, A., MacNeice, P.J., and Zheng, Y.: *Astrophys J.*,
2408 *812:145*, doi:10.1088/004-637X/812/2/145, 2015.

McComas, D.J. et al.: Ulysses second fast latitude scan; complexity near solar maximum and the reformation of polar coronal holes, *Geophys. Res. Lett., 29(9)*, 1290, doi:10.1029/2001GL014164, 2002.

McDonald, F.B., Teegarden, B.J., Trainor, J.H., Von Rosenvinge, T.T., and Webber, W.R.: The interplanetary acceleration of energetic nucleons, *Astrophys. J. Lett., 203*, L149, 1976.

Mendes, O., Domingues, M. O., Echer, E., Hajra, R., and Menconi, V. E.: Characterization of high-intensity, long-duration continuous auroral activity (HILDCAA) events using recurrence quantification analysis, *Nonlin. Processes Geophys., 24*, 407-417, 2017.

Meng, X., Tsurutani, B.T., and Mannucci, A.J.: The solar and interplanetary causes of superstorms (minimum *Dst* ≤ −250 nT) during the space age, *J. Geophysi. Res., 124*. https://doi.org/10.1029/2018JA026425, 2019a.

Meng, X., Mannucci, A.J., Verkhoglyadova, O.P., Tsurutani, B.T., Ridley, A.J., and Shim, J.S.: Thermosphere-ionosphere modeling with forecastable inputs: Case study of the June 2012 high speed stream geomagnetic storm, submitted to *J. Geophys. Res., Spa. Phys.*, 2019b.

Meredith, N. P., Horne, R.B., Iles, R.H.A., Thorne, R.M., Heynderickx, D., and Anderson, R. R: Outer zone relativistic electron acceleration associated with substorm-enhanced whistler mode chorus, *J. Geophys. Res., 107*, A7, 1144, doi:10.1029/2001JA900146, 2002.

Miyake, F., Nagaya, K., Masuda, K., and Nakamura, T.: A signature of cosmic-ray increase in AD 774-775 from tree rings in Japan, *Nature Lett.*, doi:10.1038/nature11123, 2012.

Miyoshi, Y., Jordanova, V.K., Morioka, A., and Evans, D.S.: Solar cycle variations of the electron radiation belts: Observations and radial diffusion simulation, *Space Weather, 2*, S10S02, doi:10.1029/2004SW000070, 2004.

Monreal MacMahon, R., and Llop, C.: Ring current decay time model during geomagnetic storms: A simple analytical approach, *Ann. Geophys., 26*, 2543-2550, 2008.

Mostl, C., Rollett, T., Frahm, R.A., Liu, Y.D., Long, D.M., Colaninno, R.C., Reiss, M.A., Temmer, M., Farrugia, C.J., Posner, A., Dumbovic, M., Janvier, M., Demoulin, P., Boakes, P., Devos, A., Kraaikamp, E., Mays, M.L., and Vrsnak, B.: Strong coronal channeling and interplanetary evolution of a solar storm up to Earth and Mars, *Nat. Comm., 6:7135*, doi:10.1038/ncomms8135, 2015.

Newton, H.W.: Solar flares and magnetic storms, *Mon. Not. R. Astron. Soc., 103*, 244, 1943.

2439 Ngwira, C.M., Pulkkinen, A., Kuznetsova, M.M., and Glocer, A.: Modeling extreme "Carrington-
2440 type" space weather events using three dimensional global MHD simulations, *J. Geophys. Res.*
2441 *Spa. Phys. 119*, 4456-4474, https://doi.org/10.1002/2013JA019661, 2014.
2442 Ngwira, C.M., Pulkkinen, A., Kuznetsova, M.M., and Glocer, A.: Reply to comments by Tsurutani
2443 et al. on "Modeling extreme 'Carrington-type' space weather events using three-dimensional
2444 global MHD simulations", *J. Geophys. Res. 123,* 1393-1395.
2445 https://doi.org/10.1002/201/2017ja024928, 2018.
2446 Nishida, A., and Jacobs, J.A.: Equatorial enhancement of world-wide changes, J. Geophys. Res.,
2447 67, 12, 4937-4940, 1962.
2448 Nishida, A.: Coherence of geomagnetic DP2 fluctuations with interplanetary magnetic variations,
2449 *J. Geophys. Res., 73*, 5549, 1968.
2450 Nishida, A.: *Geomagnetic Diagnosis of the Magnetosphere*, Springer-Verlag, New York, 1978.
2451 Nishiura, M., Yoshida, Z., Saitoh, H., Yano, Y., Kawazura, Y., Nogami, T., Yamasaki, M.,
2452 Mushiake, T., and Kashyap, A.: Improved beta (local beta > 1) and density in electron cyclotron
2453 resonance heating on the RT-1 magnetosphere plasma, *Nuc. Fus., 55*, 053019, doi:10.1088/0029-
2454 5515/5/053019, 2015.
2455 Obayashi, T.: The interaction of solar plasma with geomagnetic field, disturbed conditions, in *Sol.*
2456 *Terr. Phys*., edited by J.W. King and W.S. Newman, 107 pp., Academic Press, London, 1967.
2457 O'Brien, T. P., and McPherron, R. L.: An empirical phase space analysis of ring current dynamics:
2458 Solar wind control of injection and decay, *J. Geophys. Res., 105*(A4), 7707–7719,
2459 doi:10.1029/1998JA000437, 2000.
2460 O'Brien, T.P., McPherron, R.L., Sornette, D., Reeves, G.D., Friedel, R., and Singer, H.J.: Which
2461 magnetic storms produce relativistic electrons at geosynchronous orbit?, *J. Geophys. Res., 106*,
2462 15533, 2001.
2463 Odstrcil, D., and Pizzo, V.J.: Three-dimensional propagation of coronal mass ejections (CMEs) in
2464 a structured solar wind flow 1. CME launched within the streamer belt, *J. Geophys. Res., 104,* A1,
2465 483-492, 1999a.
2466 Odstrcil, D., and Pizzo, V.J.: Three-dimensional propagation of coronal mass ejections (CMEs) in
2467 a structured solar wind flow 2. CME launched adjacent to the streamer belt, *J. Geophys. Res., 104,*
2468 493-503, 1999b.

2469 Olsen, J.V., and Lee, L.C.: PC1 wave generation by sudden impulses, *Plan. Spa. Sci., 31*, 295,
2470 1983.
2471 Palmerio, E., Kilpua, E.K.J., Mostl, C., Bothmer, V., James, A.W., Green, L.M., Isavnin, A.,
2472 Davies, J.A., and Harrison, R.A.: Coronal magnetic structure of earthbound CMEs and in situ
2473 comparison, *Space Weather 16*, 442-460, 2018.
2474 Pérez-Peraza, J., Vashenyuk, E. V., Miroshnichenko, L. I., Balabin, Yu. V., and Gallegos-Cruz,
2475 A.: Impulsive, stochastic, and shock wave acceleration of relativistic protons in large solar events
2476 of 1989 September 29, 2000 July 14, 2003 October 28, and 2005 January 20, *Astrophys. J.*, *695*,
2477 865-873, 2009.
2478 Perreault, P., and Akasofu, S. I.: A study of geomagnetic storms, *Geophysical Journal*
2479 *International*, *54*, 547-573, https://doi.org/10.1111/j.1365-246X.1978.tb05494.x, 1978.
2480 Pesses, M.E., Van Allen, J.A., and Goertz, C.K.: Energetic protons associated with interplanetary
2481 active regions 1-5 AU from the sun, *J. Geophys. Res.*, *83*, 553, 1978.
2482 Pesses, M.E, Tsurutani, B.T., Van Allen, J.A., and Smith, E.J.: Acceleration of energetic protons
2483 by interplanetary shocks, *J. Geophys. Res.*, *84*, 7297, 1979.
2484 Phillips, J.L., Bame, S.J., Feldman, W.C., Goldstein, B.E., Gosling, J.T., Hammond, C.M.,
2485 McComas, D.J., Neugebauer, M., Scime, E.E., and Suess, S.T.: Ulysses solar wind plasma
2486 observations at high southerly latitudes, *Science*, *268*, 1030, 1995.
2487 Pizzo, V.J., Koning, C., Cash, M., Millward, G., Biesecker, D.A., Puga, L., Codrescu, M., and
2488 Odstrcil, D.: Theoretical basis for operational ensemble forecasting of coronal mass ejections,
2489 *Space Weather 13*, 676-697. https://doi.org/10.1002/2015SW001221, 2015.
2490 Rae, I.J., Murphy, K.R., Watt, C.E.J., Halford, A.J., Mann, I.R., Ozeke, L.G., Sibeck, D.G.,
2491 Clilverd, M.A., Rodger, C.J., Degeling, A.W., Forsyth, C., Singer, H.J.: The role of localized
2492 compressional ultra-low frequency waves in energetic electron precipitation, *J. Geophys. Res. 123*,
2493 1900-1914. https://doi.org/10.1002/2017JA024674, 2018.
2494 Randall, C.E., Harvey, V.L., Singleton, C.S., Bailey, S.M., Bernath, P.F., Codrescu, M., Nakajima,
2495 H., and Russell, J.M.: Energetic particle precipitation effects on the Southern Hemisphere
2496 stratosphere in 1992-2005, *J. Geophys. Res. 112*, D08308. https://doi.org/10.1029/2006JD007696,
2497 2007.

Randall, C.E., Harvey, V.L., Siskind, D.E., France, J., Bernath, P.F., Boone, C.D., and Walker, K.A.: NOx descent in the Arctic middle atmosphere in early 2009, *Geophys. Res. Lett. 36*, L18811. https://doi.org/10.1029/2009GL039706, 2009.

Reames, D.V.: Particle acceleration at the Sun and in the heliosphere, *Spa. Sci. Rev.*, *90*, 413-491, 1999.

Reeves, G.D., Spence, H.E., Henderson, M.G., Morley, S.K., Friedel, R.H.W., Funsten, H.O., Baker, D.N., Kanekal, S.G., Blake, J.B., Fennell, J.F., Claudepierre, S.G., Thorne, R.M., Turner, D.L., Kletzing, C.A., Kurth, W.S., Larsen, B.A., and Niehof, J.T.: Electron acceleration in the heart of the Van Allen radiation belts, *Science, 341*, 991-994, https://doi.org/10.1126/science.1237743, 2013.

Reeves, G.D., Friedel, R.H.W., Larsen, B.A., Skoug, R.M., Funsten, H.O., Claudepierre, S.G., Fennell, J.F., Turner, D.L., Denton, M.H., Spence, H.E., Blake, J.B., and Baker, D.N.: Energy dependent dynamics of keV to MeV electrons in the inner zone, outer zone, and slot regions, *J. Geophys. Res. 121*, 397-412, https://doi.org/10.1002/2015JA021569, 2016.

Reikard, G.: Forecasting geomagnetic activity at monthly and annual horizons: Time series models, *J. Atmos. Sol.-Terr. Phys., 133*, 111-120, 2015.

Reikard, G.: Forecasting space weather over short horizons: Revised and updated estimates, *New Astron., 62*, 62-69, 2018.

Remya, B., Tsurutani, B.T., Reddy, R.V., Lakhina, G.S., and Hajra, R.: Electromagnetic cyclotron waves in the dayside subsolar outer magnetosphere generated by enhanced solar wind pressure: EMIC wave coherency, *J. Geophys. Res. Spa. Phys.*, *120*, 7536-7551, doi:10.1002/2015JA021327, 2015.

Riley, P., Caplan, R.M., Giacalone, J., Lario, D., and Liu, Y.: Properties of the fast forward shock driven by the 2012 July 23 extreme coronal mass ejection, *Astrophys. J.*, *819*:57, doi:10.3847/0004-637X/819/1/57, 2016.

Saikin, A.A., Zhang, J.-C., Smith, C., Spence, H.E., Torbert, R.B., and Kletzing, C.A.: The dependence on geomagnetic conditions and solar wind dynamic pressure of the spatial distributions of EMIC waves observed by the Van Allen Probes, *J. Geophys. Res. Spa. Phys.*, *121*, 4362-4377, doi:10.1002/2016JA022523, 2016.

2527 Saitoh, H., Yano, Y., Yoshida, Z., Nishiura, M., Morikawa, J., Kawazura, Y., Nogami, T., and
2528 Yamasaki, M.: Observation of a new high-β and high-density state of a magnetospheric plasma in
2529 RT-1, *Phys. Plas. 21*, 082511, 2014.
2530 Saldanha, R., S. Krucker, and R.P. Lin, Hard x-ray spectral evolution and production of solar
2531 energetic particle events during the January 2005 x-class flares, *Astrophys. J., 673*, 1169-1173,
2532 2008.
2533 Savani, N.P., Vourlidas, A., Szabo, A., Mays, M.L., Richardson, I.G., Thompson, B.J., Pulkkinen,
2534 A., Evans, R., Nieves-Chinchilla, T.: Predicting the magnetic vectors within coronal mass ejections
2535 arriving at Earth: 1. Initial architecture, *Space Weather 13*, 374-385, doi:10.1002/2015SW001171,
2536 2015.
2537 Savani, N. P., Vourlidas, A., Richardson, I. G., Szabo, A., Thompson, B. J., Pulkkinen, A., et al.:
2538 Predicting the magnetic vectors within coronal mass ejections arriving at Earth: 2. Geomagnetic
2539 response, *Space Weather 15*, 441-461. https://doi.org/10.1002/2016SW001458, 2017.
2540 Scherhag, R.: Stratospheric temperature changes and the associated changes in pressure
2541 distribution, *J. Meteor., 17*, 575, doi:10.1175/1520-0469(1960)017<0575:STCATA>2.0.CO;2,
2542 1960.
2543 Schrijver, C.J., Kauristie, K., Aylward, A.D., Denardini, C.M., Gibson, S.E., Glover, A.,
2544 Gopalswamy, N., Grande, M., Hapgood, M., Heynderickx, D., Jakowski, N., Kalegaev, V.V.,
2545 Lapenta, G., Linker, J.A., Liu, S., Mandrini, C.H., Mann, I.R., Nagatsuma, T., Nandy, D., Obara,
2546 T., O'Brien, T.P., Onsager, T., Opgenoorth, H.J., Terkildsen, M., Valladares, C.E., Vilmer, N.:
2547 Understanding space weather to shield society: A global road map for 2015-2025 commissioned
2548 by COSPAR and ILWS, A*dv. Spa. Res. 55*, 2745-2807, 2015.
2549 Sckopke, N.: A general relation between the energy of trapped particles and the disturbance field
2550 near the Earth, *J. Geophys. Res., 71*, 3125, 1966.
2551 Schrijver, C. J., Beer, J., Baltensperger, U., Cliver, E. W., Güdel, M., Hudson, H. S., McCracken,
2552 K. G., Osten, R. A., Peter, T., Soderblom, D. R., Usoskin, I. G., and Wolff, E. W.: Estimating the
2553 frequency of extremely energetic solar events, based on solar, stellar, lunar, and terrestrial records,
2554 *J. Geophys. Res., 117*, A08103, doi: 10.1029/2012JA017706, 2012.
2555 Sharma, S., Kamide, Y., and Lakhina, G.S. (editors): *Storm-Substorm Relationship*, Amer.
2556 Geophys. Un. Press, Wash. D.C.,142, 2004.

2557 Sheeley, N.R. Jr., Harvey, J.W., and Feldman, W.C.: Coronal holes, solar wind streams and
2558 recurrent geomagnetic disturbances: 1973-1976, *Sol. Phys., 49*, 271, 1976.
2559 Sheeley, N.R. Jr., Asbridge, J.R., Bame, S.J., and Harvey, J.W.: A pictoral comparison of
2560 interplanetary magnetic field polarity, solar wind speed and geomagnetic disturbance index during
2561 the sunspot cycle, *Sol. Phys., 52*, 485, 1977.
2562 Simpson, J.A., Lentz, G.A., McKibben, R.B., O'Gallagher, J.J., Schroeder, W., and Tuzzolino,
2563 A.J.: Preliminary documentation for the University of Chicago charged particle instrument data
2564 from the Pioneer 10.11 spacecraft as submitted to NASA NSSDG, *NSSDC Doc. B.*, GSFC,
2565 Greenbelt, Md, 1974.
2566 Siscoe, G. L.: A quasi-self-consistent axially symmetric model for the growth of a ring current
2567 through earthward motion from a pre-storm configuration, *Planet. Spa. Sci., 27*, 285-295, 1979.
2568 Smith, E.J., Connor, B.V., and Foster Jr., G.T.: Measuring the magnetic fields of Jupiter and the
2569 outer solar system, IEE Trans. Magn., MAG-11, 962, 1975.
2570 Smith, E.J., and Wolfe, J.H.: Observations of interaction regions and corotating shocks between
2571 one and five AU: Pioneers 10 and 11, *Geophys. Res. Lett., 3*, 137-140, 1976.
2572 Smith, E.J., Tsurutani, B.T., and Rosenberg, R.L.: Observations of the interplanetary sector
2573 structure up to heliographic latitudes of 16°: Pioneer 11, *J. Geophys. Res., 83*, 717-723, 1978.
2574 Soraas, F., Aarsnes, K., Oksavik, K., Sandanger, M.I., Evans, D.S., and Greer, M.S.: Evidence for
2575 particle injection as the case of Dst reduction during HILDCAA events, *J. Atmos. Sol.-Terr. Phys.,*
2576 *66*, 177-187, 2004.
2577 Souza, A. M., Echer, E., Bolzan, M. J. A., and Hajra, R.: A study on the main periodicities in
2578 interplanetary magnetic field Bz component and geomagnetic AE index during HILDCAA events
2579 using wavelet analysis, *J. Atmos. Sol. Terr. Phys., 149*, 81-86, 2016.
2580 Souza, A. M., Echer, E., Bolzan, M. J. A., and Hajra, R.: Cross-correlation and cross-wavelet
2581 analyses of the solar wind IMF Bz and auroral electrojet index AE coupling during HILDCAAs,
2582 *Ann. Geophys., 36*, 205-211, 2018.
2583 Srivastava, N.: A logistic regression model for predicting the occurrence of intense geomagnetic
2584 storms, *Ann. Geophys 23*, 2969-2974, 2005.
2585 Stern, D.P.: The motion of a proton in the equatorial magnetosphere, *J. Geophys. Res., 80*, 595,
2586 1975.

Suess, S., and Tsurutani, B.T. (editors): *From the Sun: Auroras, Magnetic Storms, Solar Flares, Cosmic Rays*, AGU monograph, Wash. D. C. 1998.

Sugiura, M.: Hourly values of equatorial Dst for the IGY, *Annual International Geophysical Year, vol. 35*, Pergamon, New York, p. 9, 1964.

Summers, D., Ni, B., and Meredith, N.P.: Timescale for radiation belt electron acceleration and loss due to resonant wave-particle interactions: 2. Evaluation for VLF chorus, ELF hiss, and electromagnetic ion cyclotron waves, *J. Geophys. Res.*, *112*. A04207, https://doi.org/10.1029/2006JA011993, 2007.

Tan, B.: Small-scale microwave bursts in long-duration solar flares, *Astrophys. J.*, *773*, 165, 2013.

Thomson, N. R., Rodger, C. J., and Clilverd, M. A.: Large solar flares and their ionospheric D region enhancements, *J. Geophys. Res., 110*, A06306, doi: 10.1029/2005JA011008, 2005.

Tang, F., Tsurutani, B.T., Gonzalez, W.D., Akasofu, S.I., and Smith, E.J.: Solar sources of interplanetary southward Bz events responsible for major magnetic storms (1978-9), *J. Geophys. Res*. *94*, A4, 3535-3541, 1989.

Thorne, R.M., Smith, E.J., Fiske, K.J., and Church, S.R.: Intense variation of ELF hiss and chorus during isolated substorms, *Geophys. Res. Lett.*, *1*, 193-196, doi:10.1029/GL001i005p00193, 1974.

Thorne, R.M., O'Brien, T.P., Shprits, Y.Y., Summers, D., and Horne, R.B.: Timescale for MeV electron microburst loss during geomagnetic storms, *J. Geophys. Res.*, *110*. A09202, https://doi.org/10.1029/2004JA010882, 2005.

Thorne, R.M., Li, W., Ni, B., Ma, Q., Bortnik, J., Chen, L., Baker, D.N., Spence, H.E., Reeves, G.D., Henderson, M.G., Kletzing, C.A., Kurth, W.S., Hospodarsky, G.B., Blake, J.B., Fennell, J.F., Claudepierre, S.G., and Kanekal, S.G.: Rapid local acceleration of relativistic radiation-belt electrons by magnetospheric chorus, *Nature 504*, 411-414, 2013.

Thomson, N.R., Rodger, C.J., and Dowden, R.L.: Ionosphere gives the size of the greatest solar flare, *Geophys. Res. Lett.*, *31*, L06803, doi:10.1029/2003GL019345, 2004.

Tinsley, B.A., and Deen, G.W.: Apparent tropospheric response to MeV-GeV particle flux variations: A connection via electrofreezing of supercooled water in high-level clouds?, *J. Geophys. Res.*, *96*, 22,283, doi:10.1029/91JD02473, 1991.

Tsurutani, B.T., and Smith, E.J.: Postmidnight chorus: A substorm phenomenon, *J. Geophys. Res.*, *79*, 1, 118-127, 1974.

2617 Tsurutani, B.T., Smith, E.J., West Jr., H.I., and Buck, R.M.: Chorus, energetic electrons and
2618 magnetospheric substorms, in *Wave Instabilities in Space Plasmas*, edited by P.J. Palmadesso and
2619 K. Papadopoulos, 55, 1979.
2620 Tsurutani, B.T., Smith, E.J., Pyle, K.R., and Simpson, J.A.: Energetic protons accelerated at
2621 corotating shocks: Pioneer 10 and 11 observations from 1 to 6 AU, *J. Geophys. Res, 87*, A9, 7389-
2622 7404, 1982.
2623 Tsurutani, B.T., and Lin, R.P.: Acceleration of >47 keV ions and > 2 keV electrons by
2624 interplanetary shocks at 1 AU, *J. Geophys. Res., 90*, A1, 1-11, 1985.
2625 Tsurutani, B.T., and Gonzalez, W.D.: The cause of high-intensity long-duration continuous AE
2626 activity (HILDCAAs): Interplanetary Alfvén wave trains, *Plan. Spa. Sci., 35, 4*, 405-412, 1987.
2627 Tsurutani, B.T., Gonzalez, W.D., Tang, F., Akasofu, S.-I., and Smith, E.J.: Origin of interplanetary
2628 southward magnetic fields responsible for major magnetic storms near solar maximum (1978-
2629 1979), *J. Geophys. Res., 93*, A8, 8518-8531, 1988.
2630 Tsurutani, B.T., Gould, T., Goldstein, B.E., and Gonzalez, W.D.: Interplanetary Alfvén waves and
2631 auroral (substorm) activity: IMP 8, *J. Geophys. Res., 95*, A3, 2241-2252, 1990.
2632 Tsurutani, B.T., Gonzalez, W.D., Tang, F., and Lee, Y.T.: Great magnetic storms, *Geophys. Res.*
2633 *Lett., 19*, 73-76, 1992a.
2634 Tsurutani, B.T., Gonzalez, W.D., Tang, F., Lee, Y.T., Okada, M., and Park, D.: Reply to L.J.
2635 Lanzerotti: Solar wind ram pressure corrections and an estimation of the efficiency of viscous
2636 interaction, *Geophys. Res. Lett., 19*, 19, 1993-1994, 1992b.
2637 Tsurutani, B.T., and Gonzalez, W.D.: The causes of geomagnetic storms during solar maximum,
2638 *EOS, 75*, 5, 49-56, 1994.
2639 Tsurutani, B.T., Gonzalez, W.D., Zhou, X.-Y., Lepping, R.P., and Bothmer, V.: Properties of slow
2640 magnetic clouds, *J. Atmos. Sol.-Terr. Phys., 66*, 147-151, 1994.
2641 Tsurutani, B.T., Gonzalez, W.D., Gonzalez, A.L.C., Tang, F., Arballo, J.K., and Okada, M.:
2642 Interplanetary origin of geomagnetic activity in the declining phase of the solar cycle, *J.*
2643 *Geophys.Res., 100*, 21,717, 1995.
2644 Tsurutani, B.T., and Lakhina, G.S.: Some basic concepts of wave-particle interactions in
2645 collisionless plasmas, *Rev. Geophys., 35*, 4, 491-502, 1997.
2646 Tsurutani, B.T., Gonzalez, W.D., Kamide, Y., and Arballo, J.K. (editors): *Magnetic Storms*, Amer.
2647 Geophys. Un. Press, Wash. D.C., *98*, 1997a.

2648 Tsurutani, B.T., and Gonzalez, W.D.: The interplanetary causes of magnetic storms: A review, in
2649 *Magnetic Storms*, edited by Tsurutani, Gonzalez, Kamide and Arballo, AGU Press, Wash. D.C.,
2650 *98*, 77-89, 1997b.
2651 Tsurutani, B.T., Arballo, J.K., Lakhina, G.S., Ho, C.M., Ajello, J., Pickett, J.S., Gurnett, D.A.,
2652 Lepping, R.P., Peterson, W.K., Rostoker, G., Kamide, Y., and Kokubun, S.: The January 10, 1997
2653 auroral hot spot, horseshoe aurora and first substorm: A CME loop?, *Geophys. Res. Lett., 25*, 15,
2654 3047-3050, 1998.
2655 Tsurutani, B. T., Arballo, J. K., Lakhina, G. S., Ho, C. M., Ajello, J., Pickett, J. S., Gurnett, D. A.,
2656 Lepping, R. P., Peterson, W. K., Rostoker, G., Kamide, Y., and Kokubun, S.: The January 10,
2657 1997 auroral hot spot, horseshoe aurora and first substorm: A CME loop?, *J. Geophys. Res.*, *25*,
2658 3047-3050, 1998.
2659 Tsurutani, B.T., Solar/interplanetary plasma phenomena causing geomagnetic activity at Earth, in
2660 *Proc. Inter. Sch. Phys."Enrico Fermi" Course CXLII*, edited by B. Coppi, A. Ferrari and E.
2661 Sindoni, IOS Press, Amsterdam, 273, 2000.
2662 Tsurutani, B.T., Gonzalez, W.D., Lakhina, G.S., and Alex, S.: The extreme magnetic storm of 1-
2663 2 September 1859, *J. Geophys. Res. 108*, A7, 1268, doi:10.1029/JA009504, 2003.
2664 Tsurutani, B.T., Gonzalez, W.D., Zhou, X.-Y., Lepping, R.P., and Bothmer, V.: Properties of slow
2665 magnetic clouds, *J. Atmos. Sol.-Terr. Phys., 66*, 147-151, 2004a.
2666 Tsurutani, B.T., Gonzalez, W.D., Guarnieri, F., Kamide, Y., Zhao, X., and Arballo, J.K.: Are high-
2667 intensity long-duration continuous AE activity (HILDCAA) events substorm expansion events*?*,
2668 *J. Atmos. Sol.-Terr. Phys., 66*, 167-176, 2004b.
2669 Tsurutani, B.T., Mannucci, A., Iijima, B., Abdu, M.A., Sobral, J.H.A., Gonzalez, W., Guarnieri,
2670 F., Tsuda, T., Saito, A., Yumoto, K., Fejer, B., Fuller-Rowell, T.J., Kozyra, J., Foster, J.C., Coster,
2671 A., and Vasyliunas, V.M.: Global dayside ionospheric uplift and enhancement associated with
2672 interplanetary electric fields, *J. Geophys. Res. 109*, A08302, doi:10.1029/2003JA010342, 2004c.
2673 Tsurutani, B.T., Gonzalez, W.D., Lakhina, G.S., and Alex, S.: Reply to comment by S.-I. Akasofu
2674 and Y. Kamide on "The extreme magnetic storm of 1-2 September 1859", *J. Geophys. Res.*, *110*,
2675 A09227, doi:10.1029/2005JA011121, 2005a.
2676 Tsurutani, B.T., Judge, D.L., Guarnieri, F.L., Gangopadhyay, P., Jones, A.R., Nuttall, J., Zambon,
2677 G.A., Didkovsky, L., Mannucci, A.J., Iijima, B., Meier, R.R., Immel, T.J., Woods, T.N., Prasad,
2678 S., Floyd, L., Huba, J., Solomon, S.C., Straus, P., and Viereck, R.: The October 38, 2003 extreme

EUV solar flare and resultant extreme ionospheric effects: Comparison to other Halloween events and the Bastille day event, *Geophys. Res. Lett., 32*, L03S09, doi:10.1029/2004GL021475, 2005b.

Tsurutani, B.T., McPherron, R.L., Gonzalez, W.D., Lu, G., Sobral, J.H.A., and Gopalswamy, N. (editors): *Recurrent Magnetic Storms: Corotating Solar Wind Streams*, Amer. Geophys. Un. Press, Wash. D.C., 167, 2006a.

Tsurutani, B.T., Gonzalez, W.D., Gonzalez, A.L.C., Guarnieri, F.L., Golpalswamy, N., Grande, M., Kamide, Y., Kasahara, Y., Lu, G., Mann, I., McPherron, R., Soraas, F., and Vasyliunas, V.: Corotating solar wind streams and recurrent geomagnetic activity: A review, *J. Geophys. Res., 111*, A07S01, doi:10.1029/2005JA011273, 2006b.

Tsurutani, B.T., McPherron, R.L., Gonzalez, W.D., Lu, G., Gopalswamy, N., and Guarnieri, F.L.: Magnetic storms caused by corotating solar wind streams, in *Recurrent Magnetic Storms Corotating Solar Wind Streams*, edited by B.T. Tsurutani et al., AGU Press, Wash. DC, 167, 1-17, 2006c.

Tsurutani, B.T., Echer, E., Guarnieri, F.L., and Kozyra, J.U.: CAWSES November 7-8, 2004 superstorm: Complex solar and interplanetary features in the post-solar maximum phase, *Geophys. Res. Lett., 35*, L06S05, doi:10.1029/2007GL031473, 2008a.

Tsurutani, B.T., Verkhoglyadova, O.P., Mannucci, A.J., Saito, A., Araki, T., Yumoto, K., Tsuda, T., Abdu, M.A., Sobral, J.H.A., Gonzalez, W.D., McCreadie, H., Lakhina, G.S., and Vasyliunas, V.M.: *J. Geophys. Res., 113*, A05311, doi:10.1029/2007HA012879, 2008b.

Tsurutani, B.T., Horne, R.B., Pickett, J.S., Santolik, O., Schriver, D., and Verhoglyadova, O.P.: *J. Geophys. Res., 115*, AF0010, doi:10.1029/2010JA015870, 2010.

Tsurutani, B.T., Lakhina, G.S., Verkhoglyadova, O.P., Gonzalez, W.D., Echer, E., and Guarnieri, F.L.: A review of interplanetary discontinuities and their geomagnetic effects, *J. Atmos. Sol.-Terr. Phys., 73*, 5-19, 2011.

Tsurutani, B.T., Verkhoglyadova, O.P., Mannucci, A.J., and Lakhina, G.S.: Extreme changes in the dayside ionosphere during a Carrington-type magnetic storm, *J. Spa. Weath. Spa. Clim., 2*, A05, doi:10.1051/swsc/2012004, 2012.

Tsurutani, B.T., and Lakhina, G.S.: An extreme coronal mass ejection and consequences for the magnetosphere and Earth, *Geophys. Res. Lett., 41*, doi:10.1002/203GL058825, 2014.

Tsurutani, B.T., Echer, E., Shibata. K., Verkhoglyadova, O.P., Mannucci, A.J., Gonzalez, W.D., Kozyra, J.U., and Paetzold, M.: The interplanetary causes og geomagnetic activity during the 7-

17 March 2012 interval: a CAWSES II overview, *J. Spa. Weath. Spa. Clim., 4*, A02, doi:10.1051/swsc/2013056, 2014.

Tsurutani, B. T., Hajra, R., Echer, E., and Gjerloev, J. W.: Extremely intense (SML ≤ −2500 nT) substorms: isolated events that are externally triggered?, *AnGeo Comm., 33*, 519-524, 2015.

Tsurutani, B. T., Hajra, R., Echer, E., Gonzalez, W. D., and Santolik, O.: Predicting magnetospheric relativistic >1 MeV electrons, *NASA Tech Briefs, 40*, 20, 2016a.

Tsurutani, B.T., Hajra, R., Tanimori, T., Takada, A., Bhanu, R., Mannucci, A.J., Lakhina, G.S., Kozyra, J.U., Shiokawa, K., Lee, L.C., Echer, E., Reddy, R.V., and Gonzalez, W.D.: Heliospheric plasma sheet (HPS) impingement onto the magnetosphere as a cause of relativistic electron dropouts (REDs) via a coherent EMIC wave scattering with possible consequences for climate change mechanisms, *J. Geophys. Res. Spa. Phys., 121*, doi:10.1002/2016JA022499, 2016b.

Tsurutani, B.T., Lakhina, G.S., Echer, E., Hajra, R., Nayak, C., Mannucci, A.J., and Meng, X.: Comment on "Modeling extreme "Carrington-type" space weather events using three-dimensional global MHD simulations" by C.M. Ngwira, A. Pulkkinen, M.M Kuznetsova and A. Glocer", *J. Geophys. Res. Spa. Phys., 123*, 1388-1392, https://doi.org/10.1002/2017JA024779, 2018a.

Tsurutani, B.T., Lakhina, G.S., Sen, A., Hellinger, P., Glassmeier, K.-H., and Mannucci, A.J.: A review of Alfvénic turbulence in high-speed solar wind streams: Hints from cometary plasma turbulence, *J. Geophys. Res. Spa. Phys., 123*, https://doi.org/10.1002/2017JA024203, 2018b.

Turner, N. E., Mitchell, E. J., Knipp, D. J., and Emery, B. A.: Energetics of magnetic storms driven by corotating interaction regions: a study of geoeffectiveness, in *Recurrent Magnetic Storms: Corotating Solar Wind Streams*, Geophys. Monogr. Ser., vol. 167, edited by B. T. Tsurutani et al., pp. 113, AGU, Washington, D.C., doi:10.1029/167GM11, 2006.

Turner, D.L., and Li, X.: Quantitative forecast of relativistic electron flux at geosynchronous orbit based on low energy electron flux, *Space Weather, 6*, S05005, https://doi.org/10.1029/2007SW000354, 2008.

Usanova, M.E., Mann, I.R., Bortnik, J., Shao, L., and Angelopoulos, V.: THEMIS observations of electromagnetic ion cyclotron wave occurrence: Dependence on AE, SYMH and solar wind dynamic pressure, *J. Geophys. Res., 117*, A10218, doi:10.1029/2012JA018049, 2012.

Usoskin, I.G., and Kovaltsov, G.A.: Occurrence of extreme solar particle events: Assessment from historical proxy data, *Astrophys. J.*, 757:92, doi:10.1088/0004-637X/757/1/92, 2012.

2740 Usoskin, I.G., Kromer, B., Ludlow, F., Beer, J., Friedrich, M., Kovaltsov, G.A., Solanki, S.K., and
2741 Wacker, L.: The AD775 cosmic event revisited: the Sun is to blame, *Astron. Astrophys., L3*,
2742 doi:10.1051/0004-6361/201321080, 2013.
2743 Vaisberg, O.L., and Zastenker, G.N.: Solar wind and magnetosheath observations at Earth during
2744 August 1972, *Spa. Sci. Rev., 19*, 687, 1976.
2745 Volland, H.: A semi-empirical model of large-scale magnetospheric electric fields, *J. Geophys.*
2746 *Res., 78*, 171, 1973.
2747 Wang, C. B., Chao, J. K., and Lin, C.-H.: Influence of the solar wind dynamic pressure on the
2748 decay and injection of the ring current, *J. Geophys. Res.*, *108*(A9), 1341,
2749 doi:10.1029/2003JA009851, 2003.
2750 Wang, J., Zhao, M., and Zhou, G.: Magnetic changes in the course of the X7.1 solar flare on 2005
2751 January 20, *Astrophys. J.*, *690*, 862-874, 2009.
2752 Wanliss, J. A., and Showalter, K. M.: High-resolution global storm index: Dst versus SYM-H,
2753 *Journal of Geophysical Research, 111*, A02202. https://doi.org/10.1029/2005JA011034, 2006.
2754 West, H.I., Jr., Buck, R.M, and Walton, J.R.: Shadowing of electron azimuthal-drift motions near
2755 the noon magnetopause, *Nature Phys. Sci., 240*, 6, doi:10.1038/physci240006a0, 1972.
2756 Weygand, J. M., and McPherron, R. L.: Dependence of ring current asymmetry on storm phase, *J.*
2757 *Geophys. Res.*, *111*, A11221, doi:10.1029/2006JA011808, 2006.
2758 Wilcox, J.M., Scherrer, P.H., Svalgaard, L., Roberts, W.O., and Olson, R.H.: Solar magnetic sector
2759 structure: Relation to circulation of the Earth's atmosphere, *Science, 180*, 185,
2760 doi:10.1126/science.180.4082.185, 1973.
2761 Williams, D. J., Mitchell, D. G., Huang, C. Y., Frank, L. A., and Russell, C. T.: Particle
2762 acceleration during substorm growth and onset, *Geophys. Res. Lett., 17*, 587-590,
2763 https://doi.org/10.1029/GL017i005p00587, 1990.
2764 Wing, S., Johnson, J.R., Jen, J., Meng, C.I., Sibeck, D.G., Bechtold, K., Freeman, J., Costello, K.,
2765 Balikhin, M., and Takahashi, K.: Kp forecast models, *J. Geophys. Res. 110*, A04203,
2766 doi:10.1029/2004JA0105002005.
2767 Wing, S., Johnson, J.R., Camporeale, E., Reeves, G.D.: Information theoretical approach to
2768 discovering solar wind drivers of the outer radiation belt, *J. Geoophys. Res. Spa. Phys.*, *121*, 9378-
2769 9399, 2016.

Winterhalter, D.E., Smith, E.J., Burton, M.E., Murphy, N., and McComas, D.J.: The heliospheric plasma sheet, J. *Geophys. Res.*, *99*, 6667, doi:10.1029/93JA03481, 1994.

Wolff, E.W., Bigler, M., Curran, M.A.J., Dibb, J.E., Frey, M.M., Legrand, M., and McConnell, J.R.: The Carrington event not observed in most ice core nitrate records, *Geophys. Res. Lett.*, *39*, L08503, doi:10.1029/2012GL051603, 2012.

Wygant, J., Mozer, F., Temerin, M., Blake, J., Maynard, N., Singer, H., and Smiddy, M.: Large amplitude electric and magnetic field signatures in the inner magnetosphere during injection of 15 MeV electron drift echos, *Geophys. Res. Lett.*, *21*, 16, 1739-1742, 1994.

Wygant, J., Rowland, D., Singer, H.J., Temerin, M., Mozer, F., and Hudson, M.K.: Experimental evidence on the role of the large spatial scale electric field in creating the ring current, J. Geophys. Res., 103, A12, 29527-29544, 1998.

Yashiro, S., Gopalswamy, N., Michalek, G., St. Cyr, O. C., Plunkett, S. P., Rich, N. B., and Howard, R. A.: A catalog of white light coronal mass ejections observed by the SOHO spacecraft, *J. Geophys. Res.*, *109*, A07105, doi:10.1029/2003JA010282, 2004.

Yurchyshyn, V., Hu, Q., Lepping, R.P., Lynch, B.J., Krall, J.: Orientations of LASCO halo CMEs and their connection to the flux rope structure of interplanetary CMEs, *Adv. Spa. Res.*, *40*, 1821-1826, 2007.

Zastenker, G.N., Temny, V.V., d'Uston, C., and Bosqued, J.M.: The form and energy of the shock waves from the solar flares of August 2, 4 and 7, 1972, *J. Geophys. Res.*, *83*, 1035, 1978.

Zhao, X., and Dryer, M.: Current status of CME/shock arrival time prediction, *Spa. Weath.*, *12*, 448-469, doi:10.1002/2014SW001060, 2014.

Zhang, J., Woch, J., and Solanki, S.: Polar coronal holes during solar cycles 22 and 23, *Chin. J. Astron. Astrophys.*, *5*, 5, 531-538, 2005.

Zhou, X., and Tsurutani, B. T.: Rapid intensification and propagation of the dayside aurora: Large scale interplanetary pressure pulses (fast shocks*), Geophys. Res. Lett.*, *26*, 8, 1097-1100, 1999.

Zhang, J., et al.: Solar and interplanetary sources of major geomagnetic storms (Dst ≤ -100 nT) during 1996-2005, *J. Geophys. Res.*, *112*, A10102, doi:10.1029/2007JA012321, 2007.

Zhou, X., and Tsurutani, B.T.: Interplanetary shock triggering of nightside geomagnetic activity: Substorms, pseudobreakups, and quiescent events, *J. Geophys. Res.*, *106*, A9, 18,957-18,967, 2001.

Zhou, X.-Y., Strangeway, R.J., Anderson, P.C., Sibeck, D.G., Tsurutani, B.T., Haerendel, G., Frey, H.U., and Arballo, J.K.: Shock aurora: FAST and DMSP observations, *J. Geophys. Res.*, *108,* A4, doi:10.1029/2002JA009701, 2003.

Acknowledgements. This paper was solicited by an Editor of Reviews of Geophysics to be the main article for Space Weather for the AGU Centennial. The paper was written with that in mind but was rejected by two referees. GSL thanks the National Academy of Sciences, India for support under the NASI-Senior Scientist Platinum Jubilee Fellowship Scheme. The work of RH is funded by the Science & Engineering Research Board (SERB), a statutory body of the Department of Science & Technology (DST), Government of India through the Ramanujan Fellowship.